

DESIGN OF MAGNETO-ELECTRIC DIPOLE ANTENNA FOR WIDEBAND
COMMUNICATION SYSTEMS

A THESIS SUBMITTED TO
THE GRADUATE SCHOOL OF NATURAL AND APPLIED SCIENCES
OF
MIDDLE EAST TECHNICAL UNIVERSITY

BY

SEMİH ALPARSLAN

IN PARTIAL FULFILLMENT OF THE REQUIREMENTS
FOR
THE DEGREE OF MASTER OF SCIENCE
IN
ELECTRICAL AND ELECTRONICS ENGINEERING

JANUARY 2018

Approval of the thesis:

**DESIGN OF MAGNETO-ELECTRIC DIPOLE ANTENNA FOR
WIDEBAND COMMUNICATION SYSTEMS**

submitted by **SEMİH ALPARSLAN** in partial fulfillment of the requirements for
the degree of **Master of Science in Electrical and Electronics Engineering**
Department, Middle East Technical University by,

Prof. Dr. Gülbin Dural Ünver
Dean, Graduate School of **Natural and Applied Sciences** _____

Prof. Dr. Tolga Çiloğlu
Head of Department, **Electrical and Electronics Eng.** _____

Assoc. Prof. Dr. Lale Alatan
Supervisor, **Electrical and Electronics Eng. Dept.,METU** _____

Examining Committee Members:

Prof. Dr. Sencer Koç
Electrical and Electronics Eng. Dept.,METU _____

Assoc. Prof. Dr. Lale Alatan
Electrical and Electronics Eng. Dept.,METU _____

Prof. Dr. Nilgün Günel
Electrical and Electronics Eng. Dept.,METU _____

Prof. Dr. Özlem Aydın Çivi
Electrical and Electronics Eng. Dept.,METU _____

Prof. Dr. Birsan Saka
Electrical and Electronics Eng. Dept. Hacettepe Uni. _____

Date: **08.01.2018**

I hereby declare that all information in this document has been obtained and presented in accordance with academic rules and ethical conduct. I also declare that, as required by these rules and conduct, I have fully cited and referenced all material and results that are not original to this work.

Name, Last name: Semih ALPARSLAN

Signature:

ABSTRACT

DESIGN OF MAGNETO-ELECTRIC DIPOLE ANTENNA FOR WIDEBAND COMMUNICATION SYSTEMS

Alparslan, Semih

M. S., Department of Electrical and Electronics Engineering

Supervisor: Assoc. Prof. Dr. Lale Alatan

January 2018, 86 pages

This thesis includes the design, simulation, production and measurement of a differential fed magneto-electric dipole antenna with cavity operating at ultra-wideband (3.3 GHz – 10 GHz). This antenna consists of a differential feeding structure, an electric dipole, a magnetic dipole and a cavity. The ultra-wideband operation is achieved through the use of differential feeding structure and cavity. A step-by-step procedure is followed during the design process of the differential fed magneto-electric dipole antenna with cavity. First, a gamma-shaped strip fed magneto-electric dipole antenna is designed to study the effects of the antenna parameters on the return loss and the characteristics of the antenna gain. These parametric analyses are done in Ansys HFSS, a high frequency electromagnetic field simulation program. By the help of the experience gained through these parametric analyses, a differential fed magneto-electric dipole antenna is designed and simulated. Then, in order to achieve design requirements a cavity is incorporated into the design.

Finally, the designed differential fed magneto-electric dipole antenna with cavity is manufactured, measured, and its performance is compared with simulation results.

KEYWORDS: Magneto-Electric Dipole, Differential Feeding Structure, Cavity, Ultra-wideband, Unidirectional

ÖZ

GENİŞ BANTLI HABERLEŞME SİSTEMLERİ İÇİN MANYETO-ELEKTRİK DİPOL ANTEN TASARIMI

Alparslan, Semih

Yüksek Lisans, Elektrik ve Elektronik Mühendisliği Bölümü

Tez Yöneticisi: Doç. Dr. Lale Alatan

Ocak 2018, 86 sayfa

Bu tez ultra-geniş bantta (3.3 GHz – 10 GHz) çalışacak duvarlı, ayırık beslemeli manyeto-elektrik dipol anten tasarımını, benzeşimini, üretimini ve ölçümünü içerir. Bu anten bir ayırık besleme yapısı, bir elektrik dipol, bir manyetik dipol ve bir duvardan meydana gelmektedir. Ayırık besleme altyapısı ve duvar sayesinde ultra-genişbantlı bir çalışma yapısına sahiptir. Tasarım kısmında duvarlı, ayırık beslemeli manyeto-elektrik dipol anten adım adım geliştirilmiştir. İlk olarak, anten parametrelerin yansıma katsayısı ve kazanç üzerindeki etkilerinin analizini çalışmak için gama-şekilli beslemeli manyeto-elektrik dipol anten tasarlanmıştır. Bu parametrik analizler yüksek frekanslı elektromanyetik alan benzeşim programı Ansys HFSS kullanılarak yapılmıştır. Parametrik analizlerden elde edilen tecrübeyle, ayırık beslemeli manyeto-elektrik dipol anten tasarımı ve benzeşimi tamamlanmıştır. Sonrasında, tasarım gereksinimlerini sağlayabilmek için, tasarıma duvar yapısı eklenmiştir. En son aşamada ise duvarlı, ayırık beslemeli manyeto-elektrik dipol antenin üretimi yapılmış, ölçümleri alınmış ve bu antenin performansı benzeşim programı sonuçları ile karşılaştırılmıştır.

ANAHTAR KELİMELEER: Manyeto-Elektrik Dipol, Ayrık Besleme Yapısı, Duvar,
Ultra-Geniş bant, Tek Yönlü

To my wife, Güler

ACKNOWLEDGEMENTS

I would like to express my sincere gratitude to my advisor, Assoc. Prof. Dr. Lale Alatan, for her valuable guidance, support and technical suggestions throughout the study.

I would also like to thank Prof. Dr. Özlem Aydın Çivi, Prof. Dr. Sencer Koç, Prof. Dr. Nilgün Günel and Prof. Dr. Birsen Saka being in my jury and sharing their opinions.

I am grateful to ASELSAN INC. for the financial and technical opportunities provided for the completion of this thesis.

I would also like to express my sincere appreciation for Kenan Çapraz, Durmuş Gebeşoğlu, Ali Murat Kayıran and Kamil Karacığer for their valuable friendship, motivation and help.

Lastly, for her great support, understanding, being with me in every moment of this work and giving me the strength and courage to finish it, I am also grateful to my wife, Güler.

TABLE OF CONTENTS

ABSTRACT	v
ÖZ.....	7
ACKNOWLEDGEMENTS	x
TABLE OF CONTENTS	xi
LIST OF TABLES	xiii
LIST OF FIGURES	xiv
CHAPTERS	
1. INTRODUCTION	1
1.1 3G/4G/5G Frequency Band.....	4
1.2 Ultra-Wideband (UWB) Frequency Band.....	8
1.3 Millimeter Wave Band.....	11
1.4 Organization of the Thesis.....	15
2. DESIGN OF THE MAGNETO-ELECTRIC DIPOLE ANTENNA.....	17
2.1 Parametric Analysis of the Magneto-Electric Dipole Antenna.....	17
2.2 Design of the Differential Fed Magneto-Electric Dipole Antenna....	29
2.3 Design of the Differential Fed Magneto-Electric Dipole Antenna with Cavity.....	48
3. FABRICATIONS AND MEASUREMENTS OF THE MAGNETO-ELECTRIC DIPOLE ANTENNA WITH CAVITY	63
3.1 Fabrications of Differential Fed Magneto-Electric Dipole Antenna with Cavity.....	63
3.2 Measurements of Fabricated Differential Fed Magneto-Electric Dipole Antenna with Cavity.....	66

4. CONCLUSIONS	83
REFERENCES	85

LIST OF TABLES

TABLES

Table 2- 1 Nominal Values of the Gamma-Shaped Fed Magneto-Electric Dipole Antenna	18
Table 2- 2 Parameter Values of the Differential Fed Magneto-Electric Dipole Antenna	30
Table 2- 3 Final Parameter Values of the Differential Fed Magneto-Electric Dipole Antenna with Cavity.....	41
Table 3- 1 Measured 3 dB Beamwidth of the Broadside Beam of the Antenna	78

LIST OF FIGURES

FIGURES

Figure 1- 1 E and H Plane Radiation Patterns of Complementary Antenna [2].....	2
Figure 1- 2 Magneto-Electric Dipole Antenna [2]	3
Figure 1- 3 Magneto-Electric Dipole Antenna with Γ -shaped Feed [2].....	4
Figure 1- 4 Magneto-Electric Dipole Antenna with Square-Cap Feed [4]	5
Figure 1- 5 Magneto-Electric Dipole Antenna with Coaxial Feed [5]	6
Figure 1- 6 Magneto-Electric Dipole Antenna with Differential Feed [5].....	7
Figure 1- 7 Magneto-Electric Dipole Antenna with Tapered H-Shaped Ground [7] 8	
Figure 1- 8 Magneto-Electric Dipole Antenna with Differential and Multi-Layer Feed [8].....	9
Figure 1- 9 Differential and Multi-Layer Feeding Structure of the Magneto-Electric Dipole Antenna [8]	9
Figure 1- 10 Magneto-Electric Dipole Antenna with Bow-Tie Structure [9]	10
Figure 1- 11 Microstrip to Parallel Plate Feeding Mechanism [9]	11
Figure 1- 12 Magneto-Electric Dipole Antenna for Millimeter-Wave Applications-1 [10]	12
Figure 1- 13 Magneto- Electric Antenna for Millimeter Wave Applications-2 [11]	13
Figure 1- 14 Magneto-Electric Dipole Antenna with Dual-Polarization [12].....	14
Figure 1- 15 Magneto-Electric Dipole Antenna with Box-Shaped Reflector [13] .	14
Figure 2- 1 Structure of the Gamma-Shaped Strip Fed Magneto-Electric Dipole Antenna [4]	17
Figure 2- 2 Input Impedance of the Gamma-Shaped Strip Fed Magneto-Electric Dipole Antenna with Nominal Values	19

Figure 2- 3 Return Loss of the Gamma-Shaped Strip Fed Magneto-Electric Dipole Antenna with Nominal Values	20
Figure 2- 4 Gain of the Gamma-Shaped Strip Fed Magneto-Electric Dipole Antenna with Nominal Values.....	20
Figure 2- 5 Return Loss of the Gamma-Shaped Strip Fed Magneto-Electric Dipole Antenna with L Sweep	21
Figure 2- 6 Gain of the Gamma-Shaped Strip Fed Magneto-Electric Dipole Antenna with L Sweep.....	21
Figure 2- 7 Return Loss of the Gamma-Shaped Strip Fed Magneto-Electric Dipole Antenna with W Sweep	22
Figure 2- 8 Gain of the Gamma-Shaped Strip Fed Magneto-Electric Dipole Antenna with W Sweep	23
Figure 2- 9 Return Loss of the Gamma-Shaped Strip Fed Magneto-Electric Dipole Antenna with H Sweep.....	24
Figure 2- 10 Gain of the Gamma-Shaped Strip Fed Magneto-Electric Dipole Antenna with H Sweep	24
Figure 2- 11 Return Loss of the Gamma-Shaped Strip Fed Magneto-Electric Dipole Antenna with Feed2L Sweep	25
Figure 2- 12 Gain of the Gamma-Shaped Strip Fed Magneto-Electric Dipole Antenna with Feed2L Sweep	25
Figure 2- 13 Return Loss of the Gamma-Shaped Strip Fed Magneto-Electric Dipole Antenna with Feed3H Sweep	26
Figure 2- 14 Gain of the Gamma-Shaped Strip Fed Magneto-Electric Dipole Antenna with Feed3H Sweep	27
Figure 2- 15 Return Loss of the Gamma-Shaped Strip Fed Magneto-Electric Dipole Antenna with FeedW Sweep	28
Figure 2- 16 Gain of the Gamma-Shaped Strip Fed Magneto-Electric Dipole Antenna with FeedW Sweep.....	28

Figure 2- 17 HFSS Model of the Differential Fed Magneto-Electric Dipole Antenna (Top View)	29
Figure 2- 18 HFSS Model of the Differential Fed Magneto-Electric Dipole Antenna (Side View).....	30
Figure 2- 19 Return Loss of the Differential Fed Magneto-Electric Dipole Antenna with Nominal Values	33
Figure 2- 20 Return Loss of the Differential Fed Magneto-Electric Dipole Antenna with Feed2L Sweep	34
Figure 2- 21 Gain of the Differential Fed Magneto-Electric Dipole Antenna with Feed2L Sweep	34
Figure 2- 22 Return Loss of the Differential Fed Magneto-Electric Dipole Antenna with FeedW Sweep	35
Figure 2- 23 Gain of the Differential Fed Magneto-Electric Dipole Antenna with FeedW Sweep	35
Figure 2- 24 Air-filled Microstrip Line	36
Figure 2- 25 Return Loss of the Differential Fed Magneto-Electric Dipole Antenna with Feed2W Sweep	36
Figure 2- 26 Gain of the Differential Fed Magneto-Electric Dipole Antenna with Feed2W Sweep	37
Figure 2- 27 Return Loss of the Differential Fed Magneto-Electric Dipole Antenna with S1 Sweep	38
Figure 2- 28 Gain of the Differential Fed Magneto-Electric Dipole Antenna with S1 Sweep	38
Figure 2- 29 Return Loss of the Differential Fed Magneto-Electric Dipole Antenna with H Sweep	39
Figure 2- 30 Gain of the Differential Fed Magneto-Electric Dipole Antenna with H Sweep	39
Figure 2- 31 Return Loss of the Differential Fed Magneto-Electric Dipole Antenna with L Sweep	40

Figure 2- 32 Gain of the Differential Fed Magneto-Electric Dipole Antenna with L Sweep	40
Figure 2- 33 Final Return Loss of the Differential Fed Magneto-Electric Dipole Antenna	41
Figure 2- 34 Final Gain of the Differential Fed Magneto-Electric Dipole Antenna	42
Figure 2- 35 Radiation Pattern of the Differential Fed Magneto-Electric Dipole Antenna at 3 GHz in E-Plane	43
Figure 2- 36 Radiation Pattern of the Differential Fed Magneto-Electric Dipole Antenna at 3 GHz in H-Plane	43
Figure 2- 37 Current distribution of the Differential Fed Magneto-Electric Dipole Antenna at 3 GHz	44
Figure 2- 38 Radiation Pattern of the Differential Fed Magneto-Electric Dipole Antenna at 9 GHz in E-Plane	45
Figure 2- 39 Radiation Pattern of the Differential Fed Magneto-Electric Dipole Antenna at 9 GHz in H-Plane	45
Figure 2- 40 Current distribution of the Differential Fed Magneto-Electric Dipole Antenna at 9 GHz	46
Figure 2- 41 Radiation Pattern of the Differential Fed Magneto-Electric Dipole Antenna at 10 GHz in E-Plane	46
Figure 2- 42 Radiation Pattern of the Differential Fed Magneto-Electric Dipole Antenna at 10 GHz in H-Plane	47
Figure 2- 43 Current distribution of the Differential Fed Magneto-Electric Dipole Antenna at 10 GHz	47
Figure 2- 44 HFSS Model of the Differential Fed Magneto-Electric Dipole Antenna with Cavity	48
Figure 2- 45 Return Loss of the Differential Fed Magneto-Electric Dipole Antenna with WallH of the Cavity Sweep	49
Figure 2- 46 Gain of the Differential Fed Magneto-Electric Dipole Antenna with WallH of the Cavity Sweep	49

Figure 2- 47 Return Loss of the Differential Fed Magneto-Electric Dipole Antenna with Length of the Cavity Sweep	50
Figure 2- 48 Gain of the Differential Fed Magneto-Electric Dipole Antenna with Length of the Cavity Sweep	50
Figure 2- 49 Final Return Loss of the Differential Fed Magneto-Electric Dipole Antenna with Cavity and without Cavity	51
Figure 2- 50 Final Gain of the Differential Fed Magneto-Electric Dipole Antenna with Cavity and without Cavity.....	51
Figure 2- 51 Radiation Pattern of the Differential Fed Magneto-Electric Dipole Antenna with and without Cavity at 3 GHz in E-Plane.....	52
Figure 2- 52 Radiation Pattern of the Differential Fed Magneto-Electric Dipole Antenna with and without Cavity at 3 GHz in H-Plane	53
Figure 2- 53 Radiation Pattern of the Differential Fed Magneto-Electric Dipole Antenna with and without Cavity at 4 GHz in E-Plane.....	53
Figure 2- 54 Radiation Pattern of the Differential Fed Magneto-Electric Dipole Antenna with and without Cavity at 4 GHz in H-Plane	54
Figure 2- 55 Radiation Pattern of the Differential Fed Magneto-Electric Dipole Antenna with and without Cavity at 5 GHz in E-Plane.....	54
Figure 2- 56 Radiation Pattern of the Differential Fed Magneto-Electric Dipole Antenna with and without Cavity at 5 GHz in H-Plane	55
Figure 2- 57 Radiation Pattern of the Differential Fed Magneto-Electric Dipole Antenna with and without Cavity at 6 GHz in E-Plane.....	55
Figure 2- 58 Radiation Pattern of the Differential Fed Magneto-Electric Dipole Antenna with and without Cavity at 6 GHz in H-Plane	56
Figure 2- 59 Radiation Pattern of the Differential Fed Magneto-Electric Dipole Antenna with and without Cavity at 7 GHz in E-Plane.....	56
Figure 2- 60 Radiation Pattern of the Differential Fed Magneto-Electric Dipole Antenna with and without Cavity at 7 GHz in H-Plane	57

Figure 2- 61 Radiation Pattern of the Differential Fed Magneto-Electric Dipole Antenna with and without Cavity at 8 GHz in E-Plane	57
Figure 2- 62 Radiation Pattern of the Differential Fed Magneto-Electric Dipole Antenna with and without Cavity at 8 GHz in H-Plane	58
Figure 2- 63 Radiation Pattern of the Differential Fed Magneto-Electric Dipole Antenna with and without Cavity at 9 GHz in E-Plane	58
Figure 2- 64 Radiation Pattern of the Differential Fed Magneto-Electric Dipole Antenna with and without Cavity at 9 GHz in H-Plane	59
Figure 2- 65 Radiation Pattern of the Differential Fed Magneto-Electric Dipole Antenna with and without Cavity at 10 GHz in E-Plane	59
Figure 2- 66 Radiation Pattern of the Differential Fed Magneto-Electric Dipole Antenna with and without Cavity at 10 GHz in H-Plane	60
Figure 2- 67 3D Radiation Patterns of the Differential Fed Magneto-Electric Dipole Antenna with Cavity	61
Figure 3- 1 Perspective View of Fabricated Differential Fed Magneto-Electric Dipole Antenna with Cavity	64
Figure 3- 2 Top View of Fabricated Differential Fed Magneto-Electric Dipole Antenna with Cavity	65
Figure 3- 3 Bottom View of the Fabricated Differential Fed Magneto-Electric Dipole Antenna with Cavity	65
Figure 3- 4 Feeding Structure of the Fabricated Differential Fed Magneto-Electric Dipole Antenna with Cavity	66
Figure 3- 5 Measured and Simulated Return Loss of the Differential Fed Magneto-Electric Dipole Antenna with Cavity	67
Figure 3- 6 General Measurement Set-up for the Differential Fed Magneto-Electric Dipole Antenna with Cavity	68
Figure 3- 7 Comparison of Simulation and Measurement Results for S_{11}	69

Figure 3- 8 Comparison of Simulation and Measurement Results for S_{21}	69
Figure 3- 9 Comparison of Simulation and Measurement Results for Differential Input Return Loss	70
Figure 3- 10 Near Field Measurement Set-up for the Differential Fed Magneto-Electric Dipole Antenna with Cavity	71
Figure 3- 11 Measured and Simulated Gains in Bore-sight Directions of the Differential Fed Magneto-Electric Dipole Antenna with Cavity	72
Figure 3- 12 E-Plane Radiation Patterns at 3 GHz	73
Figure 3- 13 H-Plane Radiation Patterns at 3 GHz	73
Figure 3- 14 E-Plane Radiation Patterns at 4 GHz	74
Figure 3- 15 H-Plane Radiation Patterns at 4 GHz	74
Figure 3- 16 E-Plane Radiation Patterns at 5 GHz	75
Figure 3- 17 H-Plane Radiation Patterns at 5 GHz	75
Figure 3- 18 E-Plane Radiation Patterns at 6 GHz	76
Figure 3- 19 H-Plane Radiation Patterns at 6 GHz	76
Figure 3- 20 E-Plane Radiation Patterns at 7 GHz	77
Figure 3- 21 H-Plane Radiation Patterns at 7 GHz	77
Figure 3- 22 E-Plane Radiation Patterns at 8 GHz	78
Figure 3- 23 H-Plane Radiation Patterns at 8 GHz	78
Figure 3- 24 E-Plane Radiation Patterns at 9 GHz	79
Figure 3- 25 H-Plane Radiation Patterns at 9 GHz	79
Figure 3- 26 E-Plane Radiation Patterns at 10 GHz	80
Figure 3- 27 H-Plane Radiation Patterns at 10 GHz	80

CHAPTER 1

INTRODUCTION

Due to recent developments in some areas like mobile communications, radar and electronic warfare (EW), novel antenna designs are required because of the inadequacy of existing antennas. These areas need wideband and low-profile antennas particularly in wireless mobile communication applications. Moreover, low back radiation, low side lobes, high gain, low input return loss and low cross polarization are other requirements for these application areas.

There are several low profile antenna types such as patch antenna, printed monopole antenna, log periodic antenna and tapered slot antenna in use for wireless mobile communication, radar and EW areas. Even though log periodic antennas and tapered slot antennas such as Vivaldi are ultra-wideband (UWB) antennas, they have relatively larger dimensions and phase center of these antennas change with frequency [1]. Thus, these antenna types are not suitable for UWB imaging radar applications.

Although microstrip patch antennas are low profile, low cost, light weight structures with easy fabrication, their bandwidths are limited. By utilizing different feeding methods like aperture coupled or L-probe, and by using stacked patches or patches with U or E shaped slots, 20% to 40% impedance bandwidth can be achieved. However the radiation pattern stability cannot be maintained throughout these wide frequency bands. In order to achieve stable radiation within a wide frequency band, complementary antenna concept is exploited by Luk and Wong and magneto-electric dipole antenna structure is proposed [2].

Electric dipole and magnetic dipole are complementary antennas. If two complementary antennas are excited simultaneously with equal amplitude and proper phase, unidirectional radiation can be obtained with low back radiation. Electric dipole has 8-shaped radiation pattern in its E-plane and omni-directional pattern in its H-plane whereas magnetic dipole has 8-shaped radiation pattern in its H-plane and omni-directional pattern in its E-plane. Hence the superposition of these two radiations with proper phase, results in a cardioid pattern as shown in Figure 1-1. Several complementary antenna structures are proposed in literature [3]. However these antennas generally exhibit narrow bandwidth.

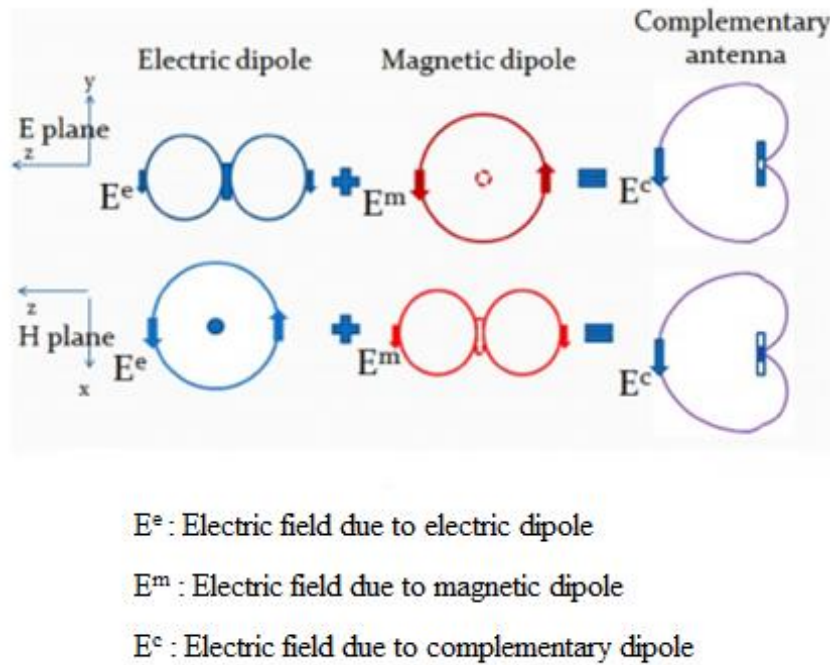


Figure 1- 1 E and H Plane Radiation Patterns of Complementary Antenna [2]

A wideband complementary antenna which is named as magneto-electric dipole antenna was proposed in 2006 [2]. The magneto-electric dipole antenna consists of a planar dipole antenna and a shorted patch antenna with air dielectric as shown in Figure 1- 2. In a patch antenna a rectangular patch of half wavelength long is placed

over a ground plane. To miniaturize the antenna, the length of the patch can be halved (i.e., $\lambda/4$) if a short circuit connection between the ground plane and the patch is established. The fringing fields at the open end of the antenna behave like a magnetic dipole. To excite the planar dipole and shorted patch antenna simultaneously Γ -shaped feed strip can be used as shown in Figure 1- 3. This magneto-electric dipole antenna has simple structure, wide bandwidth (more than 43.8% impedance bandwidth for $VSWR \leq 1.5$), low cross polarization, 8 dBi maximum gain and very low back radiation [2].

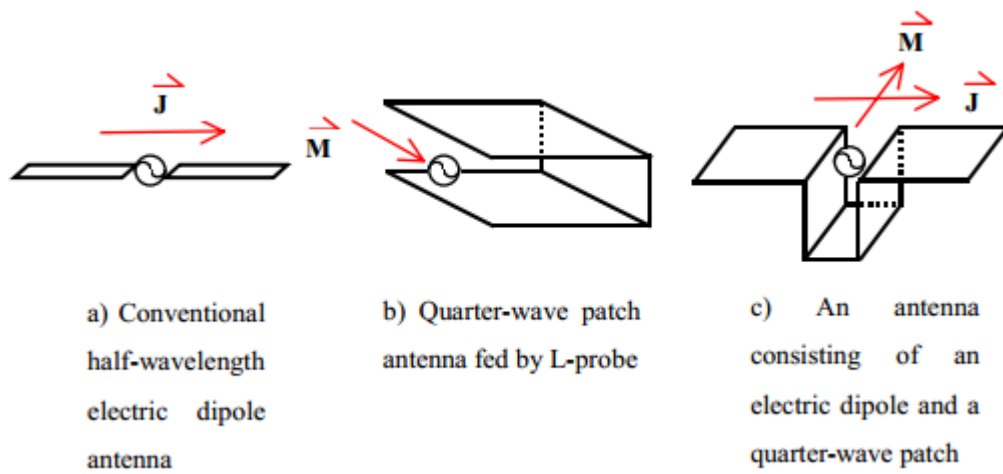


Figure 1- 2 Magneto-Electric Dipole Antenna [2]

Over the last decade various magneto-electric dipole antenna structures with different feeding methods and/or different operation bands are proposed in literature [3]. The magneto-electric dipole antenna studies can be classified into three groups in terms of the operating frequency bands. First one is the 3G/4G/5G mobile communication bands, second one is the ultra-wideband (UWB) communication band and third one is the millimeter wave band.

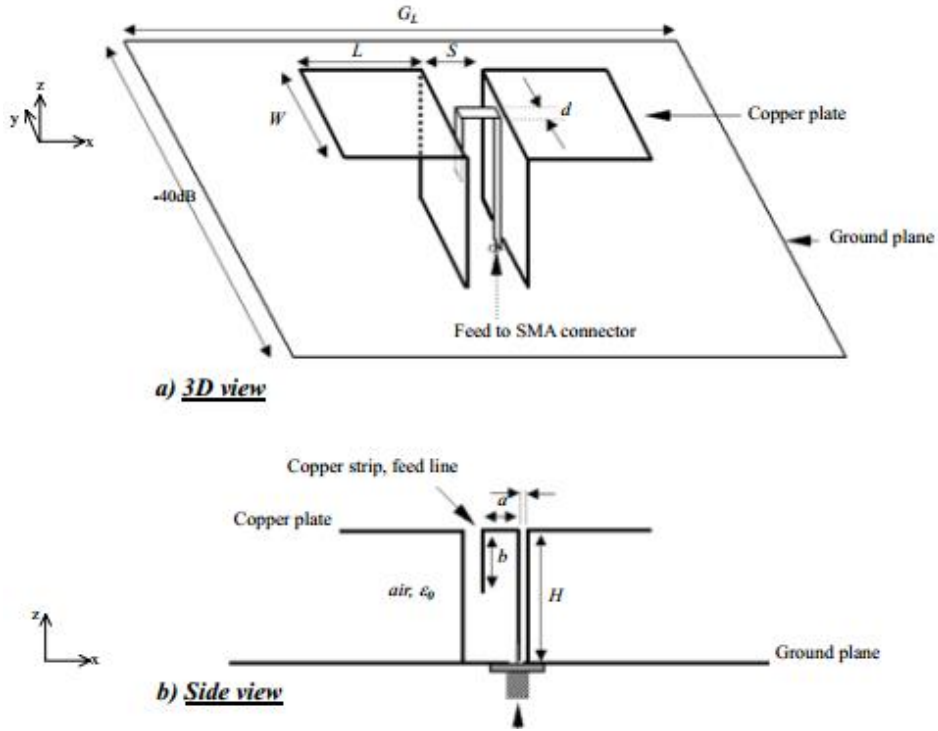


Figure 1- 3 Magneto-Electric Dipole Antenna with Γ -shaped Feed [2]

1.1 3G/4G/5G Frequency Band

The originally proposed magneto-electric dipole antenna presented in [2] was designed for 3G/4G/5G frequency band. Later the Γ -shaped feeding strip of this antenna was replaced with a square-cap coupled feed [4] as shown in Figure 1- 4. This antenna has wide bandwidth, low cross polarization, symmetrical radiation pattern and very low back radiation with 62% impedance bandwidth for $\text{VSWR} < 2$ and 8dBi maximum gain.

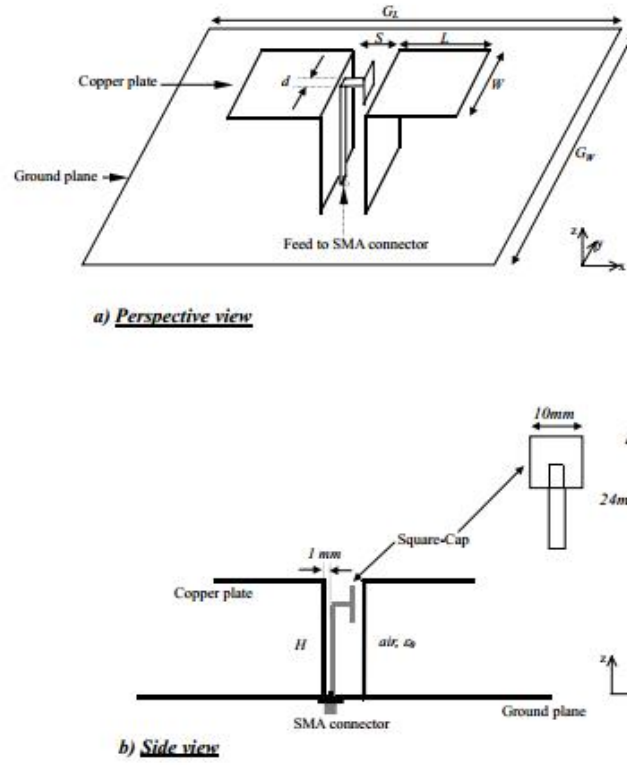


Figure 1- 4 Magneto-Electric Dipole Antenna with Square-Cap Feed [4]

In [5] a coaxial feed with a copper strip is proposed as shown in Figure 1- 5. In this antenna a rectangular cavity shaped reflector is utilized to enhance the radiation pattern stability within the impedance bandwidth. Moreover a folded shorted patch is used to reduce the height of the antenna. This antenna has 54% impedance bandwidth for $VSWR < 1.5$ and an average gain of 8.6 dBi.

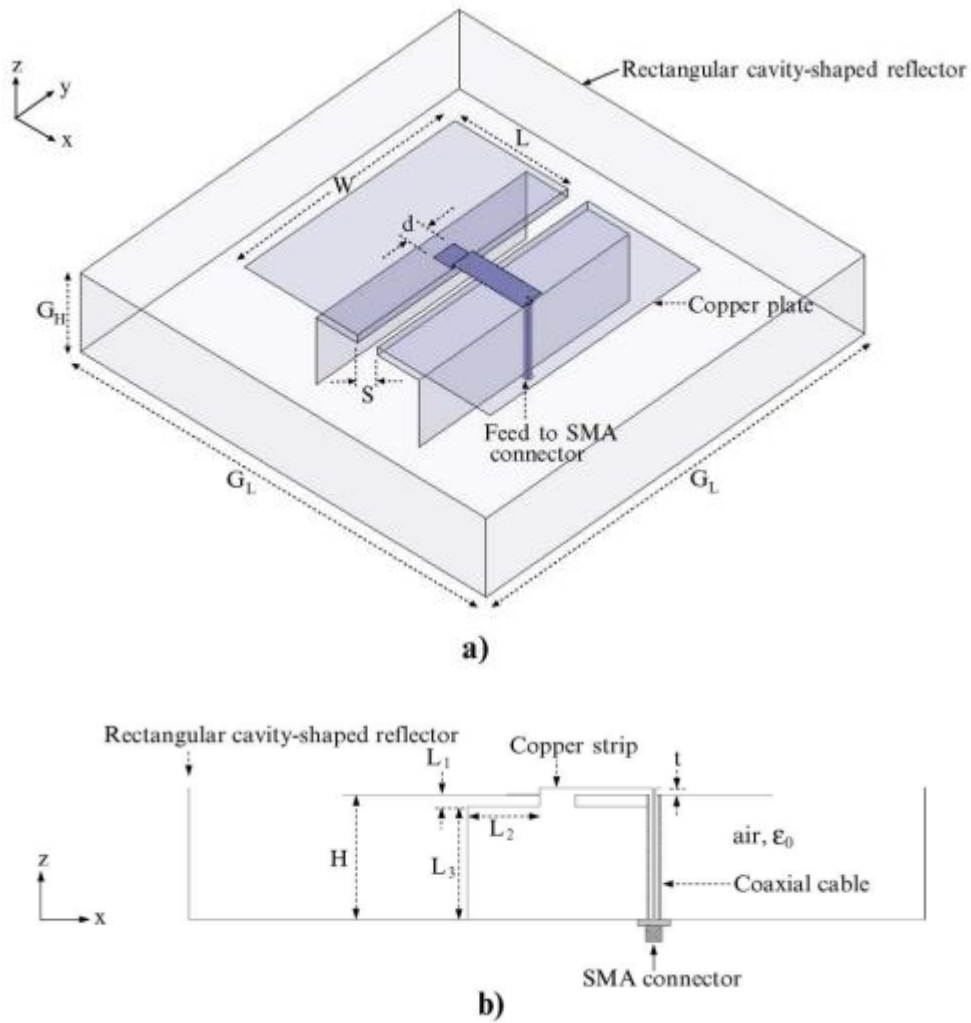


Figure 1- 5 Magneto-Electric Dipole Antenna with Coaxial Feed [5]

The antenna designs discussed so far employed unbalanced feed structures. A simple differential feed structure as shown in Figure 1- 6 is proposed in [6] to avoid the need for a balun that converts the unbalanced feed like coaxial cable to balanced antenna.

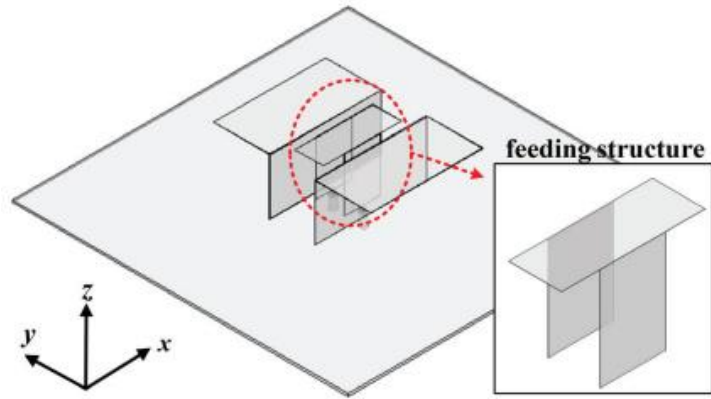


Figure 1- 6 Magneto-Electric Dipole Antenna with Differential Feed [5]

Differentially fed magneto-electric dipole antenna has 92% impedance bandwidth for $VSWR < 2$, 7.7 dBi maximum gain [6].

In [7] tapered H-shaped ground technique which is presented in Figure 1- 7 is used to reduce the thickness of the magneto-electric dipole antenna from 0.25λ to 0.11λ . This antenna can be easily fabricated using the multi-layer printed circuit board (PCB) technology. This substrate integrated magneto-electric dipole antenna has an impedance bandwidth 18.74% for $VSWR \leq 2$ and 6.8 dBi maximum gain. The bandwidth of the antenna is significantly decreased due to the reduction in the height of the antenna.

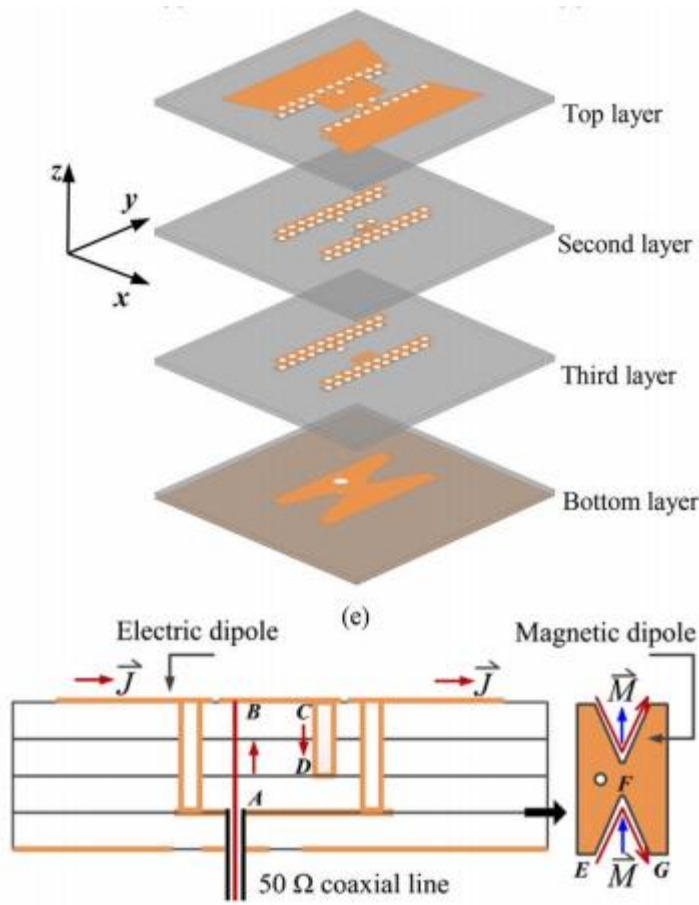


Figure 1- 7 Magneto-Electric Dipole Antenna with Tapered H-Shaped Ground [7]

1.2 Ultra-Wideband (UWB) Frequency Band

There are several studies in UWB communications area. In general, UWB studies focus on 3 GHz to 10 GHz frequency band.

As shown in Figure 1- 8 and Figure 1- 9, in [8] differential and multi-layer feeding structure is used in this design. This differential fed magneto-electric dipole antenna has a rectangular cavity, instead of the normal ground plane to realize unified gain. This antenna has flat gain of around 9 dBi for whole operating frequency band and large impedance bandwidth which is 111.4% for VSWR<2.

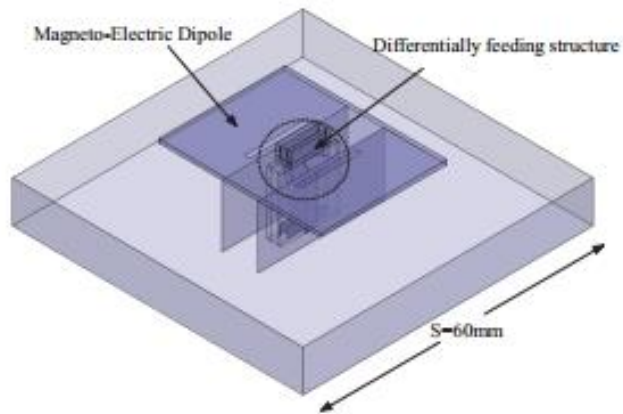


Figure 1- 8 Magneto-Electric Dipole Antenna with Differential and Multi-Layer Feed [8]

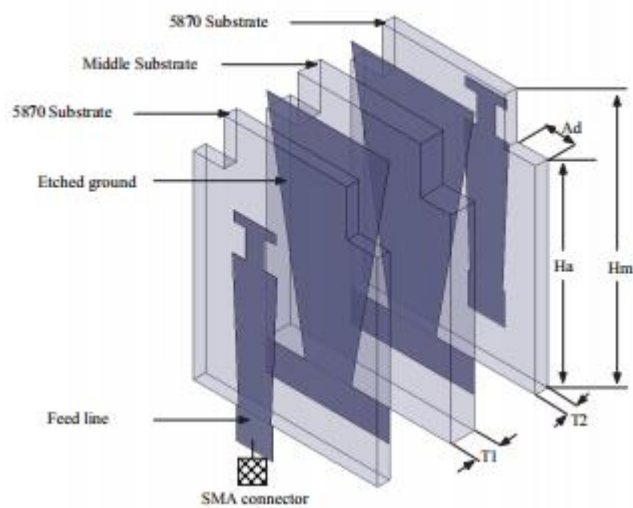


Figure 1- 9 Differential and Multi-Layer Feeding Structure of the Magneto-Electric Dipole Antenna [8]

In [9] bowtie structure which is presented in Figure 1- 10 is used as an electric dipole because of its wideband characteristic. A vertically-oriented folded patch antenna is used as a magnetic dipole. A rectangular cavity is placed to decrease the back

radiation and provide flat antenna gain up to the high frequency end of the bandwidth.

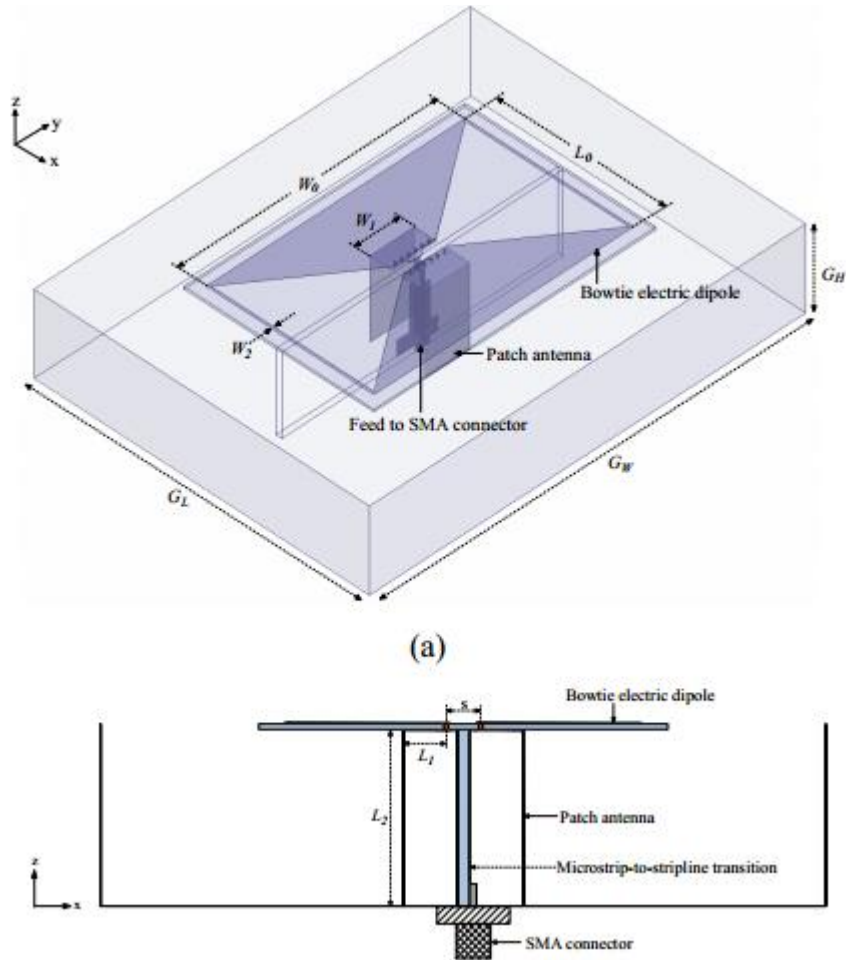


Figure 1- 10 Magneto-Electric Dipole Antenna with Bow-Tie Structure [9]

Microstrip-to-parallel-plate waveguide transition which is presented in Figure 1- 11 is used to excite simultaneously electric and magnetic dipole. This antenna has 110% impedance bandwidth, 9.9 dBi average gain and unidirectional radiation patterns with low cross polarization and low back radiation. [9].

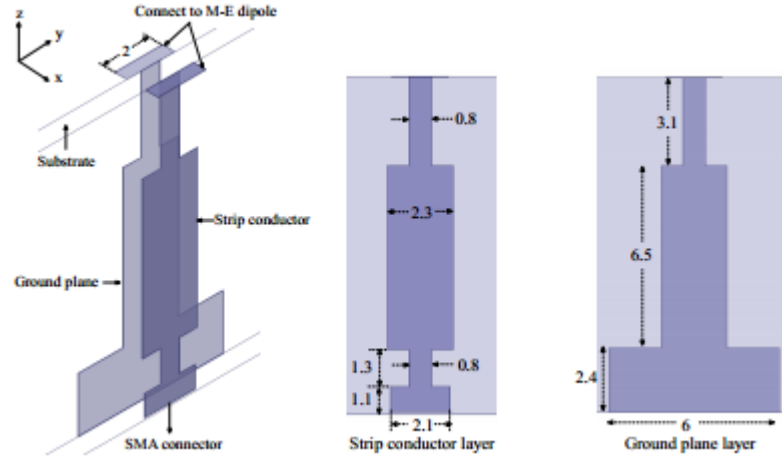


Figure 1- 11 Microstrip to Parallel Plate Feeding Mechanism [9]

1.3 Millimeter Wave Band

The millimeter-wave region of the electromagnetic spectrum is usually considered to be the range of wavelengths from 10 millimeters to 1 millimeters. The millimeter-wave region of the electromagnetic spectrum corresponds to radio band frequencies of 30 GHz to 300 GHz and is sometimes called the Extremely High Frequency (EHF) range. Usually millimeter wave studies focus on from 40 to 75 GHz frequency bands.

In [10] a planar dipole is used as an electric dipole. Three metallic vias which are shown in Figure 1- 12, act as the side walls of the vertically oriented quarter-wavelength patch antenna. T-shaped coupled strip is used to excite both electric and magnetic dipoles. This antenna provides 48% impedance bandwidth from 48 GHz to 75 GHz. The average gain of the antenna is 7.5 dBi.

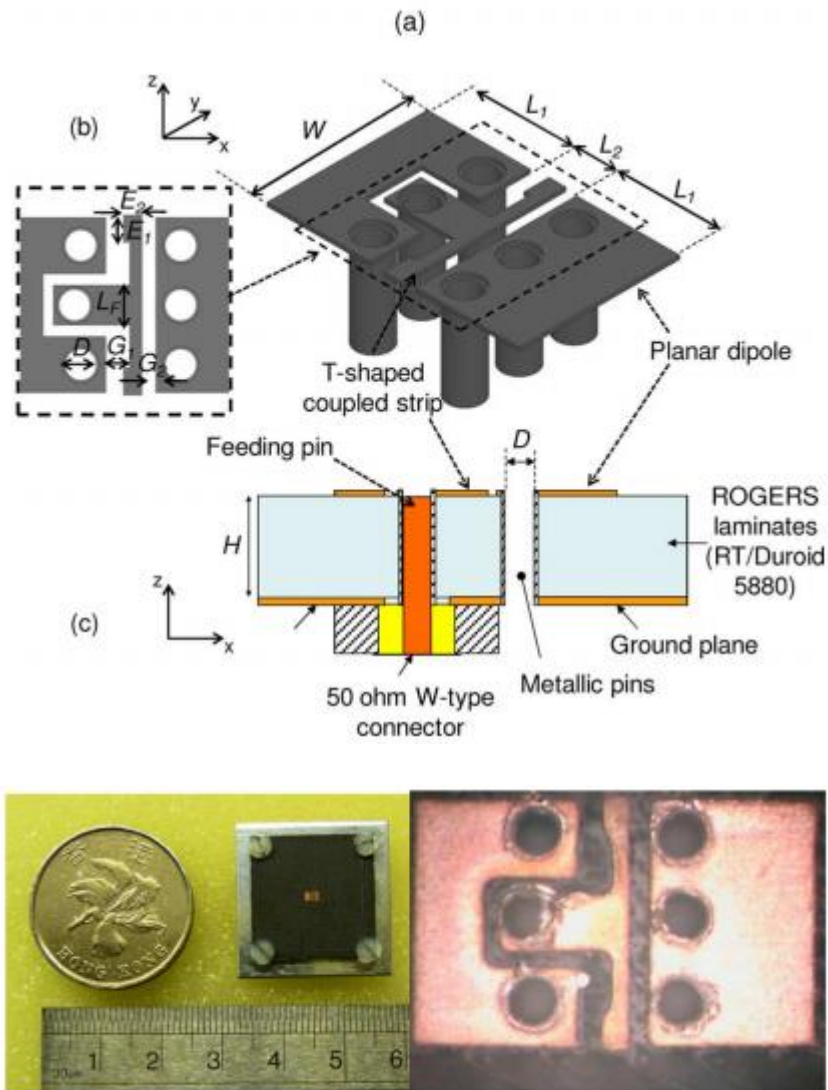


Figure 1- 12 Magneto-Electric Dipole Antenna for Millimeter-Wave Applications-
1 [10]

A similar antenna structure operating in 41.5 – 69.5 GHz band is proposed in [11]. Proposed antenna which is presented in Figure 1- 13 has four metal plates which work as a planar electric dipole. This antenna has also four sets of vias which work as quarter wave shorted patch antenna. L-shaped probe is used to excite the antenna. This antenna has impedance bandwidth of 51% and 8 dBi gain.

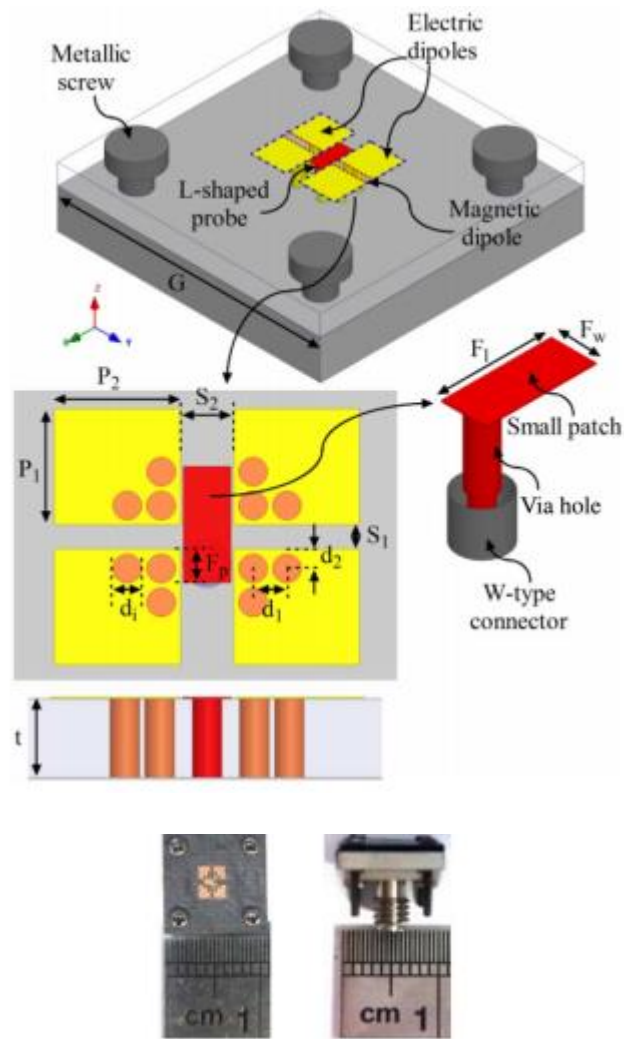


Figure 1- 13 Magneto- Electric Antenna for Millimeter Wave Applications-2 [11]

So far, single polarized magneto-electric dipole antennas are presented. There are also dual polarized magneto-electric dipole antennas which are designed and presented in the literature.

As shown in Figure 1- 14 two orthogonal Γ -shaped strip feed are used in [12] to excite two polarization. The isolation is a very critical parameter for dual polarized antennas. In order to reduce the coupling, different heights are assigned to two orthogonal Γ -shaped strip feeds. This antenna has 67% impedance bandwidth, 9 dBi maximum gain and 36 dB isolation between ports [12].

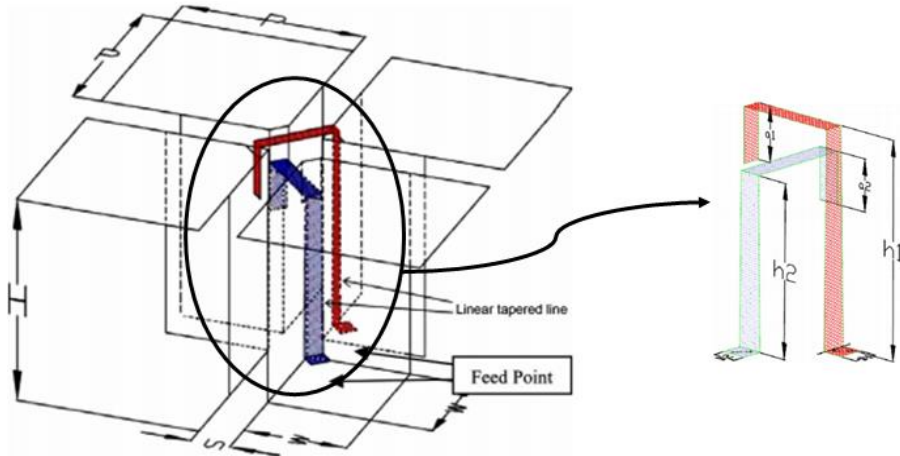


Figure 1- 14 Magneto-Electric Dipole Antenna with Dual-Polarization [12]

A similar design is proposed in [13]. Two Γ -shaped strips are orthogonally placed in the gaps between the metallic posts as shown in Figure 1- 15. This antenna has 48% impedance bandwidth and 36 dB isolation between the ports, with maximum broadside gain of about 9.3 dBi.

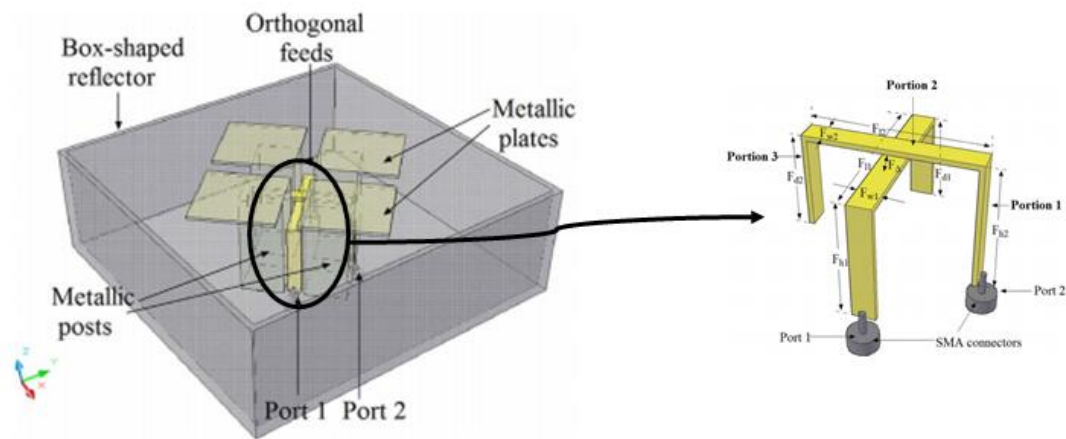


Figure 1- 15 Magneto-Electric Dipole Antenna with Box-Shaped Reflector [13]

1.4 Organization of the Thesis

As summarized in the previous section, different magneto-electric dipole antenna designs are presented in literature. The aim of this thesis is to understand the operation of the magneto-electric dipole antenna and to study the effect of the design parameters on the performance of the antenna through full wave electromagnetic simulations performed in Ansys HFSS [14]. Moreover based on these analysis a magneto-electric dipole antenna is designed to operate in the UWB (3.3 GHz to 10 GHz).

In Chapter 2, the design parameters for the magneto-electric dipole antenna are defined. Parametric analyses of the magneto-electric dipole antenna are presented. Based on the results of these analyses, radiation mechanism and operation principle of the antenna are explained. By using the experience gained through the parametric analyses, an antenna operating in 3.3 - 10 GHz band is designed.

After the optimization of the design parameters, the differential fed magneto-electric dipole antenna with cavity is fabricated and measured. This fabrication process and evaluation of the measurement results are presented in Chapter 3. Comparisons of the measurement and the simulation results are also discussed in Chapter 3.

In the last chapter of the thesis, possible future work and concluding remarks about the magneto-electric dipole antenna and its feeding structure are given.

CHAPTER 2

DESIGN OF THE MAGNETO-ELECTRIC DIPOLE ANTENNA

2.1 Parametric Analysis of the Magneto-Electric Dipole Antenna

To understand the operation of the magneto-electric dipole antenna and to investigate the effects of antenna parameters on the radiation characteristics of the antenna, an example from the literature is chosen and analyzed with Ansys HFSS [14]. The geometry of the Γ -shaped strip fed magneto-electric dipole antenna and the antenna parameters are shown in Figure 2- 1. The antenna parameter values reported in [2] are listed in Table 2- 1, and they are considered as the nominal values. The parametric analysis is performed around these nominal values.

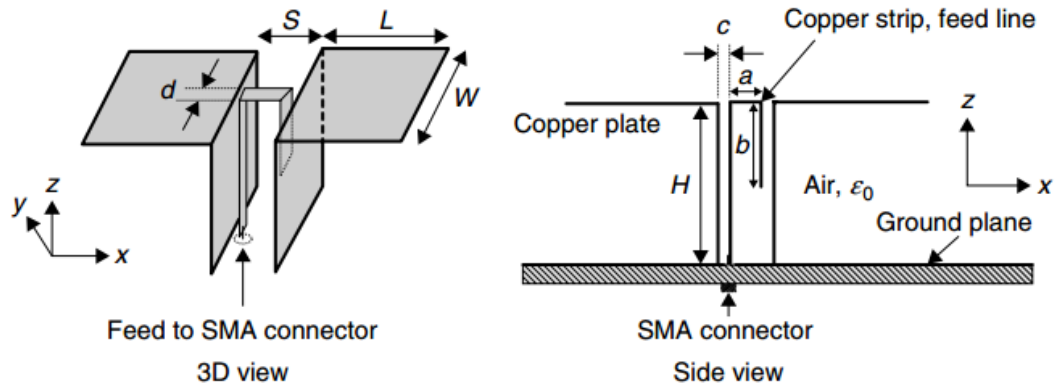


Figure 2- 1 Structure of the Gamma-Shaped Strip Fed Magneto-Electric Dipole Antenna [4]

Table 2- 1 Nominal Values of the Gamma-Shaped Strip Fed Magneto-Electric Dipole Antenna

Name of the Parameter	Nominal Value
S	17 mm
W	60 mm
L	30 mm
H	30 mm
d(FeedW)	4.91 mm
a(Feed2L)	9.5 mm
b(Feed3H)	22 mm

The first portion of the Γ -shaped feed, which is vertically oriented, is in contact with the inner conductor of the coaxial launcher mounted below the grounded plane. This portion, together with the nearest vertical conductor of the antenna, works as microstrip line and connects coaxial launcher to the second portion of the feeding structure. Excitation of the planar dipole and the shorted patch is achieved by the second portion of the feed. The third portion of the feed structure has the length 'b' as shown in Figure 2- 1. This part exhibits a capacitive reactance due to its interaction with the closest vertical conductor of the antenna. This capacitive reactance compensates for the inductive reactance introduced by the first part of the feed structure. While 'd', 'a', 'b' parameters are used in Figure 2- 1 to denote the dimensions of the feed, 'FeedW', 'Feed2L' and 'Feed3H' parameters are preferred in HFSS simulations since this kind of nomenclature makes it easier to remember.

In order to perform parametric analysis of the Γ -shaped strip fed magneto-electric dipole antenna, parameter sweep tool of HFSS is used. During the parametric studies, one of the parameters is changed, and all other parameters are kept constant at their nominal values which are listed in Table 2- 1.

Simulation results with the nominal values for the input impedance, for the input return loss and for the gain are presented in Figure 2- 2, Figure 2- 3 and Figure 2- 4, respectively. Three local minimums are observed in the return loss characteristics around 1.4 GHz, 2 GHz and 2.7 GHz. Although the imaginary part of the input impedance is not zero at these frequencies, these local minima points will be denoted as “resonance points” for the sake of brevity, throughout this thesis. The results reported in [2] are almost same with the results presented in Figure 2- 3 and Figure 2- 4. The impedance bandwidth of the antenna (return loss ≤ -10 dB), is 42%. The gain bandwidth of the antenna (gain variation less than 1 dB) is 74%.

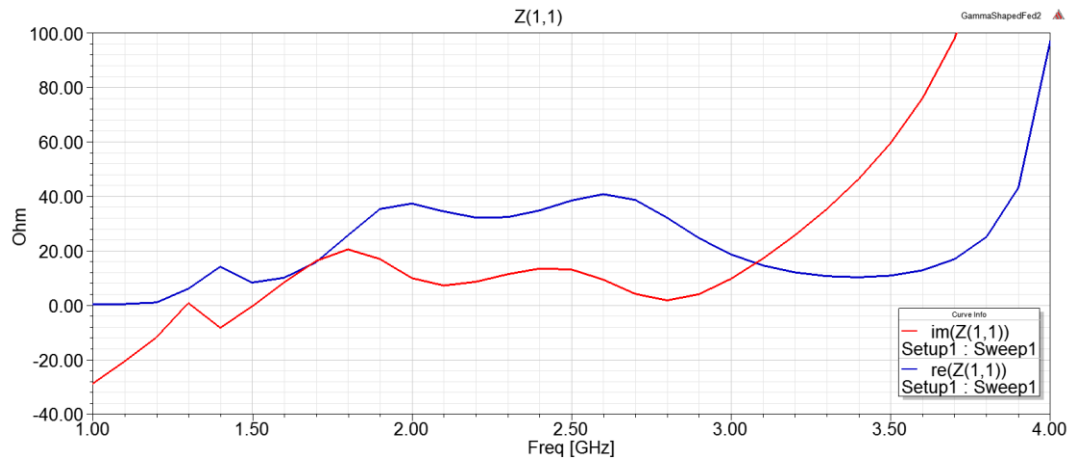


Figure 2- 2 Input Impedance of the Gamma-Shaped Strip Fed Magneto-Electric Dipole Antenna with Nominal Values

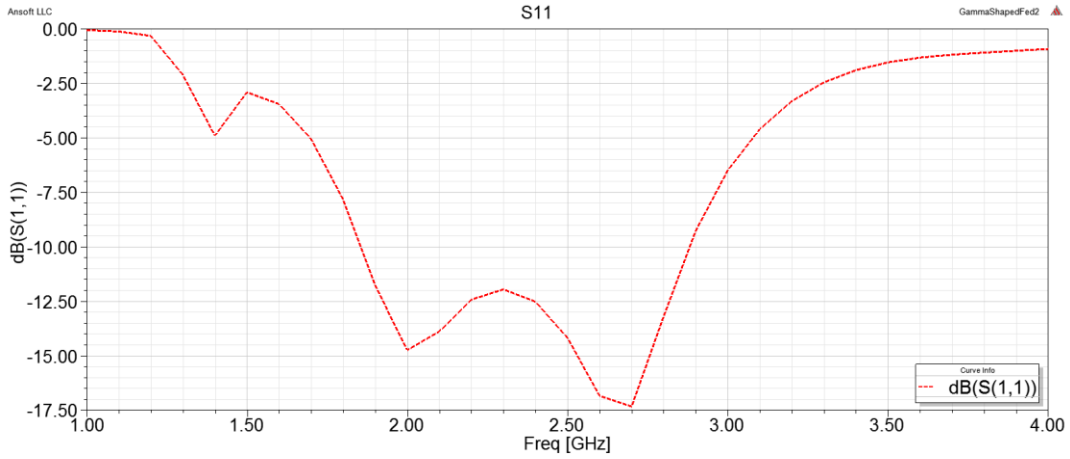


Figure 2- 3 Return Loss of the Gamma-Shaped Strip Fed Magneto-Electric Dipole Antenna with Nominal Values

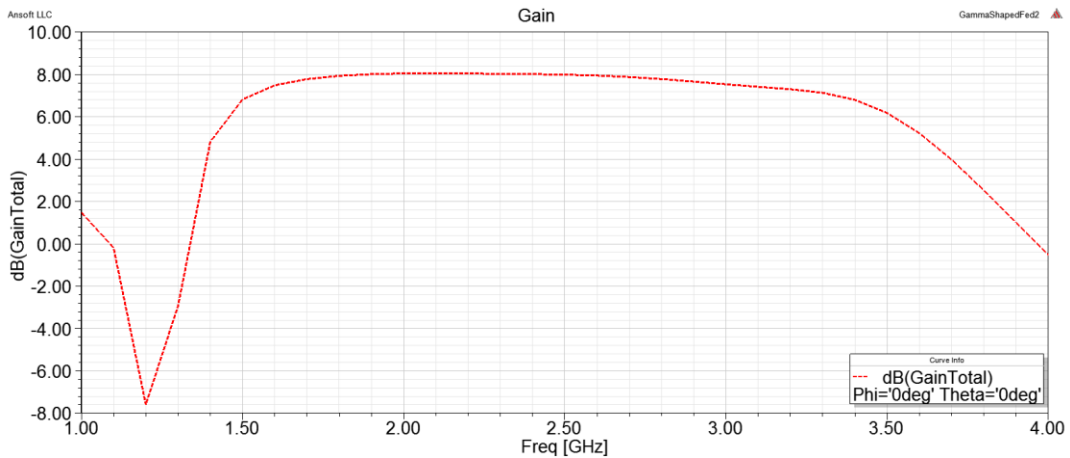


Figure 2- 4 Gain of the Gamma-Shaped Strip Fed Magneto-Electric Dipole Antenna with Nominal Values

Before analyzing the effects of the parameters of the feeding structure, parametric analysis for the length, width and height of the magneto-electric dipole antenna are performed. Nominal value of the length is $L = 30$ mm. Values of 26 mm, 28 mm, 32 mm and 34 mm are studied to observe the effect of the length on the radiation characteristic of the antenna. The return loss results presented in Figure 2- 5 demonstrate that the second resonance of the antenna is due to electric dipole since

the length of the antenna is effective in adjusting the location of this resonance. It can be observed that when the length of the magneto-electric dipole antenna decreases, the frequency of the second resonance shifts to higher frequencies. In contrast, the first and the third resonant frequencies are insensitive to the variations in the length of the antenna. The antenna gain results presented in Figure 2- 6 show that the length of the antenna is effective in determining the low frequency end of the gain bandwidth.

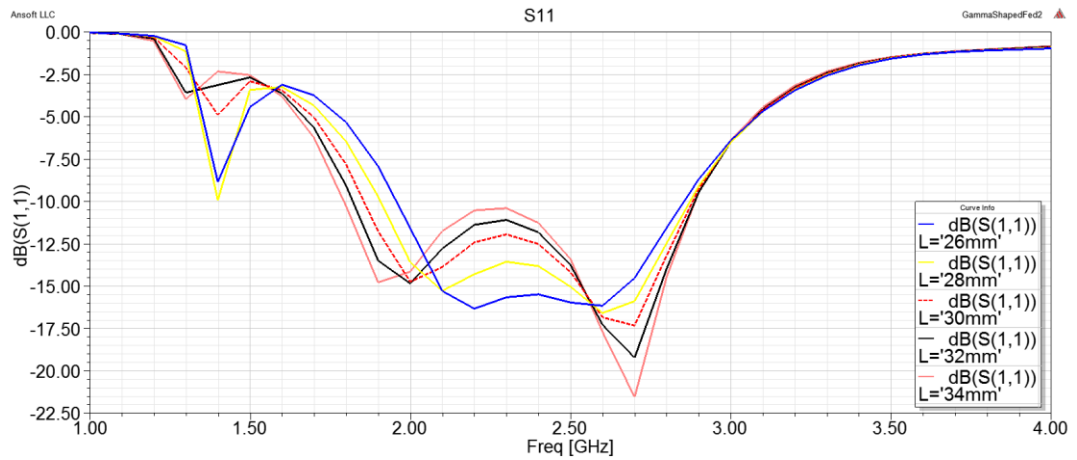


Figure 2- 5 Return Loss of the Gamma-Shaped Strip Fed Magneto-Electric Dipole Antenna with L Sweep

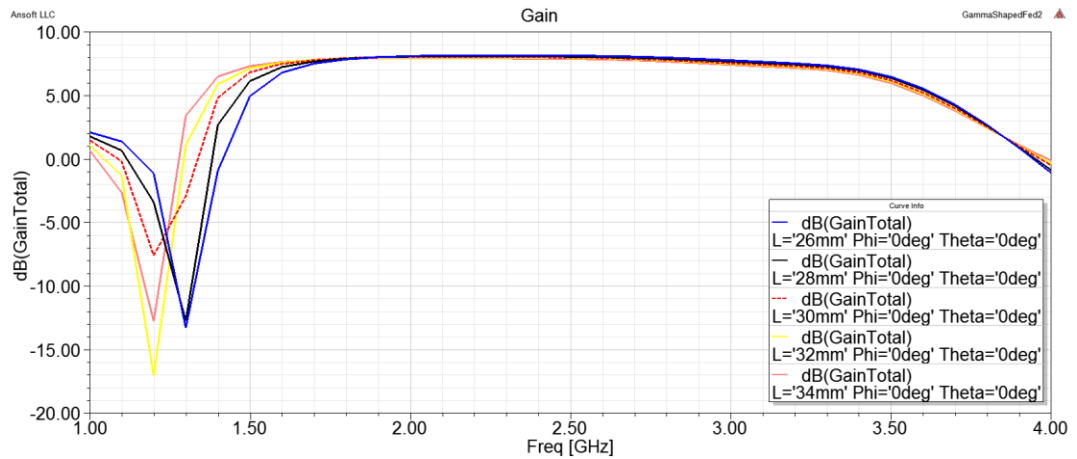


Figure 2- 6 Gain of the Gamma-Shaped Strip Fed Magneto-Electric Dipole Antenna with L Sweep

Nominal value of the width is $W = 60$ mm. Values of 40 mm, 50 mm, 70 mm and 80 mm have been studied to obtain the effect of the width and simulation results for input return loss and gain are presented in Figure 2- 7 and Figure 2- 8, respectively. It can be observed that when the width of the magneto-electric dipole antenna decreases the frequency of the third resonance shifts to higher frequencies. In contrast, the first and the second resonant frequencies are insensitive to the variations in the width of the antenna. Note that width of the antenna is the length of the magnetic dipole. Hence it may be concluded that the third resonance of the antenna is due to magnetic dipole. The gain results show that the width of the antenna is effective at the high frequency end of the gain bandwidth.

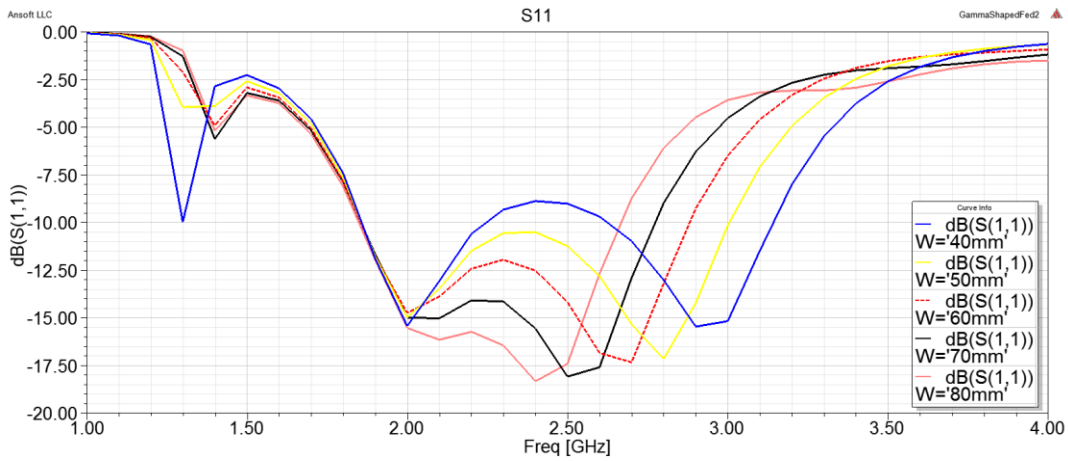


Figure 2- 7 Return Loss of the Gamma-Shaped Strip Fed Magneto-Electric Dipole Antenna with W Sweep

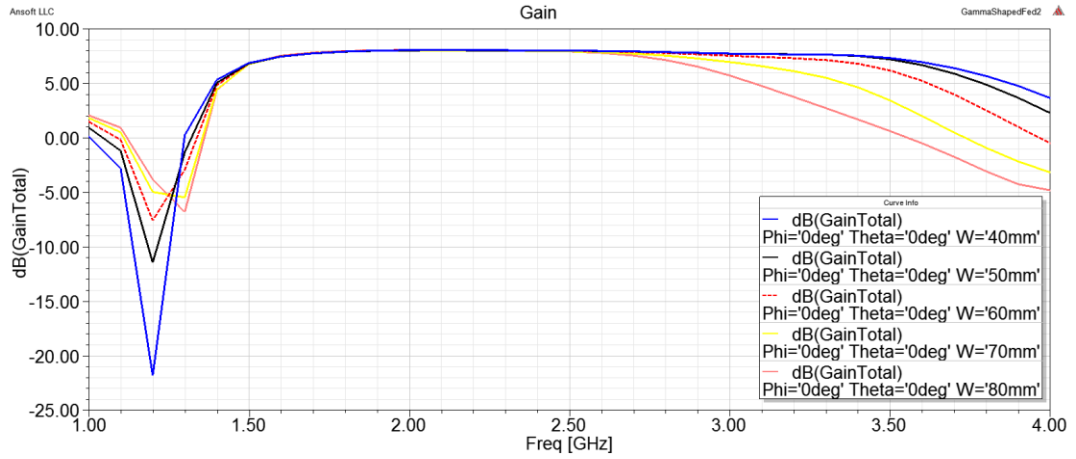


Figure 2- 8 Gain of the Gamma-Shaped Strip Fed Magneto-Electric Dipole Antenna with W Sweep

As revealed by the simulation results presented in Figure 2- 5 and Figure 2- 7, the second resonance is formed by the electric dipole and the third resonance is formed by the magnetic dipole.

The nominal value for height of the antenna is $H = 30$ mm. Values of 25 mm and 35 mm have been studied to observe the effect of the height variations. The simulation results for the input return loss and gain are presented in Figure 2- 9 and Figure 2- 10, respectively. The height of the magneto-electric dipole antenna is very effective on the return loss and the bandwidth. As the height of the antenna decreases, the dominance of the electric dipole antenna decreases, and the dominance of the magnetic dipole increases. Therefore, this value must be adjusted in order to excite with the planar dipole and the shorted patch antenna, equally. The antenna gain results indicate that, the height of the magneto-electric dipole antenna must be adjusted to achieve wideband and flat gain. 30 mm provides the largest bandwidth.

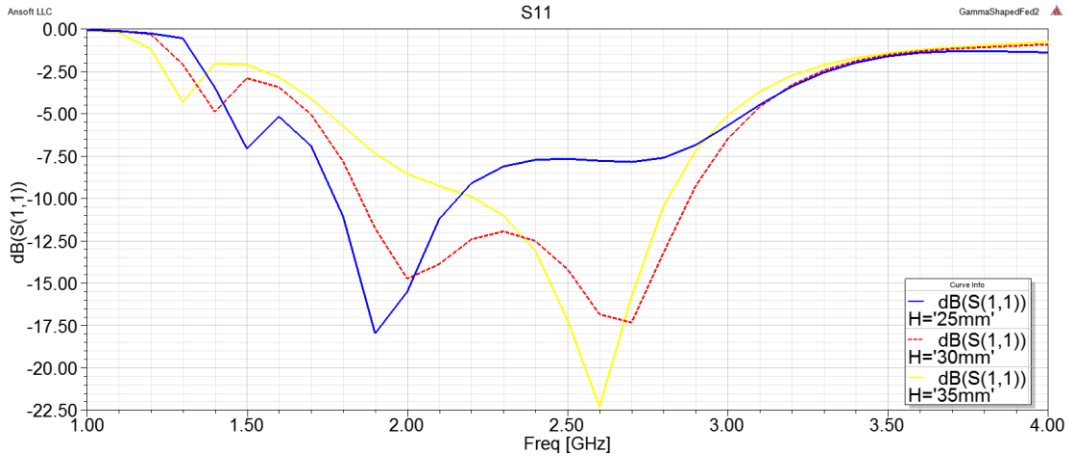


Figure 2- 9 Return Loss of the Gamma-Shaped Strip Fed Magneto-Electric Dipole Antenna with H Sweep

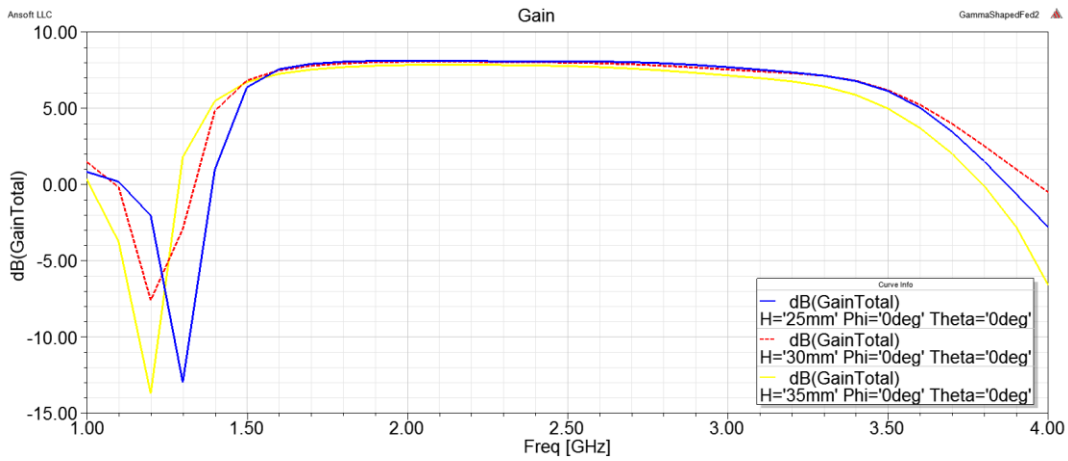


Figure 2- 10 Gain of the Gamma-Shaped Strip Fed Magneto-Electric Dipole Antenna with H Sweep

The analysis of the parameters of the feed structure starts with the length of the second portion of the feeding strip (dimension 'a' in Figure 2- 1). It has 9.5 mm nominal value. Values of 5.5 mm, 7.5 mm and 11.5 mm have been studied to observe the effect of this portion. Simulation results for the input return loss and gain are presented in Figure 2- 11 and Figure 2- 12, respectively. At first glance the results show that the length of the second portion is very effective on the return loss and the

bandwidth of the magneto-electric dipole antenna. If the length of the second portion is very short, then the planar dipole antenna is not excited. On the other hand, magnetic dipole is slightly excited when the length of this portion is too long. The antenna gain results indicate that the length of the second portion of the feeding strip has no effect on the gain of the antenna.

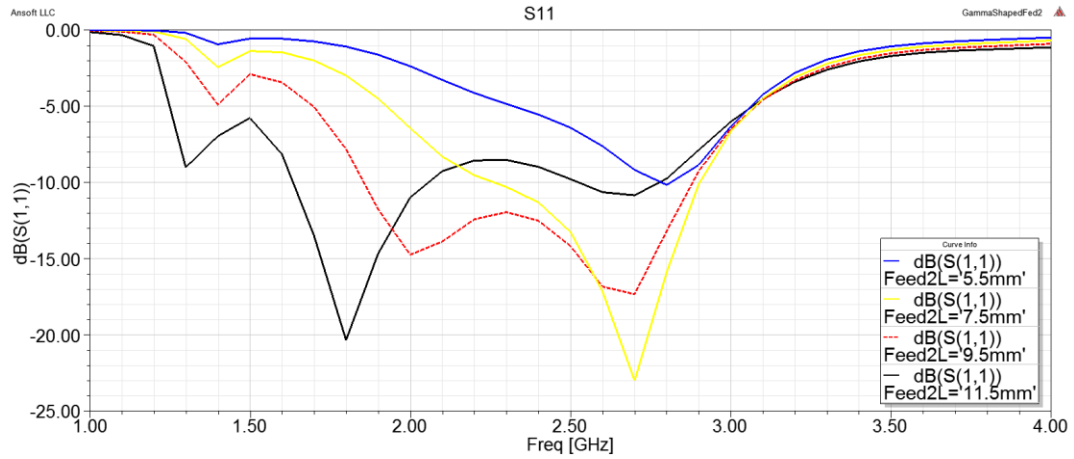


Figure 2- 11 Return Loss of the Gamma-Shaped Strip Fed Magneto-Electric Dipole Antenna with Feed2L Sweep

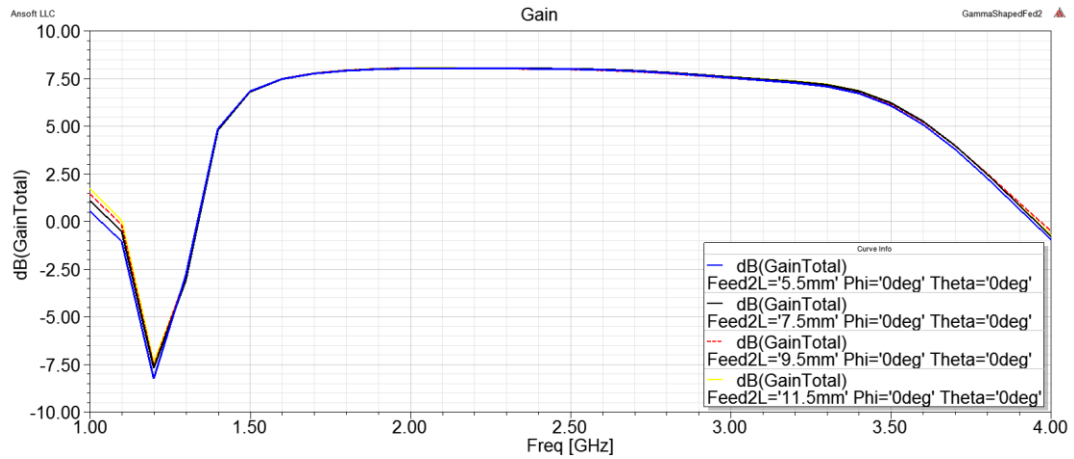


Figure 2- 12 Gain of the Gamma-Shaped Strip Fed Magneto-Electric Dipole Antenna with Feed2L Sweep

Next, the height of the third portion of the feeding strip (dimension ‘b’ in Figure 2-1) is changed, and the simulation results for the input return loss and gain are presented in Figure 2-13 and Figure 2-14, respectively. This portion has 22 mm nominal value. Values of 18 mm, 20 mm and 24 mm have been studied to obtain the effect of this portion and the results of this effect were observed. According to the input return loss results, it can be observed that the height of the third portion of the feeding strip has a significant effect on the coupling levels of the electric and magnetic dipoles. While the electric dipole is more dominantly excited with larger height values, the magnetic dipole is excited more dominantly with smaller height values. Thus, this parameter should be selected carefully to excite both dipoles equally. The antenna gain results show that the height of the third portion of the feeding strip has no effect on the gain of the antenna.

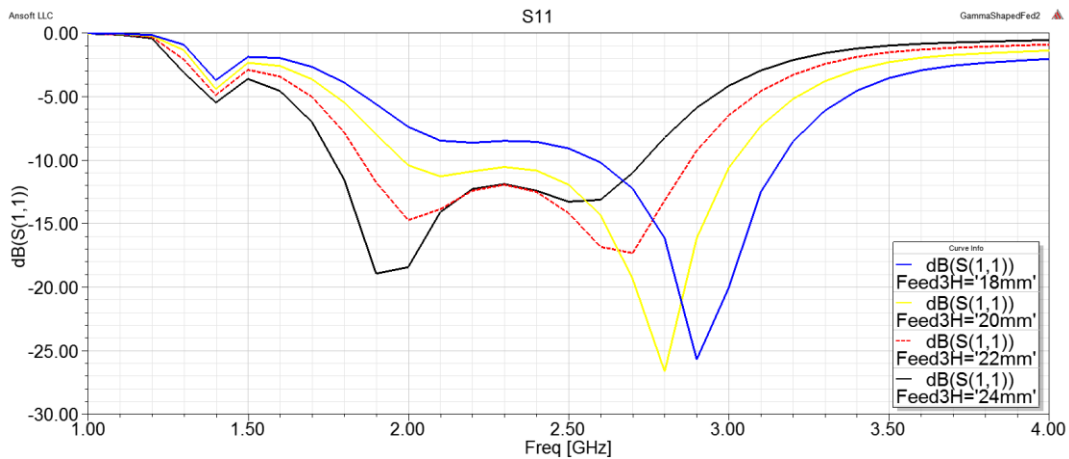


Figure 2- 13 Return Loss of the Gamma-Shaped Strip Fed Magneto-Electric Dipole Antenna with Feed3H Sweep

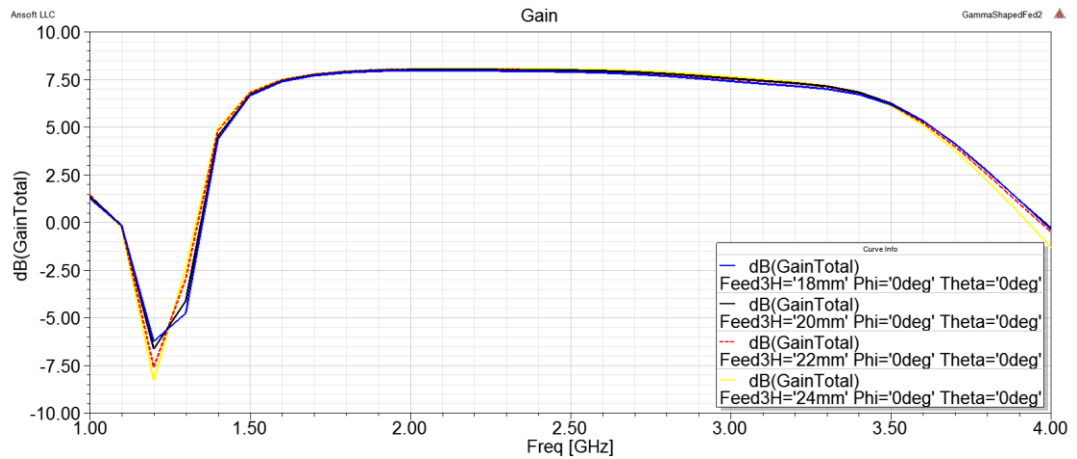


Figure 2- 14 Gain of the Gamma-Shaped Strip Fed Magneto-Electric Dipole Antenna with Feed3H Sweep

The last parametric analysis of the feeding strip is the width of the feeding structure (dimension 'd' in Figure 2- 1). The width of the feeding strip is changed, and the simulation results for the input return loss and gain are presented in Figure 2- 15 and Figure 2- 16, respectively. This portion has 4.91 mm nominal value. Values of 3 mm, 4 mm and 5 mm have been studied to obtain the effect of this portion and the results of this effect were observed. A first glimpse of the results show that the width of the feeding strip is slightly effective on the return loss characteristics of the magneto-electric dipole antenna. The width of the feeding strip also has some effect on coupling levels of electric and magnetic dipoles. The gain results show that the width of the feeding strip has no effect on the gain of the antenna.

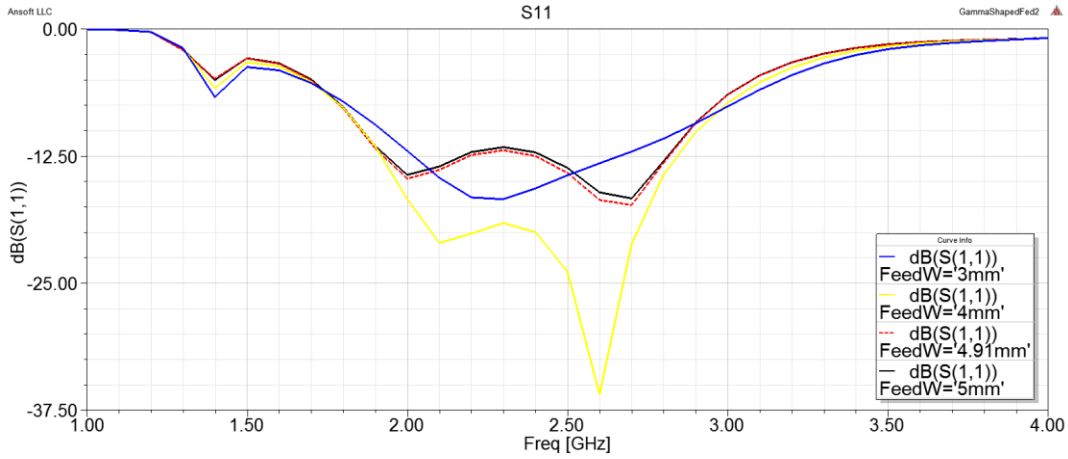


Figure 2- 15 Return Loss of the Gamma-Shaped Strip Fed Magneto-Electric Dipole Antenna with FeedW Sweep

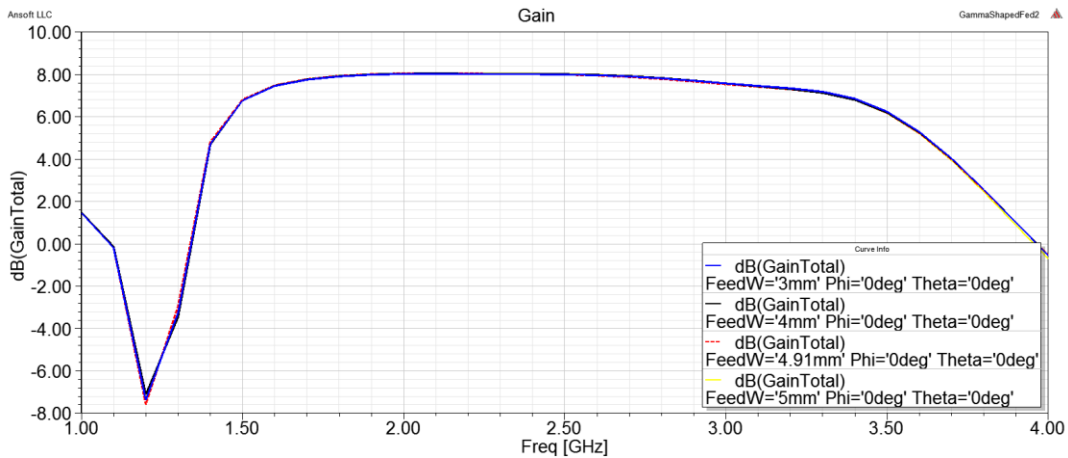


Figure 2- 16 Gain of the Gamma-Shaped Strip Fed Magneto-Electric Dipole Antenna with FeedW Sweep

After completing the parametric analysis for the gamma-shaped strip fed magneto-electric dipole antenna, the input return loss results reveal that the gamma shaped feeding structure doesn't provide ultra-wideband characteristic. Thus, differential feeding structure instead of the gamma shaped feeding structure is considered to achieve ultra-wideband antenna with a flat gain and stable radiation characteristics.

2.2 Design of the Differential Fed Magneto-Electric Dipole Antenna

By using the experience gained through the parametric analysis, an antenna operating in 3-10 GHz band with flat gain and stable radiation characteristics will be designed. An antenna operating with 92% bandwidth is proposed in [6] by using differential feeding. The top and side views of the differential fed magneto-electric dipole antenna are presented in Figure 2- 17 and Figure 2- 18, respectively. As the name implies (differential fed), Port 1 and Port 2 are excited out of phase.

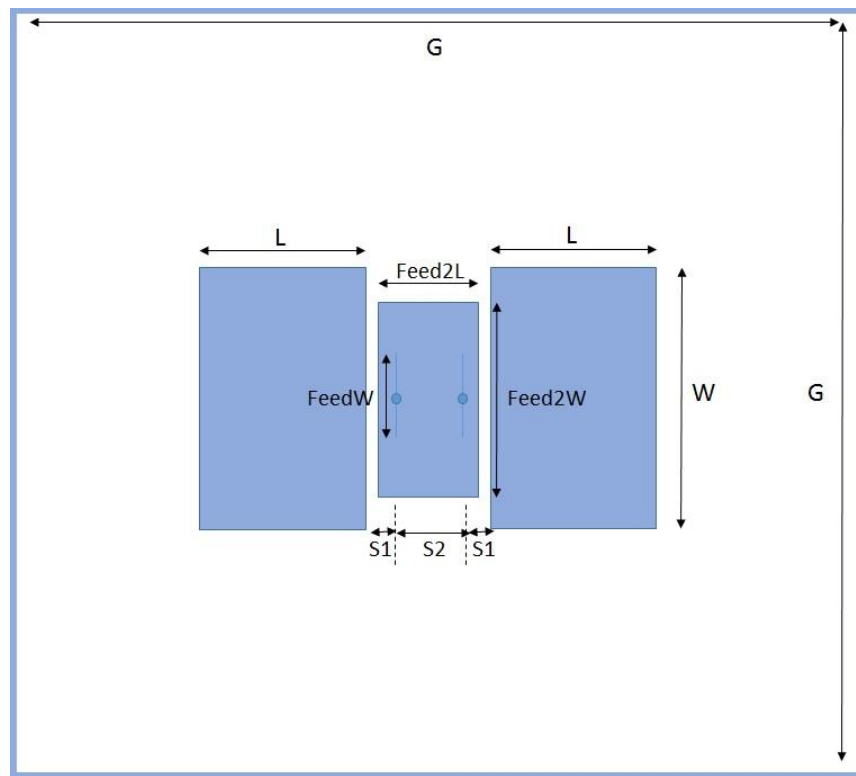


Figure 2- 17 HFSS Model of the Differential Fed Magneto-Electric Dipole Antenna (Top View)

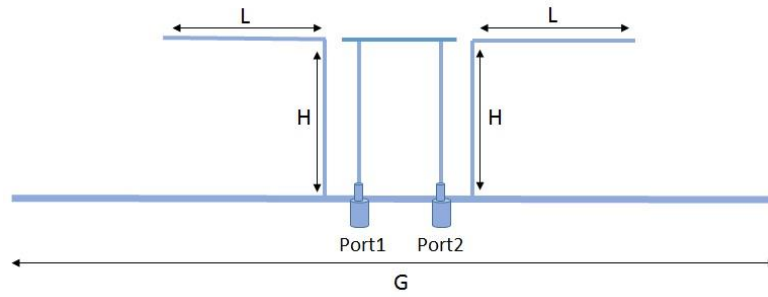


Figure 2- 18 HFSS Model of the Differential Fed Magneto-Electric Dipole Antenna (Side View)

This antenna proposed in [6] operates between 0.8-2.16 GHz. The antenna that will be designed in this thesis is specified to operate between 3-10 GHz. Hence the dimensions reported in [6] are divided by 4 to obtain a good starting point for the design of the antenna. This starting point values are listed in Table 2- 2. HFSS simulations provide the s-parameters (S_{11} , S_{12} , S_{21} , S_{22}) of the basic two port antenna.

Table 2- 2 Parameter Values of the Differential Fed Magneto-Electric Dipole Antenna

Name of the Parameter in HFSS	Nominal Value
S1	1.7875 mm
S2	6.425 mm
W	26 mm
L	12 mm
H	12.5 mm
FeedW	8 mm
Feed2L	6.425 mm
Feed2W	17.5 mm

In a two-port circuit, where the variables a_1 and a_2 represent the incident waves, and b_1 and b_2 represent the reflected waves, the following relation can be written in terms of scattering parameters:

$$\begin{bmatrix} b_1 \\ b_2 \end{bmatrix} = S_{sm} \begin{bmatrix} a_1 \\ a_2 \end{bmatrix} \quad (2.1)$$

Where S_{sm} represents the single mode scattering parameters of the basic two port network as:

$$S_{sm} = \begin{bmatrix} S_{11} & S_{12} \\ S_{21} & S_{22} \end{bmatrix} \quad (2.2)$$

The differential two port network model has two modes of propagation: common mode and differential mode. For both modes, incident waves a_c and a_d and reflected waves b_c and b_d are defined in equation (2.3) and (2.4).

$$a_c = \frac{1}{\sqrt{2}} \times (a_1 + a_2) \text{ and } b_c = \frac{1}{\sqrt{2}} \times (b_1 + b_2) \quad (2.3)$$

$$a_d = \frac{1}{\sqrt{2}} \times (a_1 - a_2) \text{ and } b_d = \frac{1}{\sqrt{2}} \times (b_1 - b_2) \quad (2.4)$$

If a transformation matrix M is defined as:

$$M = \frac{1}{\sqrt{2}} \begin{bmatrix} 1 & -1 \\ 1 & 1 \end{bmatrix} \quad (2.5)$$

Then common mode and differential mode incident and reflected waves can be written as:

$$\begin{bmatrix} b_d \\ b_c \end{bmatrix} = M \begin{bmatrix} b_1 \\ b_2 \end{bmatrix} \text{ and } \begin{bmatrix} a_d \\ a_c \end{bmatrix} = M \begin{bmatrix} a_1 \\ a_2 \end{bmatrix} \quad (2.6)$$

Mixed mode S-parameters are defined by:

$$S_{mm} = \begin{bmatrix} S_{dd} & S_{cd} \\ S_{dc} & S_{cc} \end{bmatrix} \text{ and } \begin{bmatrix} b_d \\ b_c \end{bmatrix} = S_{mm} \begin{bmatrix} a_d \\ a_c \end{bmatrix} \quad (2.7)$$

Bockelman et. al. [15] demonstrate that mixed mode parameters can be derived from single mode parameters:

$$S_{mm} = MS_{sm}M^{-1} \quad (2.8)$$

Hence, S_{mm} can be redefined as:

$$S_{mm} = \frac{1}{2} \begin{bmatrix} S_{11} - S_{12} - S_{21} + S_{22} & S_{11} + S_{12} - S_{21} + S_{22} \\ S_{11} - S_{12} + S_{21} - S_{22} & S_{11} + S_{12} + S_{21} + S_{22} \end{bmatrix} \quad (2.9)$$

As a result, S-parameter of the differential fed antenna (S_{d11}) can be calculated by using equation (2.10).

$$S_{d11} = \frac{1}{2}(S_{11} - S_{12} - S_{21} + S_{22}) \quad (2.10)$$

From now on, the input return loss of the differential fed antenna will be called as the differential input return loss. Simulation results of the differential input return loss are presented in Figure 2- 19 for the magneto-electric dipole antenna with parameter values listed in Table 2- 2. These results do not meet the design requirements. Hence, some parametric optimization must be applied to the differential fed magneto-electric dipole antenna. During the parametric optimizations, optimized parameters are set to their optimum values during the optimization of the later parameters.

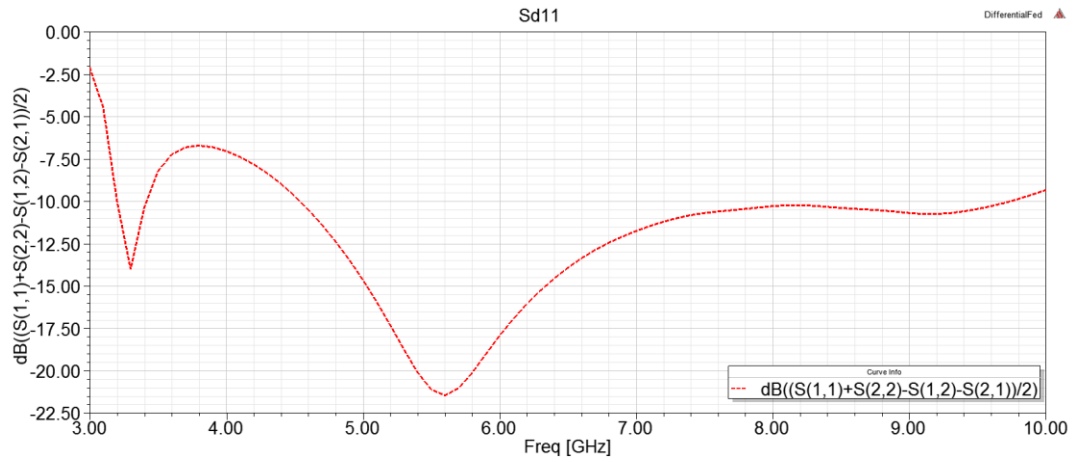


Figure 2- 19 Return Loss of the Differential Fed Magneto-Electric Dipole Antenna with Nominal Values

The first optimization is applied to the Feed2L parameter of the antenna. The length of the second portion of the feeding strip is changed (6.425 mm, 7.425 mm, 8.425 mm and 9.425 mm), and the simulation results for the differential input return loss and gain are presented in Figure 2- 20 and Figure 2- 21, respectively. Feed2L parameter of the feeding strip should be set as 7.425 mm by considering the characteristic around 4 GHz and above 7 GHz. 6.425 mm provides the best performance above 7 GHz, but the return loss at 4 GHz is maximum at this value. Hence, 7.425 mm is evaluated to be the best choice regarding this compromise.

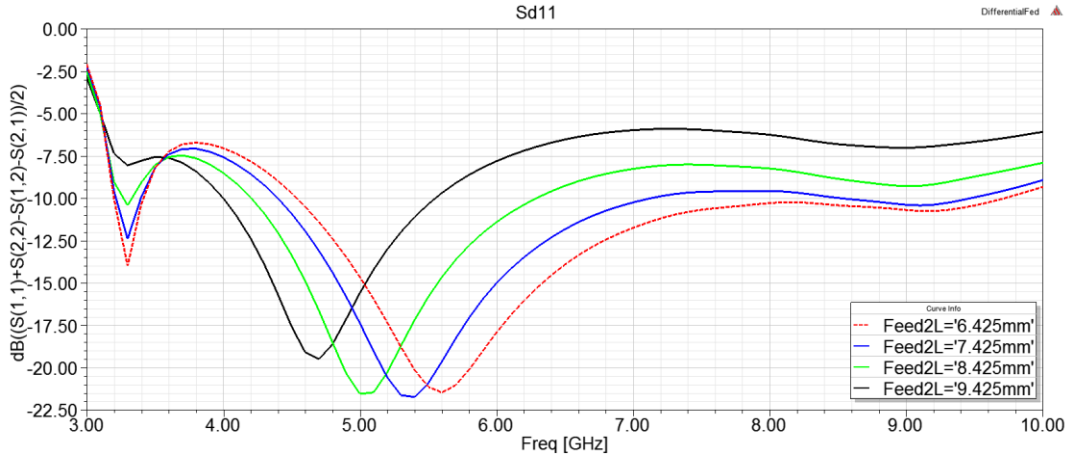


Figure 2- 20 Return Loss of the Differential Fed Magneto-Electric Dipole Antenna with Feed2L Sweep

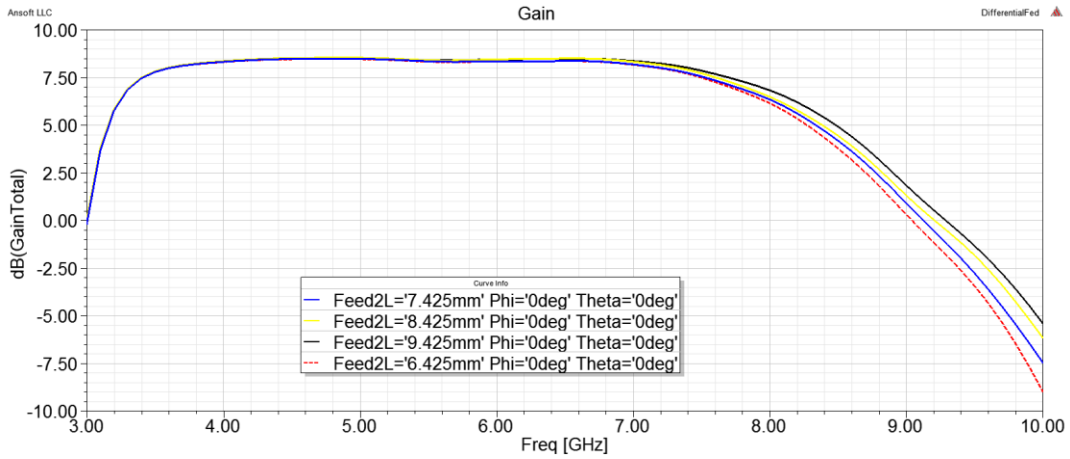


Figure 2- 21 Gain of the Differential Fed Magneto-Electric Dipole Antenna with Feed2L Sweep

The second optimization is applied to the FeedW parameter of the antenna. Simulation results of the differential input return loss and gain are presented in Figure 2- 22 and Figure 2- 23, respectively for different FeedW values (7 mm, 8 mm, 9 mm and 10 mm). It can be observed that the FeedW parameter of the feeding strip should be set as 9 mm. As shown in Figure 2- 24, vertical conductors of the antenna and the

feed forms a microstrip line. By changing FeedW, the characteristic impedance of this line changes. Hence, FeedW effects the matching level of the antenna.

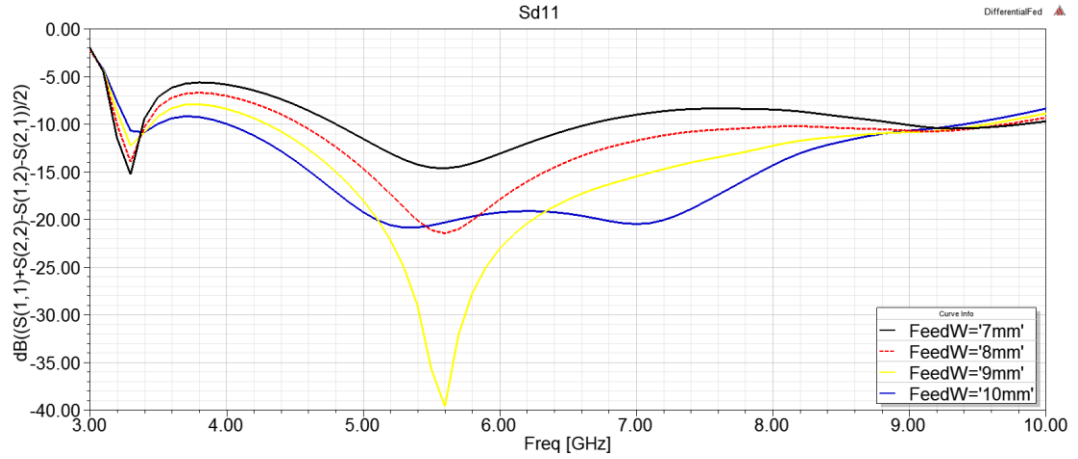


Figure 2- 22 Return Loss of the Differential Fed Magneto-Electric Dipole Antenna with FeedW Sweep

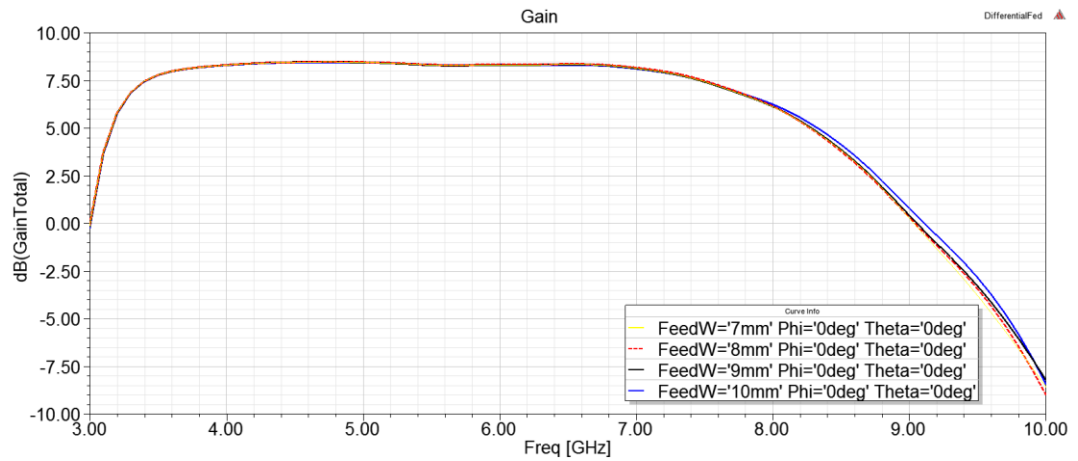


Figure 2- 23 Gain of the Differential Fed Magneto-Electric Dipole Antenna with FeedW Sweep

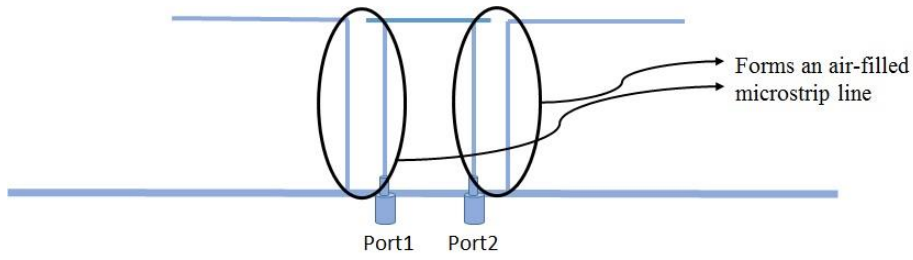


Figure 2- 24 Air-filled Microstrip Line

The third optimization is applied to the Feed2W parameter of the antenna. The Feed2W parameter of the antenna is changed (16.5 mm, 17.5 mm and 18.5 mm), and the simulation results of the differential input return loss and gain are presented in Figure 2- 25 and Figure 2- 26, respectively. The results indicate that this parameter is not very effective so it can be kept at the initial value.

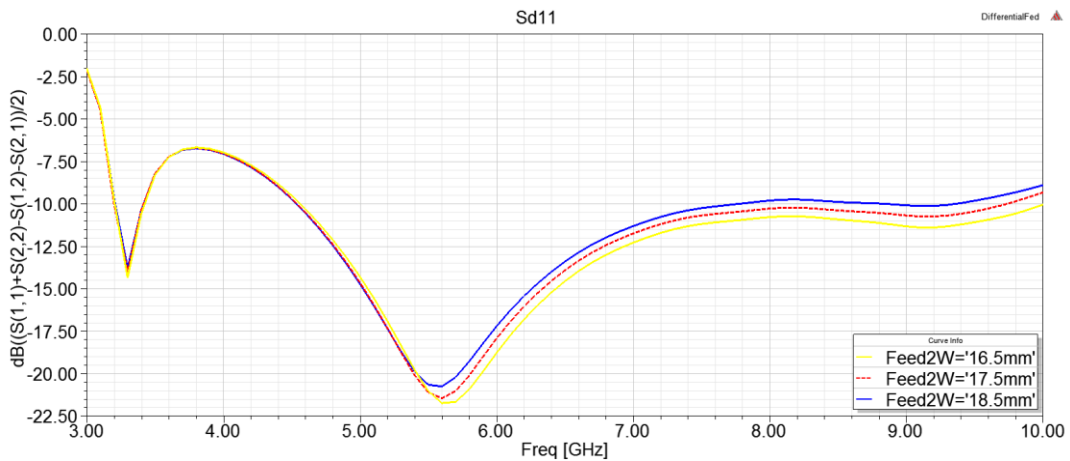


Figure 2- 25 Return Loss of the Differential Fed Magneto-Electric Dipole Antenna with Feed2W Sweep

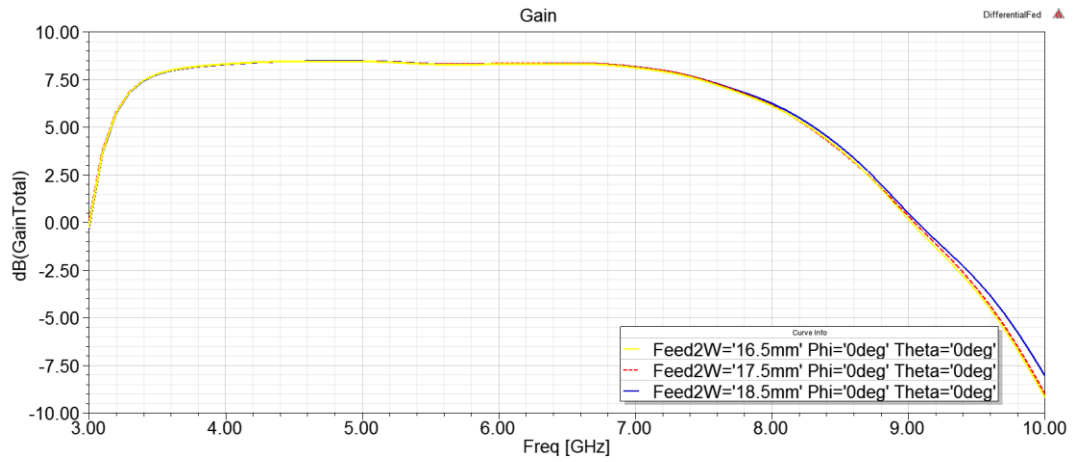


Figure 2- 26 Gain of the Differential Fed Magneto-Electric Dipole Antenna with Feed2W Sweep

The last optimization for the feeding strip is applied to the S1 parameter of the antenna. The S1 parameter of the antenna is changed (1.7875 mm, 2.2875 mm and 2.7875 mm), and the simulation results of the differential input return loss and gain are presented in Figure 2- 27 and Figure 2- 28, respectively. As discussed in Figure 2- 23, S1 also effects the characteristic impedance of the microstrip line formed by the feed and antenna. Therefore, this parameter also changes the matching characteristic of the antenna. It is set at 1.7875 for best performance.

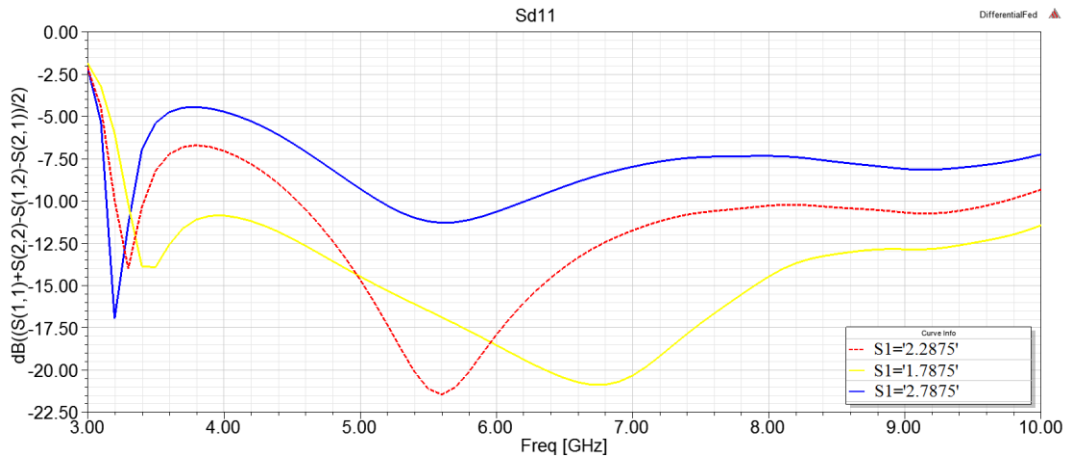


Figure 2- 27 Return Loss of the Differential Fed Magneto-Electric Dipole Antenna with S1 Sweep

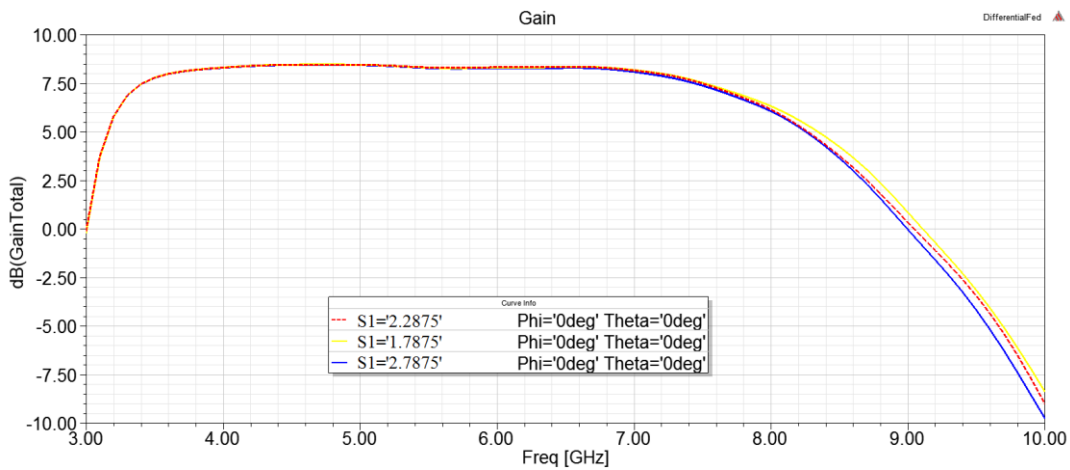


Figure 2- 28 Gain of the Differential Fed Magneto-Electric Dipole Antenna with S1 Sweep

After optimizing the parameters of the feed structure, an acceptable performance is obtained up to 8 GHz. In order to improve the matching of the antenna above 8 GHz, height, width and length parameters are optimized. The optimization is applied to the H parameter of the antenna. The H parameter of the antenna is changed (11.5 mm, 12.5 mm and 13.5 mm), and the simulation results of the differential input return loss and gain are presented in Figure 2- 27 and Figure 2- 28, respectively. The results

indicate that H=12.5 mm provides the best performance within the desired frequency band.

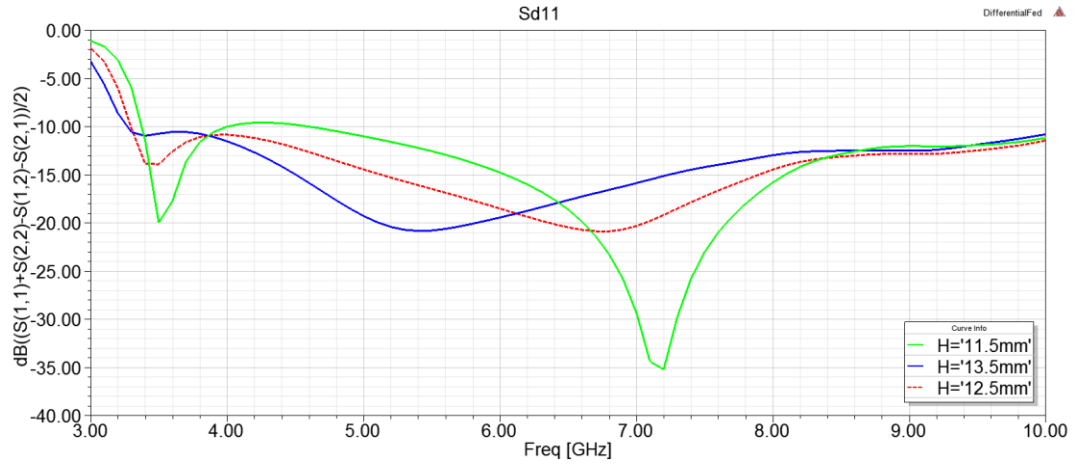


Figure 2- 29 Return Loss of the Differential Fed Magneto-Electric Dipole Antenna with H Sweep

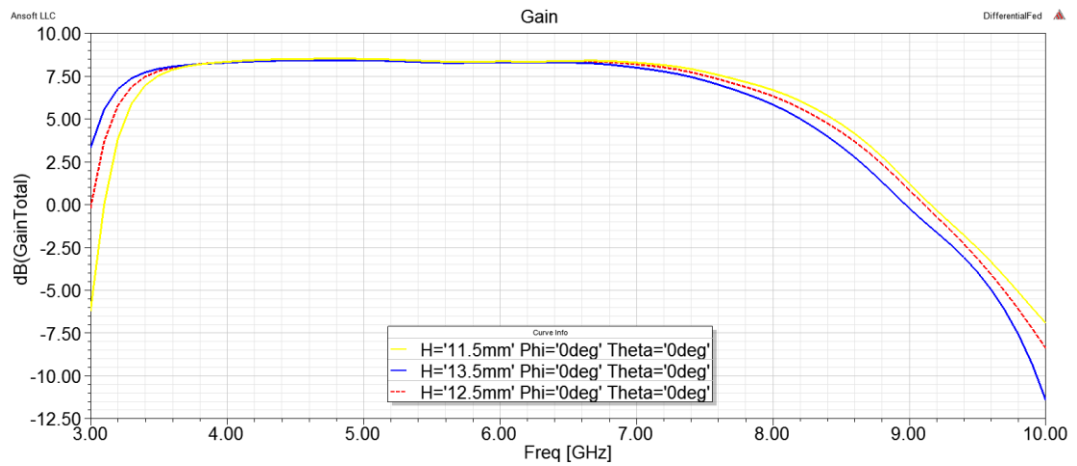


Figure 2- 30 Gain of the Differential Fed Magneto-Electric Dipole Antenna with H Sweep

The optimization is applied to the L parameter of the antenna. The L parameter of the antenna is changed (11 mm, 12 mm and 13 mm), and the simulation results of the differential input return loss and gain are presented in Figure 2- 31 and Figure 2-

32, respectively. The length of the antenna is kept at 12 mm since changes in L does not improve the performance of the antenna.

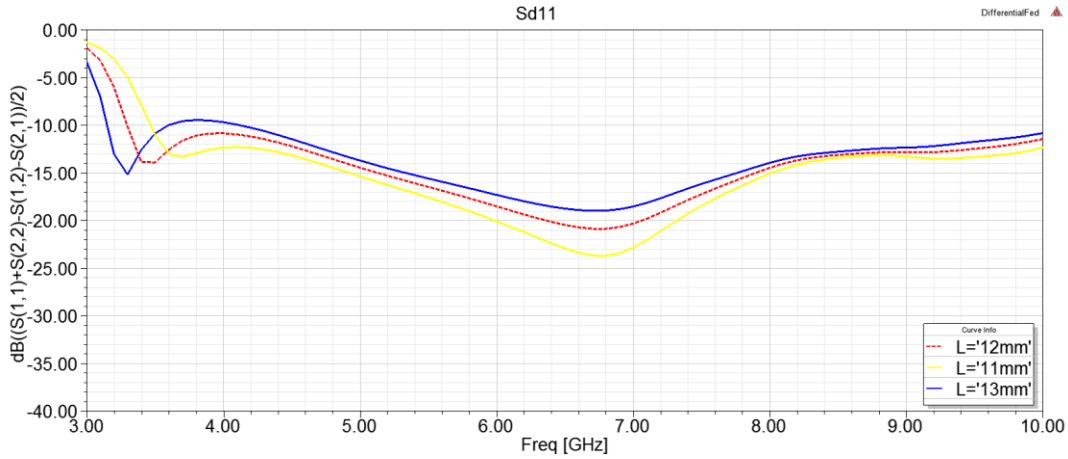


Figure 2- 31 Return Loss of the Differential Fed Magneto-Electric Dipole Antenna with L Sweep

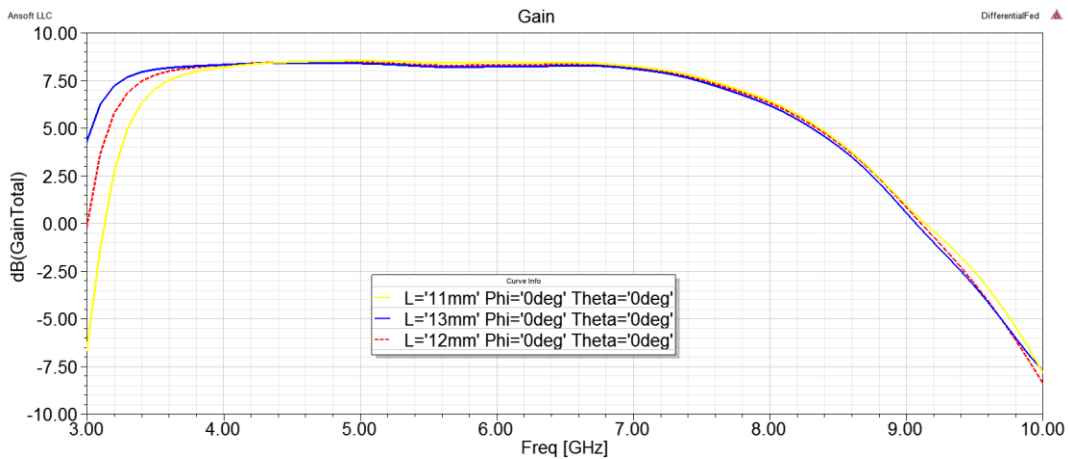


Figure 2- 32 Gain of the Differential Fed Magneto-Electric Dipole Antenna with L Sweep

The parametric analysis for the gamma-shaped strip fed antenna implies that the width of the antenna is very effective on the third resonance frequency. Since this resonance is very close to the end of the required bandwidth, width of the antenna should be longer to shift the resonance to lower frequencies. Best performance is

obtained when W is extended to 32 mm. The parameters of the optimized antenna are summarized in Table 2- 3. The simulation results of optimized antenna for the differential input return loss and gain are presented in Figure 2- 33 and Figure 2- 34, respectively.

Table 2- 3 Final Parameter Values of the Differential Fed Magneto-Electric Dipole Antenna with Cavity

Name of the Parameter in HFSS	Nominal Value
S1	1.7875 mm
S2	6.425 mm
W	32 mm
L	12 mm
H	12.5 mm
FeedW	9 mm
Feed2L	7.425 mm
Feed2W	17.5 mm

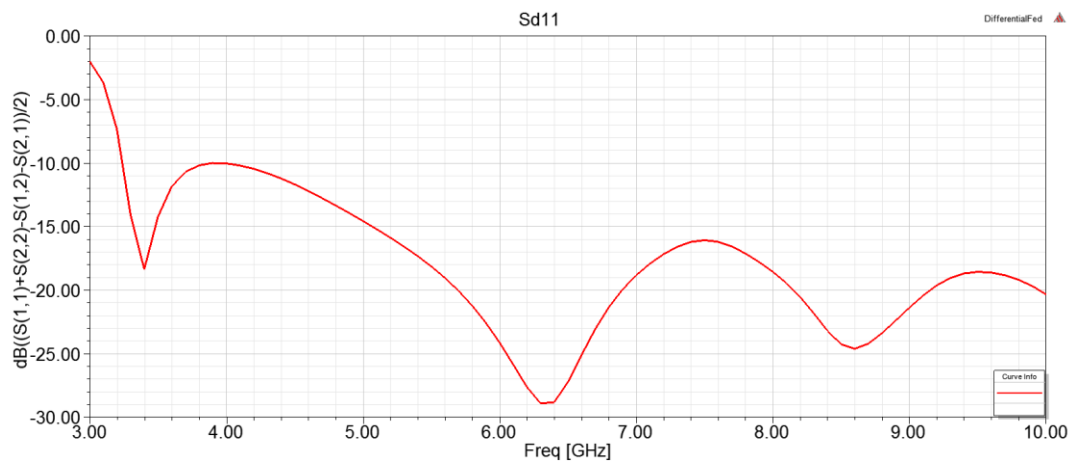


Figure 2- 33 Final Return Loss of the Differential Fed Magneto-Electric Dipole Antenna

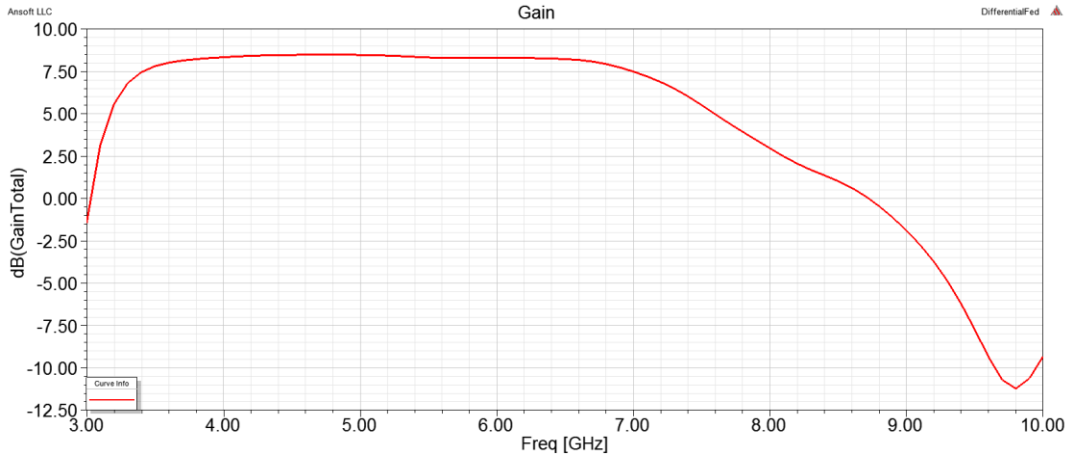


Figure 2- 34 Final Gain of the Differential Fed Magneto-Electric Dipole Antenna

The final differential return loss result of the antenna is satisfactory. However, the final gain result of the antenna does not meet our expectations, especially in high end of the frequency bandwidth. In order to investigate the reason of the decrease in the gain result, the radiation patterns and the current distributions of the antenna are studied at different frequencies. E-plane and H-plane co-polarization and cross-polarization radiation patterns at 3 GHz are presented in Figure 2- 35 and Figure 2- 36, respectively. Note that cross polarization patterns are not visible in the figures since their levels are very low (less than -50 dB) compared to co-polarized components. It can be observed that the back radiation of the antenna is higher than the front radiation of the antenna. Current distribution of the antenna at 3 GHz (presented in Figure 2- 37) shows that the current distribution on the ground plane is very high. It may be concluded that the radiation due to the induced currents on the ground plane dominates the radiation characteristics of the antenna at this frequency.

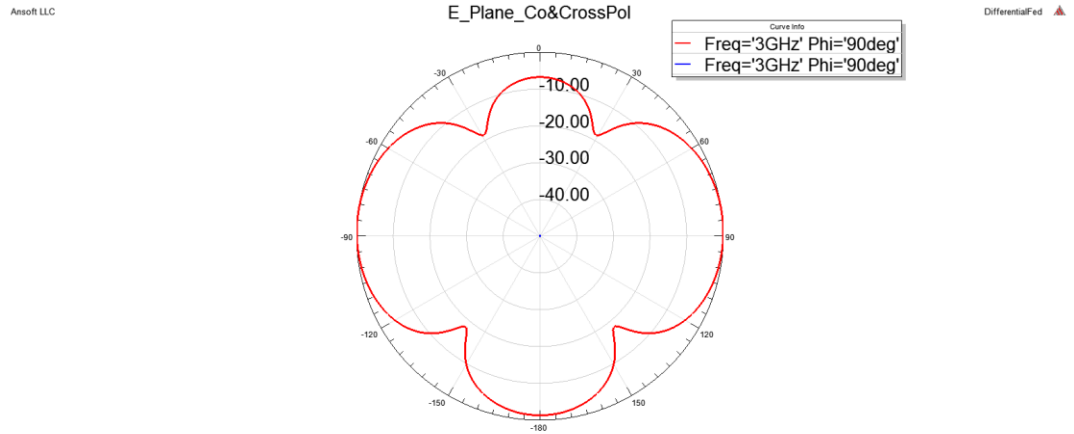


Figure 2- 35 Radiation Pattern of the Differential Fed Magneto-Electric Dipole Antenna at 3 GHz in E-Plane

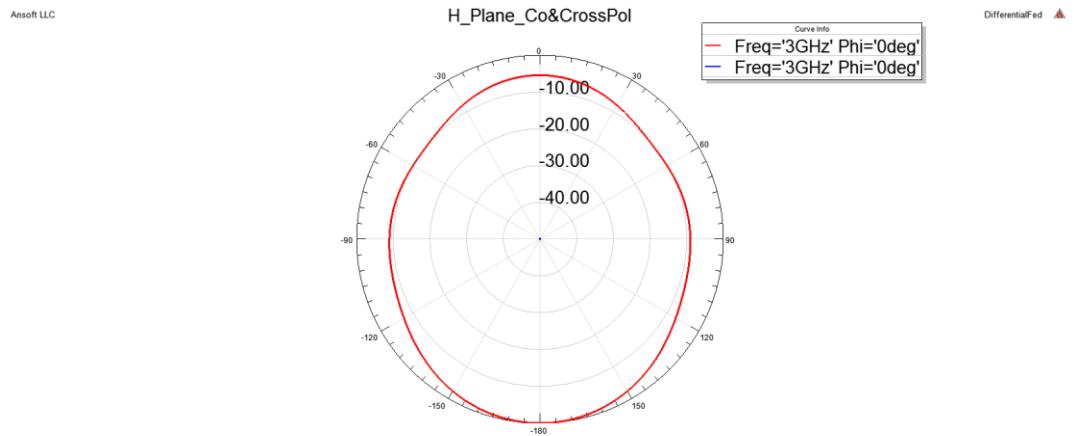


Figure 2- 36 Radiation Pattern of the Differential Fed Magneto-Electric Dipole Antenna at 3 GHz in H-Plane

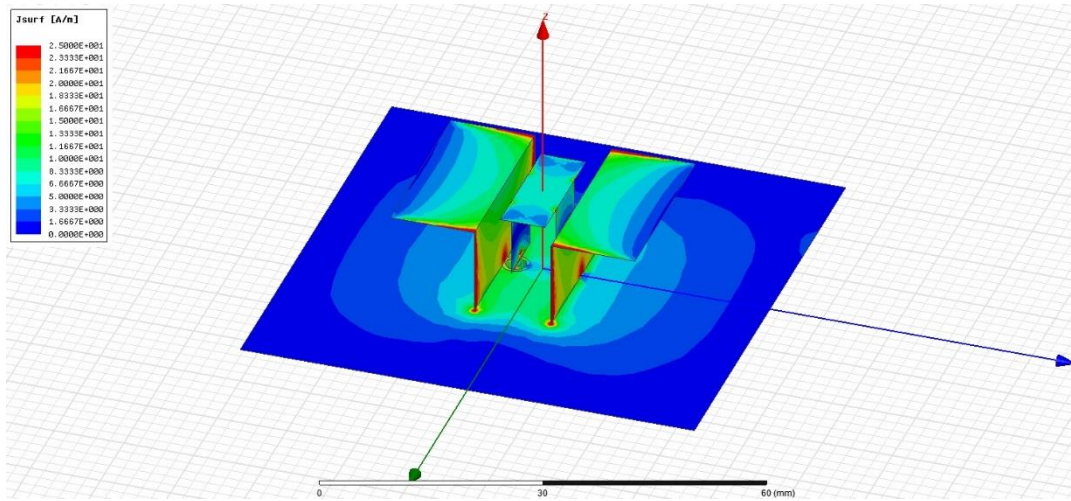


Figure 2- 37 Current distribution of the Differential Fed Magneto-Electric Dipole Antenna at 3 GHz

In Figure 2- 38 and Figure 2- 39 co- and cross-polarization patterns are sketched at 9 GHz. As revealed by these figures, main beam of the antenna is not in broadside of the antenna. The current distribution of the antenna at 9 GHz, presented in Figure 2- 40, shows that both the electric dipole and the magnetic dipole are not excited efficiently. The currents are confined within the feed structure. The even symmetry along the x-direction in the current distribution on the feed conductor result in -10 dB reduction at the broadside direction in the H-plane (xz plane) radiation pattern.

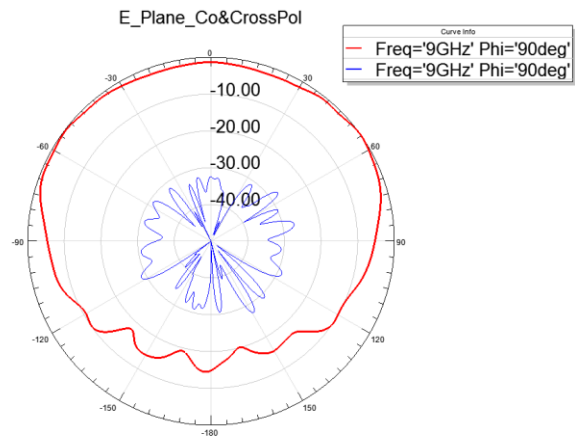


Figure 2- 38 Radiation Pattern of the Differential Fed Magneto-Electric Dipole Antenna at 9 GHz in E-Plane

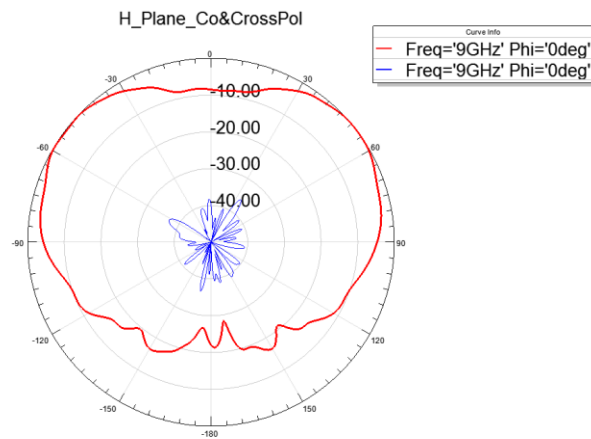


Figure 2- 39 Radiation Pattern of the Differential Fed Magneto-Electric Dipole Antenna at 9 GHz in H-Plane

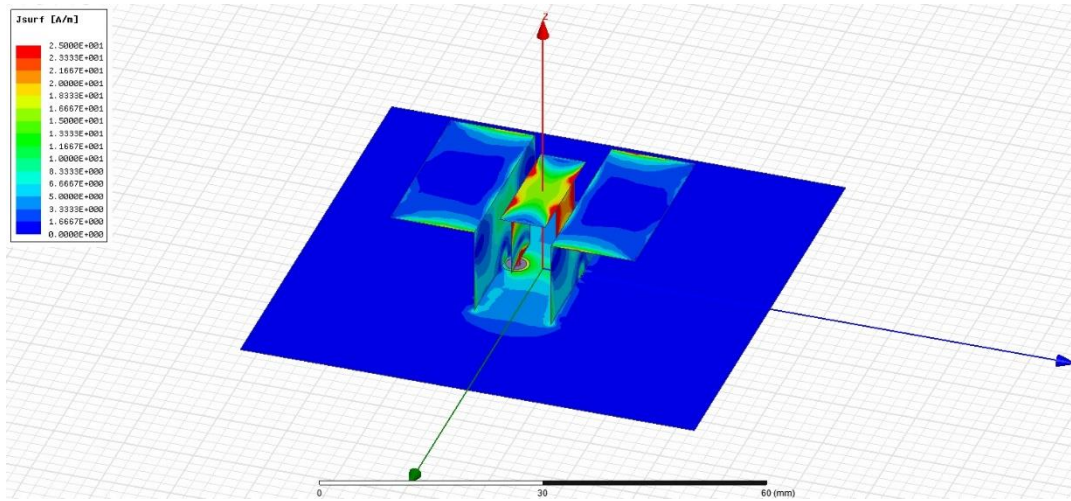


Figure 2- 40 Current distribution of the Differential Fed Magneto-Electric Dipole Antenna at 9 GHz

E-plane and H-plane radiation patterns and current distribution at 10 GHz are presented in Figure 2- 41, Figure 2- 42 and Figure 2- 43, respectively. Similar to the case at 9 GHz, higher order modes are excited at 10 GHz. Even symmetry is observed for the electric dipole antenna. Consequently, the reduction at the broadside direction in the H-plane radiation pattern became more significant.

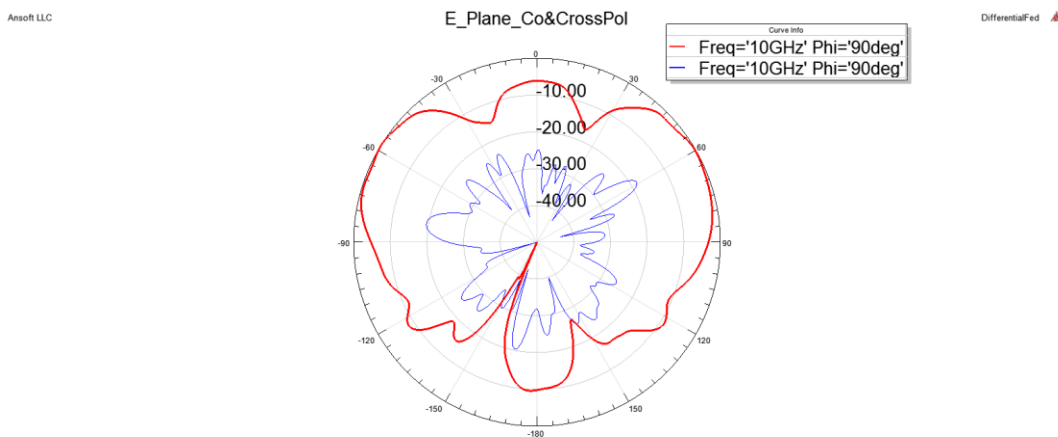


Figure 2- 41 Radiation Pattern of the Differential Fed Magneto-Electric Dipole Antenna at 10 GHz in E-Plane

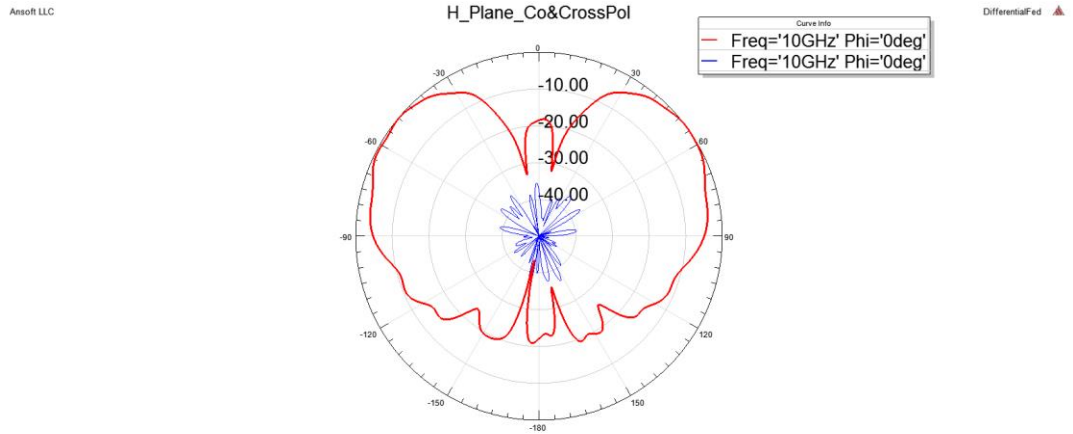


Figure 2- 42 Radiation Pattern of the Differential Fed Magneto-Electric Dipole Antenna at 10 GHz in H-Plane

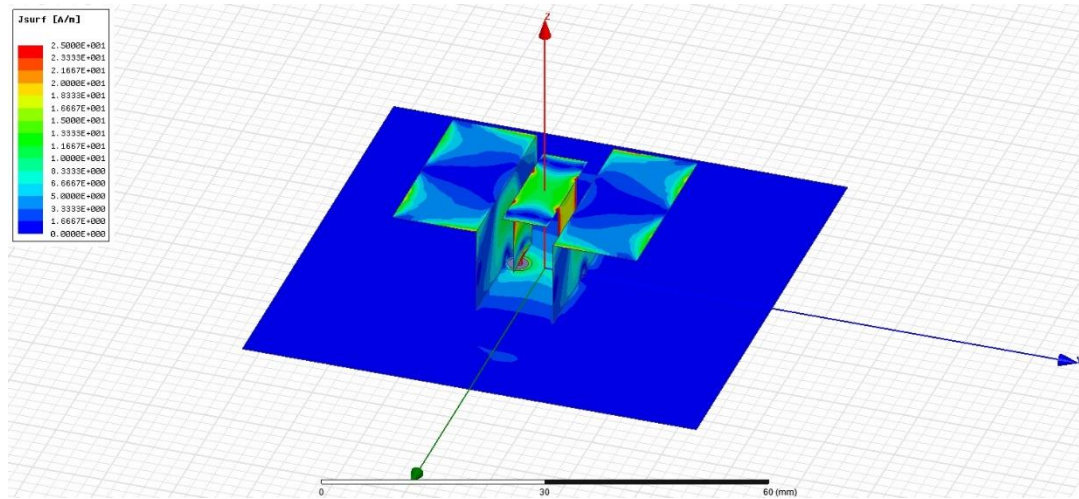


Figure 2- 43 Current distribution of the Differential Fed Magneto-Electric Dipole Antenna at 10 GHz

In order to achieve a higher and a flat broadside gain at the whole operating frequency band, placing a rectangular cavity to the antenna ground plane is proposed in [8]. The cavity suppresses the radiation of the higher order modes. Thus, the gain of the antenna at the broadside direction improves at the high end of the bandwidth.

2.3 Design of the Differential Fed Magneto-Electric Dipole Antenna with Cavity

A square cavity is considered with its width equal to its length denoted by “G” and the height of the cavity is denoted by “WallH” as seen in Figure 2- 44. In order to determine the optimum values of these parameters, parametric analyses are performed. Note that the ground plane of the designed antenna is square. Hence, length and width of the cavity are taken equal. The first optimization is applied to the height parameter of the cavity. Figure 2- 45 shows the differential input return loss. The differential input return loss results indicate that the height of the cavity affects the differential input return loss and bandwidth slightly. The simulation results of the gain are presented in Figure 2- 46. According to gain results, the best value of the cavity height is 12.5 mm.

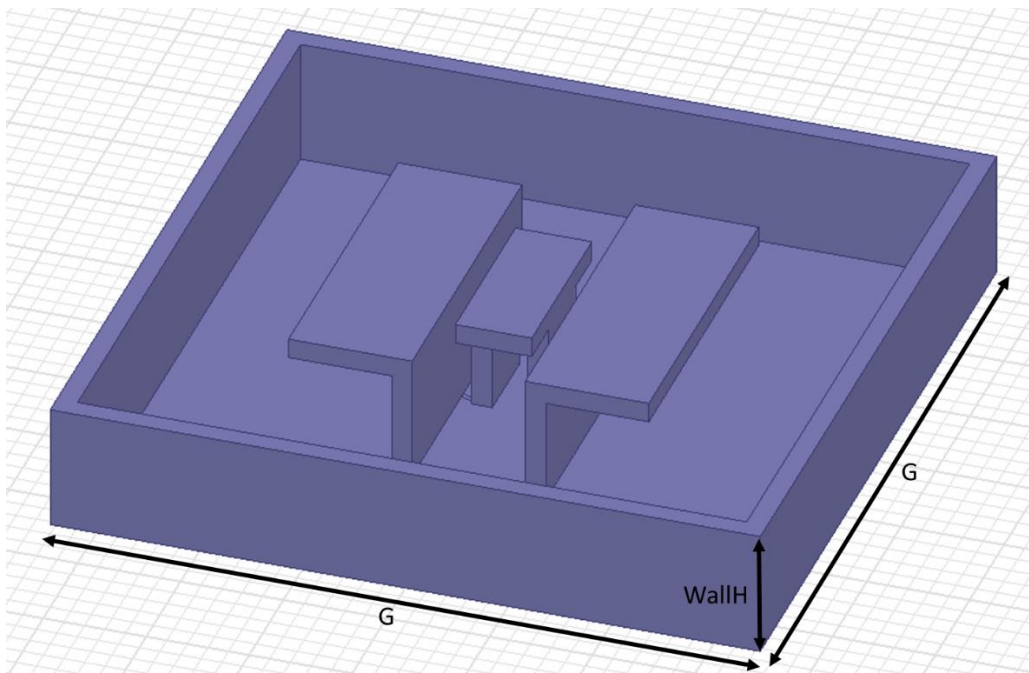


Figure 2- 44 HFSS Model of the Differential Fed Magneto-Electric Dipole Antenna with Cavity

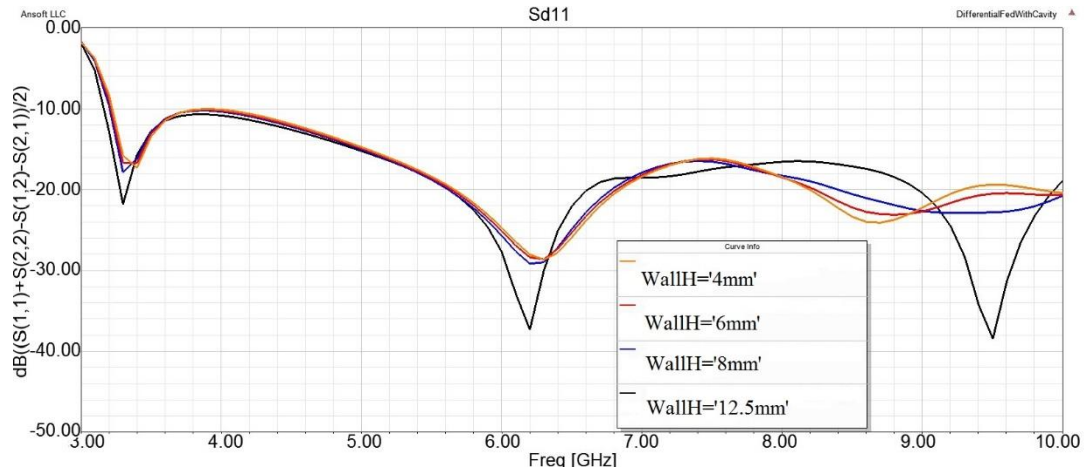


Figure 2- 45 Return Loss of the Differential Fed Magneto-Electric Dipole Antenna with WallH of the Cavity Sweep

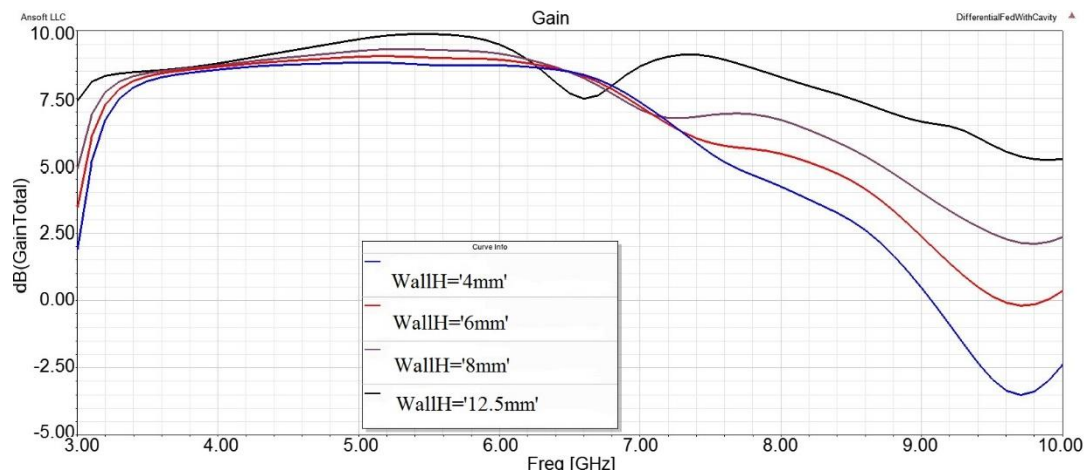


Figure 2- 46 Gain of the Differential Fed Magneto-Electric Dipole Antenna with WallH of the Cavity Sweep

The second optimization is applied to the length parameter of the cavity. The differential input return loss and gain results which are presented in Figure 2- 47 and Figure 2- 48 indicate that the length of the cavity should be set at 65 mm.

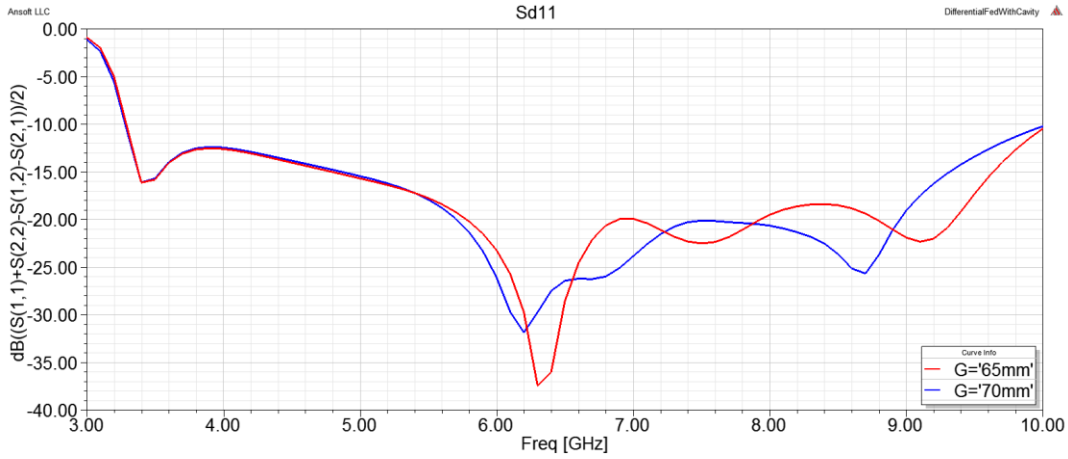


Figure 2- 47 Return Loss of the Differential Fed Magneto-Electric Dipole Antenna with Length of the Cavity Sweep

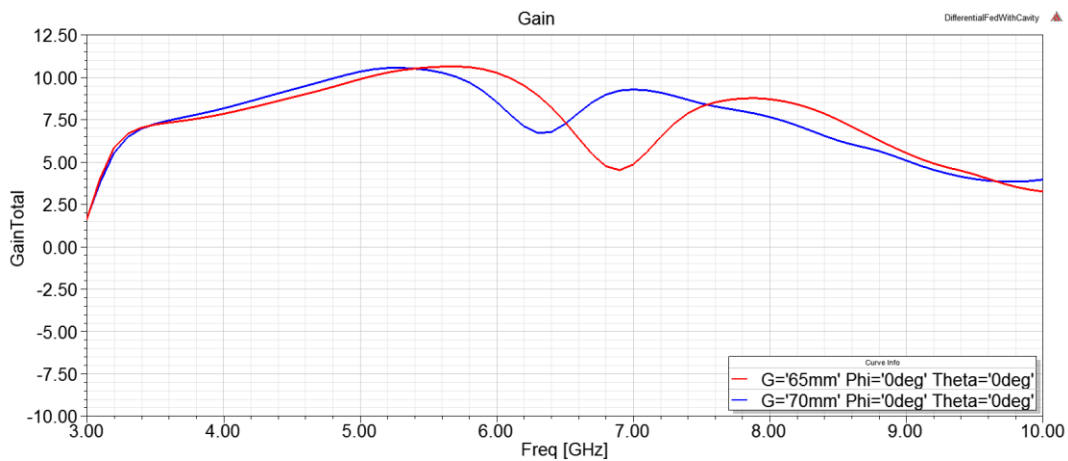


Figure 2- 48 Gain of the Differential Fed Magneto-Electric Dipole Antenna with Length of the Cavity Sweep

The final configuration of the antenna has the expected differential input return loss and almost flat gain results. A comparison of the differential input return loss and gain of the antenna with and without cavity are presented in Figure 2- 49 and Figure 2- 50, respectively.

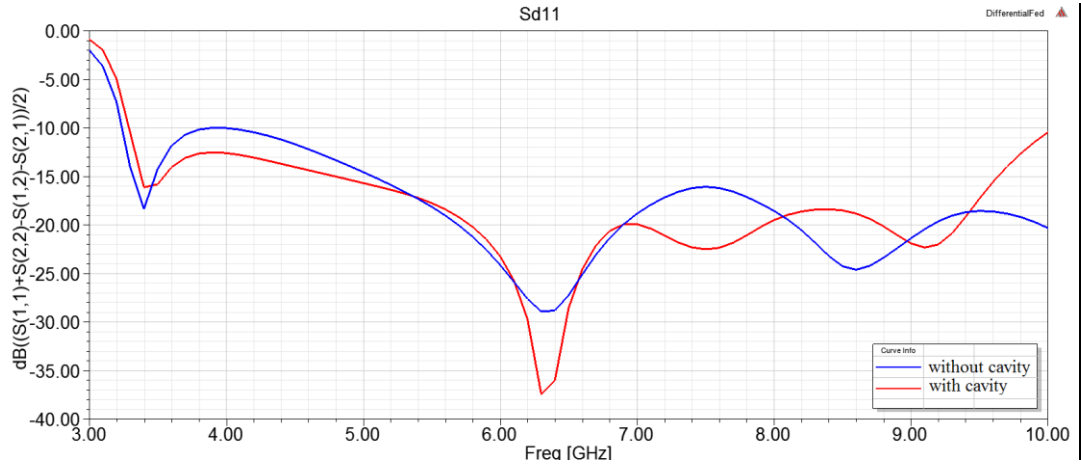


Figure 2- 49 Final Return Loss of the Differential Fed Magneto-Electric Dipole Antenna with Cavity and without Cavity

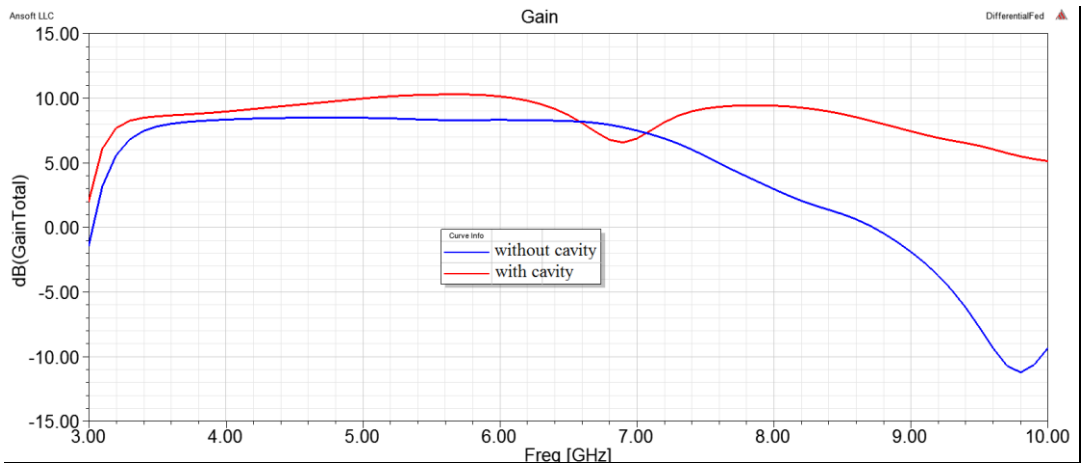


Figure 2- 50 Final Gain of the Differential Fed Magneto-Electric Dipole Antenna with Cavity and without Cavity

The radiation patterns of the differential fed magneto-electric dipole antenna with cavity and without cavity are compared in Figure 2- 51 to Figure 2- 66. The radiation patterns indicate that the differential fed magneto-electric dipole antenna with cavity has better radiation characteristics than the differential fed magneto-electric dipole antenna without cavity. The cross-polarization radiation pattern values of the designed antenna are very low compared to the co-polarization radiation pattern

values. Therefore, only co-polarization radiation patterns of the antenna with cavity and without cavity are presented comparatively.

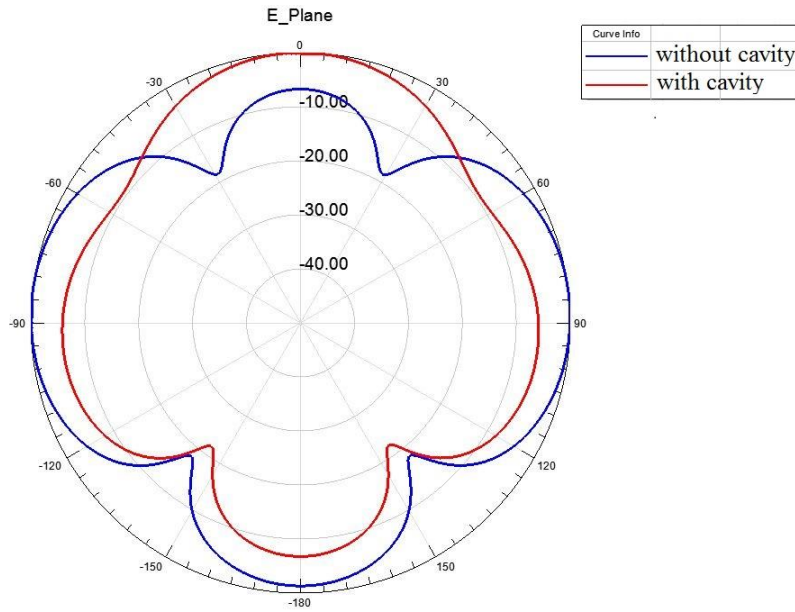


Figure 2- 51 Radiation Pattern of the Differential Fed Magneto-Electric Dipole Antenna with and without Cavity at 3 GHz in E-Plane

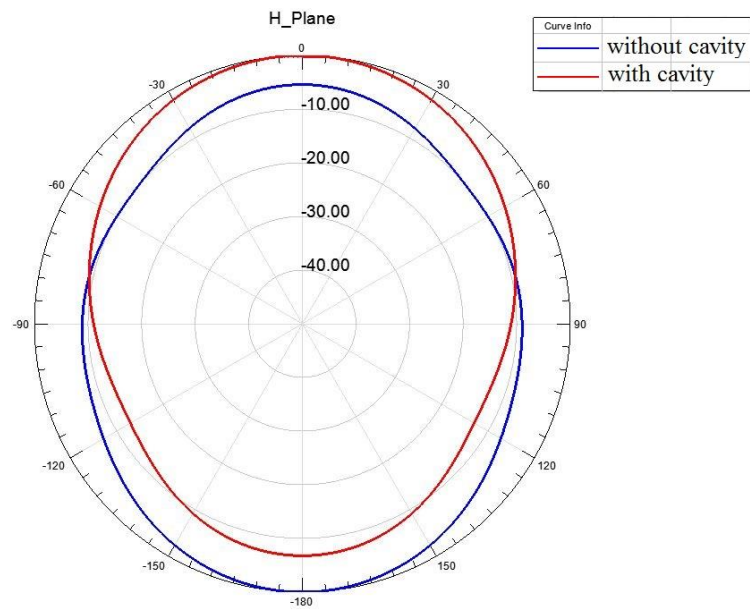


Figure 2- 52 Radiation Pattern of the Differential Fed Magneto-Electric Dipole Antenna with and without Cavity at 3 GHz in H-Plane

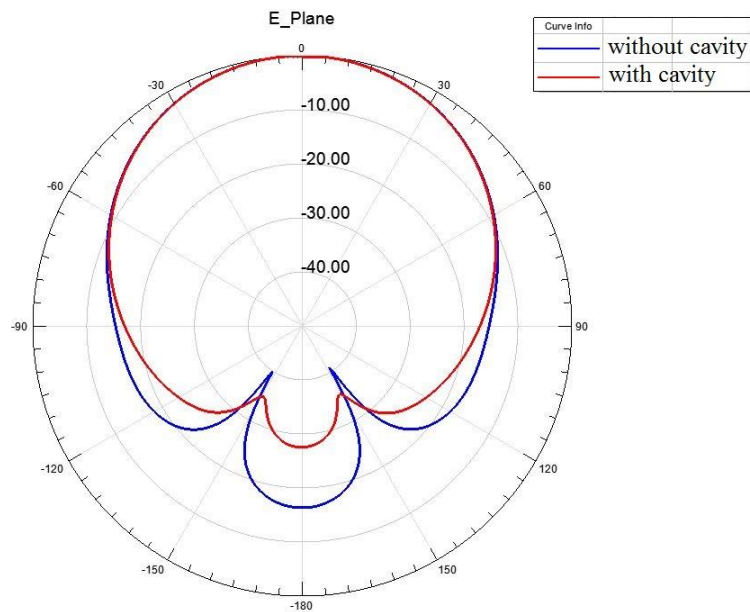


Figure 2- 53 Radiation Pattern of the Differential Fed Magneto-Electric Dipole Antenna with and without Cavity at 4 GHz in E-Plane

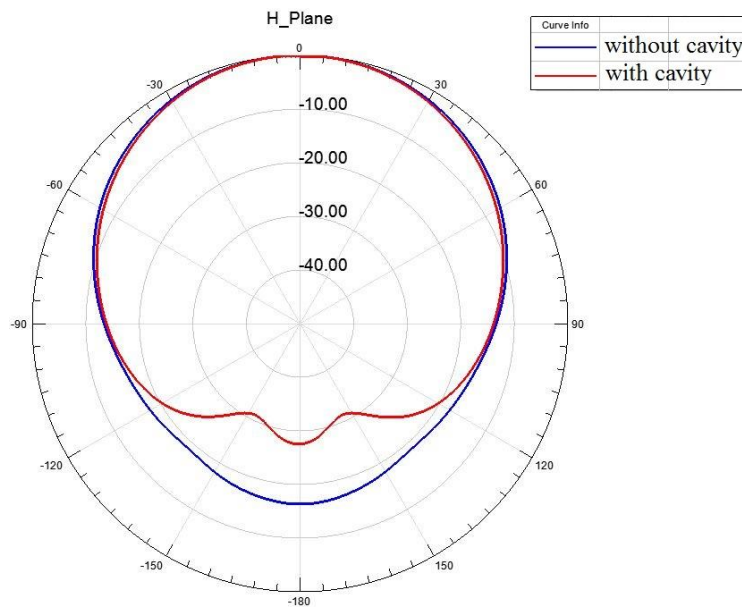


Figure 2- 54 Radiation Pattern of the Differential Fed Magneto-Electric Dipole Antenna with and without Cavity at 4 GHz in H-Plane

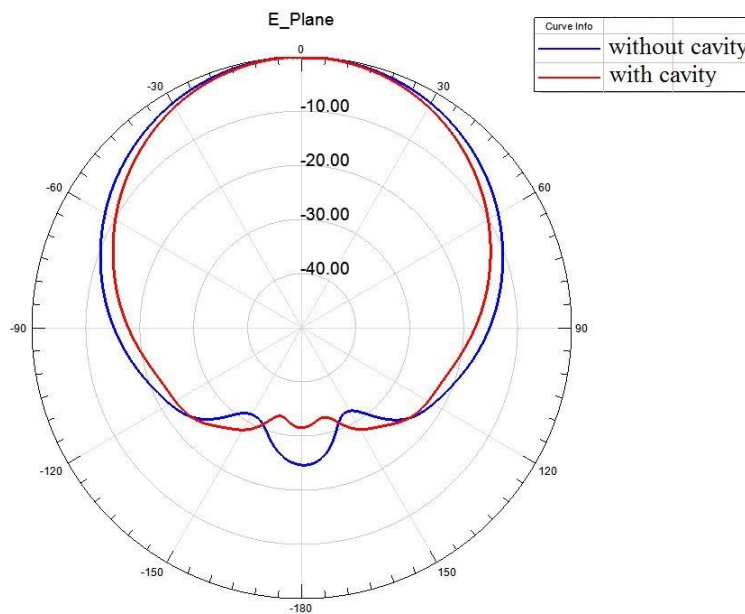


Figure 2- 55 Radiation Pattern of the Differential Fed Magneto-Electric Dipole Antenna with and without Cavity at 5 GHz in E-Plane

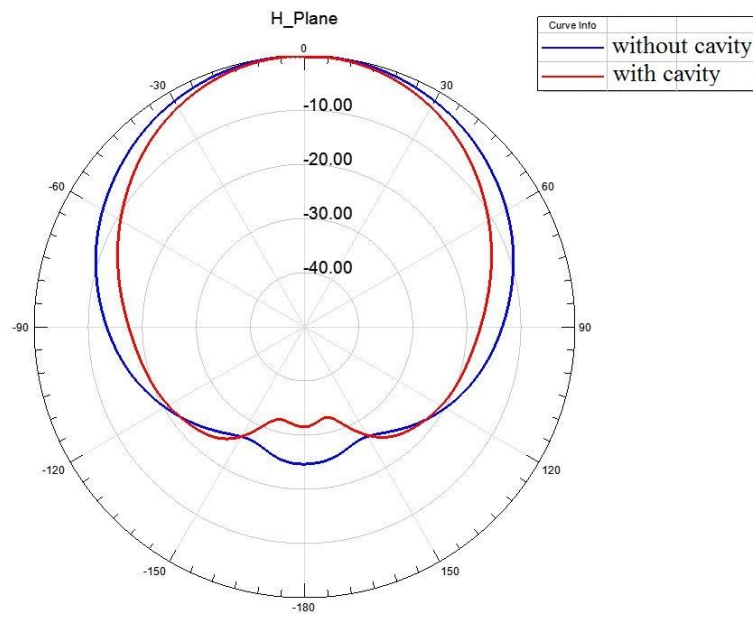


Figure 2- 56 Radiation Pattern of the Differential Fed Magneto-Electric Dipole Antenna with and without Cavity at 5 GHz in H-Plane

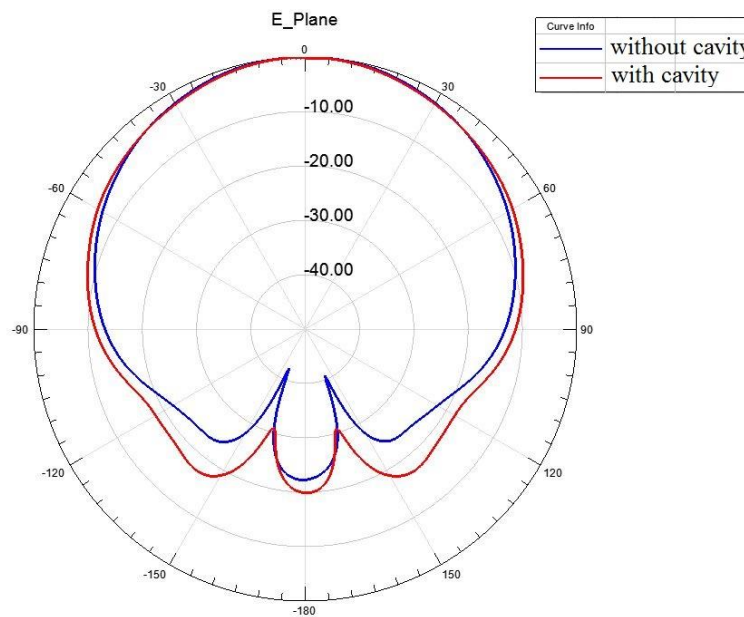


Figure 2- 57 Radiation Pattern of the Differential Fed Magneto-Electric Dipole Antenna with and without Cavity at 6 GHz in E-Plane

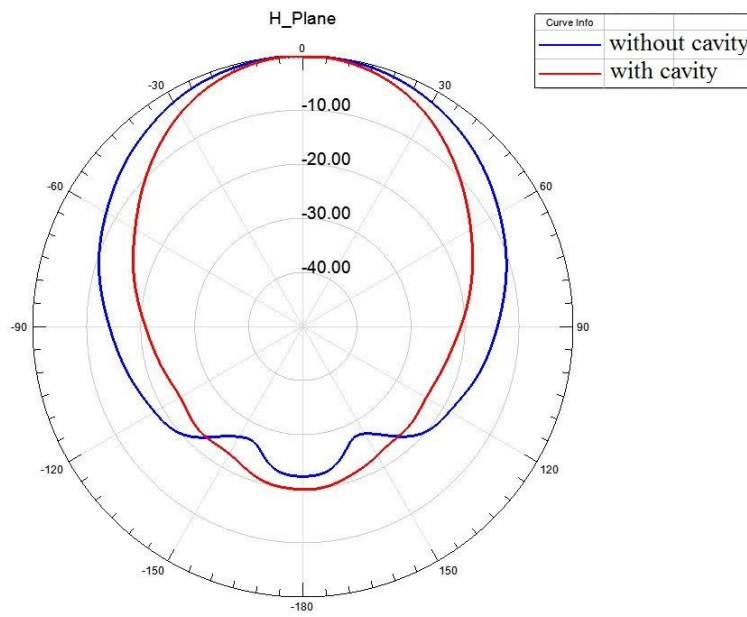


Figure 2- 58 Radiation Pattern of the Differential Fed Magneto-Electric Dipole Antenna with and without Cavity at 6 GHz in H-Plane

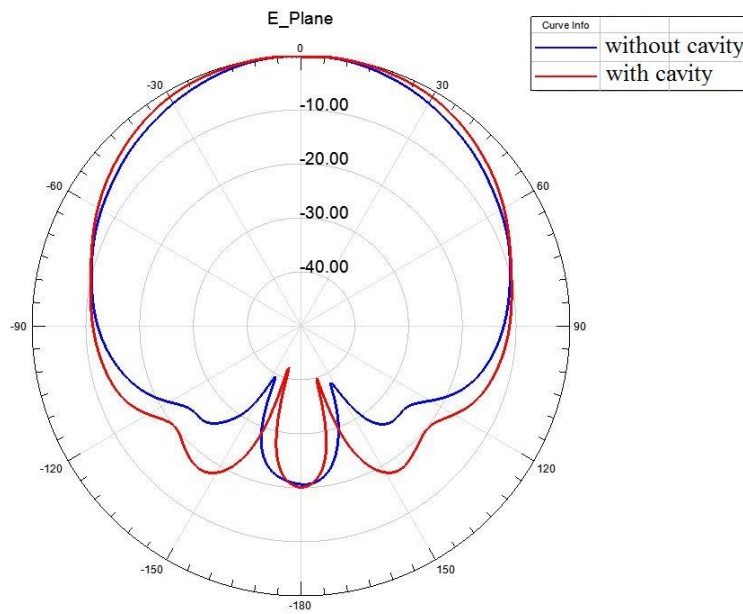


Figure 2- 59 Radiation Pattern of the Differential Fed Magneto-Electric Dipole Antenna with and without Cavity at 7 GHz in E-Plane

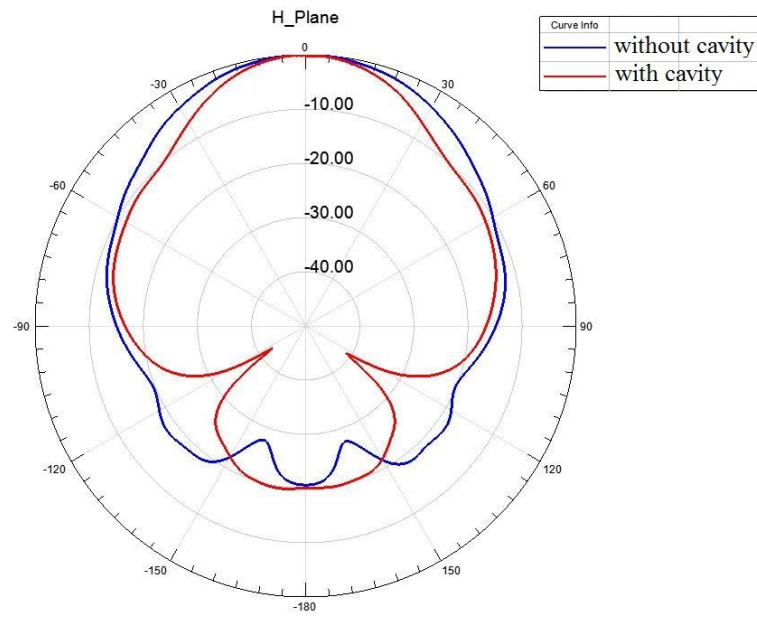


Figure 2- 60 Radiation Pattern of the Differential Fed Magneto-Electric Dipole Antenna with and without Cavity at 7 GHz in H-Plane

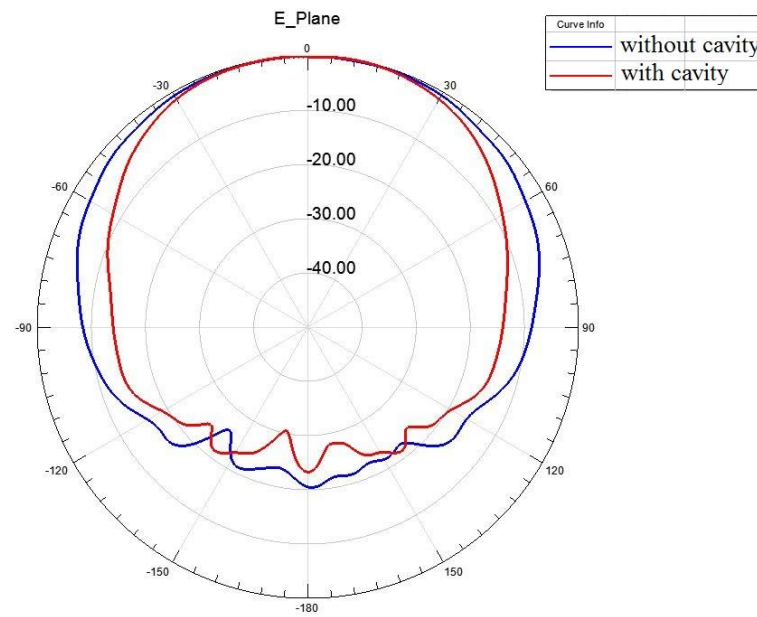


Figure 2- 61 Radiation Pattern of the Differential Fed Magneto-Electric Dipole Antenna with and without Cavity at 8 GHz in E-Plane

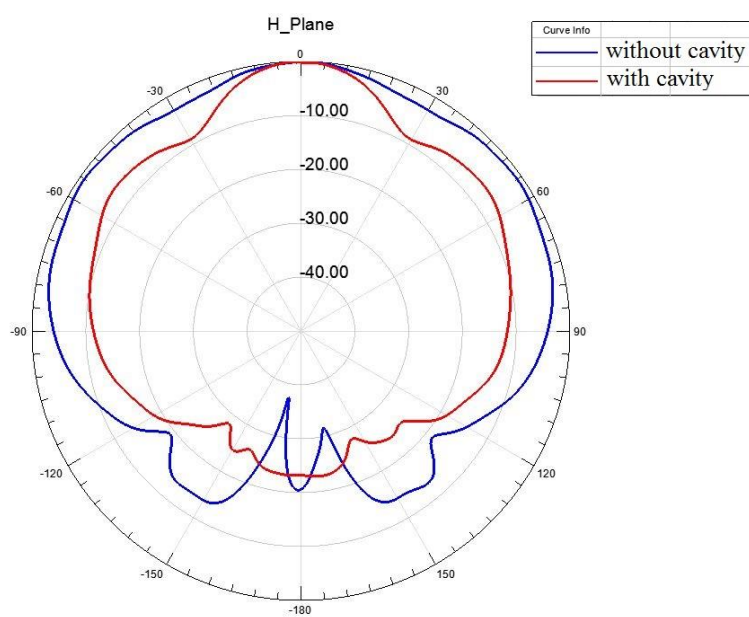


Figure 2- 62 Radiation Pattern of the Differential Fed Magneto-Electric Dipole Antenna with and without Cavity at 8 GHz in H-Plane

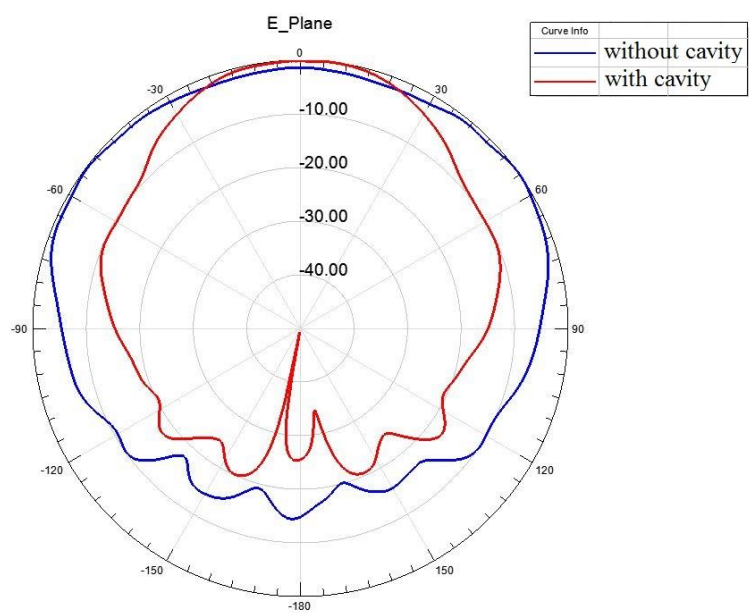


Figure 2- 63 Radiation Pattern of the Differential Fed Magneto-Electric Dipole Antenna with and without Cavity at 9 GHz in E-Plane

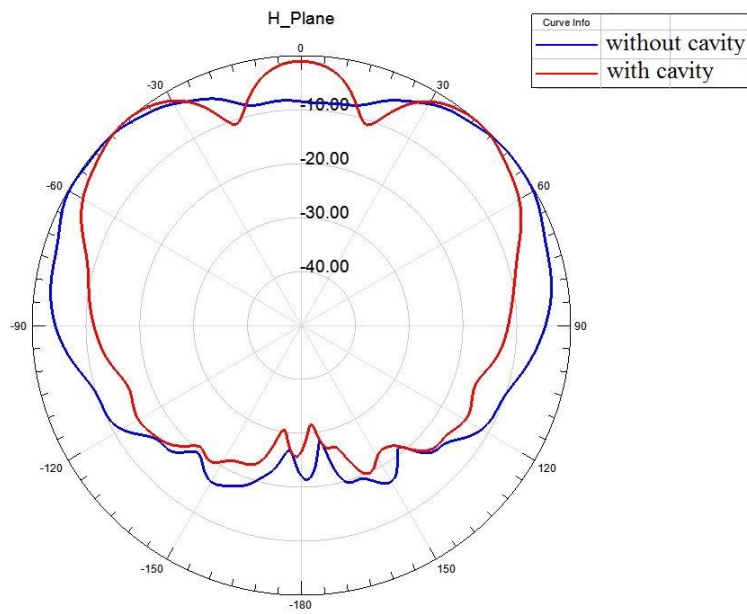


Figure 2- 64 Radiation Pattern of the Differential Fed Magneto-Electric Dipole Antenna with and without Cavity at 9 GHz in H-Plane

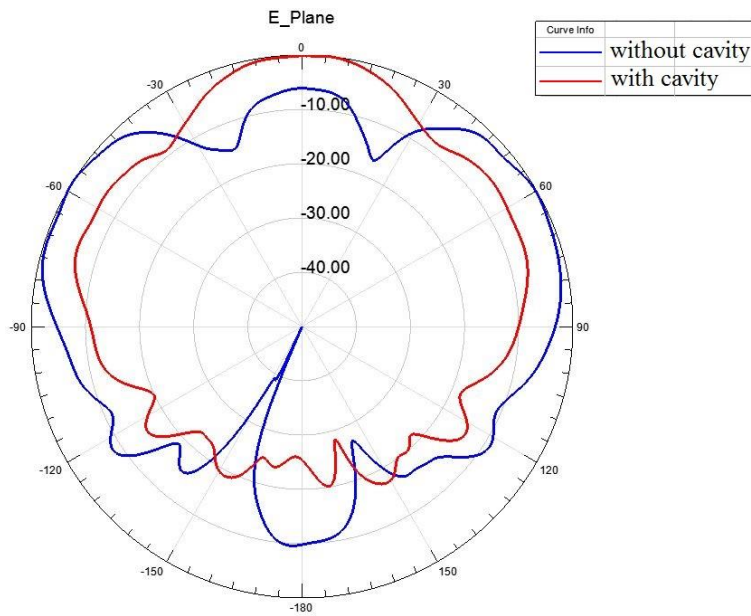


Figure 2- 65 Radiation Pattern of the Differential Fed Magneto-Electric Dipole Antenna with and without Cavity at 10 GHz in E-Plane

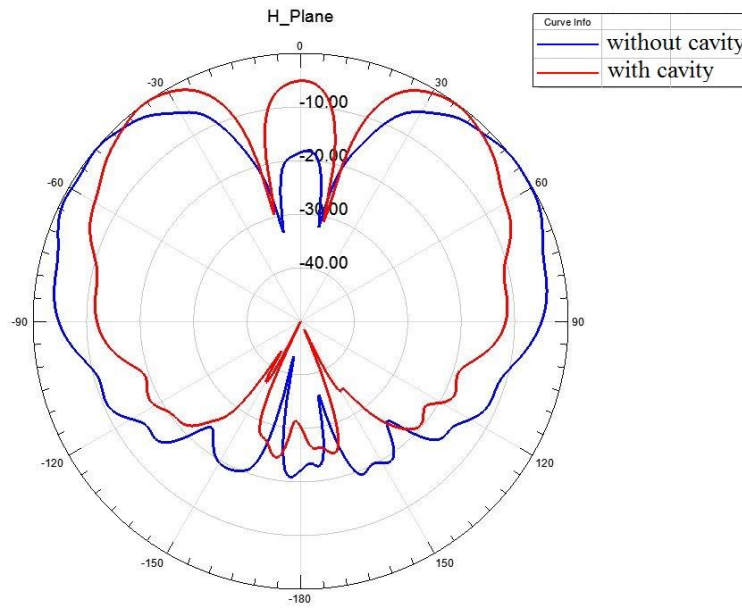


Figure 2- 66 Radiation Pattern of the Differential Fed Magneto-Electric Dipole Antenna with and without Cavity at 10 GHz in H-Plane

At all frequencies the deterioration in the H-plane patterns are more than E-plane patterns. This may be due to the radiation from the feeding structure. The dimension of the feeding structure is longer in the H-plane, therefore its effects is more dominant in this plane.

3D radiation patterns of the differential fed magneto-electric dipole antenna with cavity at 8 different frequencies between 3GHz and 10 GHz are presented in Figure 2- 67.

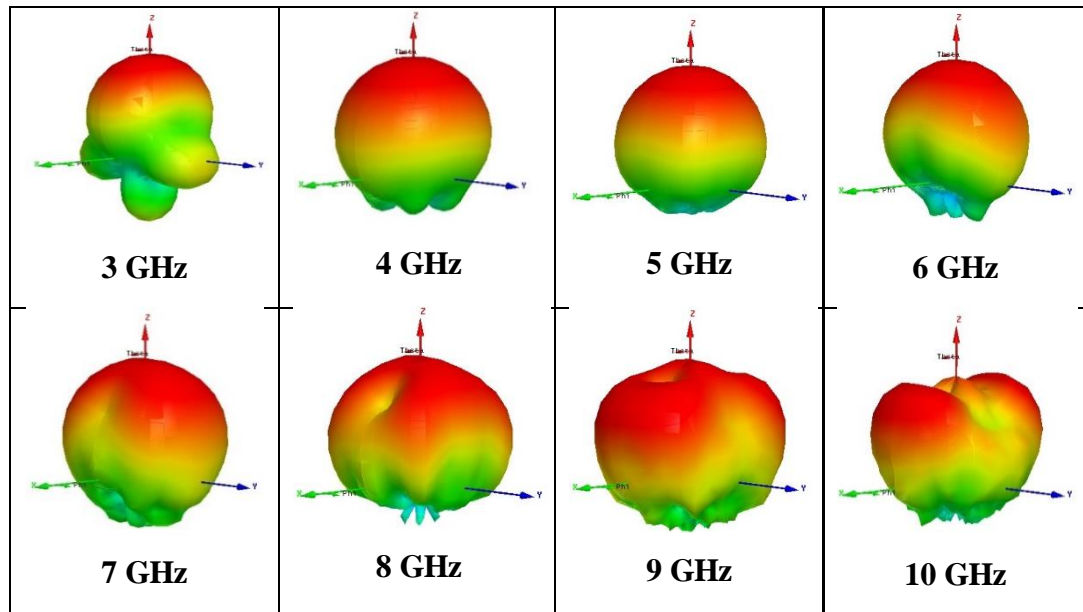


Figure 2- 67 3D Radiation Patterns of the Differential Fed Magneto-Electric Dipole Antenna with Cavity

CHAPTER 3

FABRICATIONS AND MEASUREMENTS OF THE MAGNETO-ELECTRIC DIPOLE ANTENNA WITH CAVITY

The design methodology for the different magneto-electric dipole antennas have been detailed so far. This chapter includes production and measurement of the differential fed magneto-electric dipole antenna with cavity.

3.1 Fabrications of Differential Fed Magneto-Electric Dipole Antenna with Cavity

In order to prove performance of the differential fed magneto-electric dipole antenna with cavity, prototype is produced and measured. The differential fed magneto-electric dipole antenna with cavity which is designed in Chapter 2 is fabricated in the facilities of ASELSAN Inc. Laboratories. Copper material is used for fabrication of the antenna. To obtain a rigid antenna thickness of copper is chosen to be 2 mm. However, simulation results indicated that the thickness should be reduced to 0.5 mm for the feed structure to obtain better matching characteristics.

Produced antenna prototype consists of three parts which are presented in Figure 3-1 through Figure 3-4. First part is the cavity. This first part of the antenna has four screw holes on the bottom plate to bond the electric and the magnetic dipoles of the antenna and extra two holes to solder the feeding mechanism. Second part of the produced antenna is the electric and the magnetic dipoles. These parts of the antenna are bonded to the bottom of the cavity via four screws. Last part of the produced antenna is the feeding mechanism. This feeding mechanism is soldered to the SMA connectors.

Two 50 ohm female connector of Huber & Suhner Corporation are used to feed the differential fed magneto-electric dipole antenna with cavity. The center pins of the SMA connectors are soldered to the vertical conductors of the feeding structure, and the outer surface of the SMA connectors are also soldered to the ground plane of the antenna.

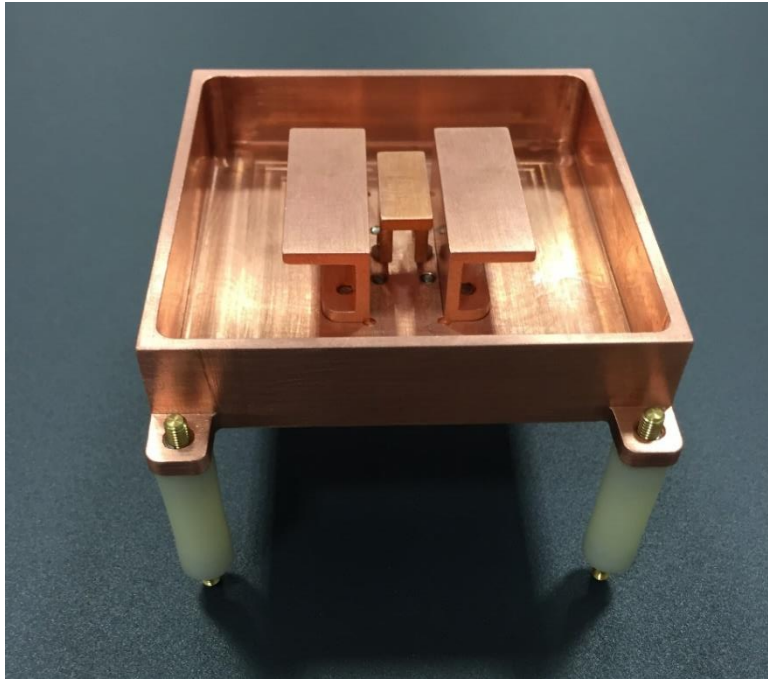


Figure 3- 1 Perspective View of Fabricated Differential Fed Magneto-Electric Dipole Antenna with Cavity

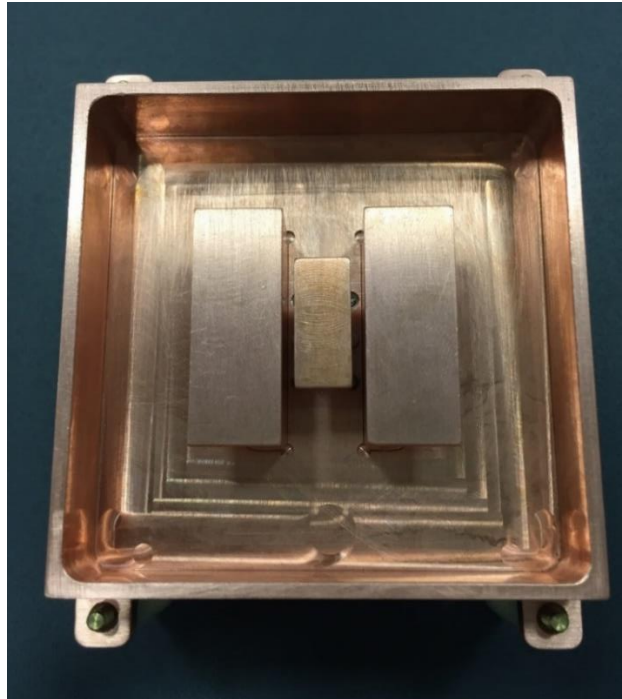


Figure 3- 2 Top View of Fabricated Differential Fed Magneto-Electric Dipole Antenna with Cavity

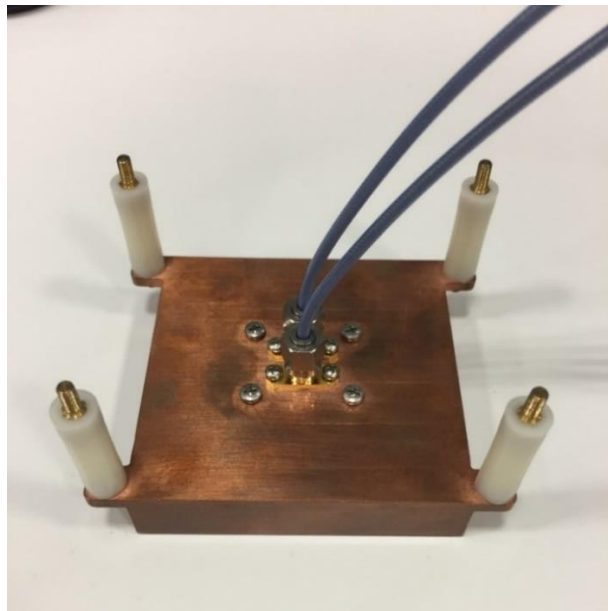


Figure 3- 3 Bottom View of the Fabricated Differential Fed Magneto-Electric Dipole Antenna with Cavity



Figure 3- 4 Feeding Structure of the Fabricated Differential Fed Magneto-Electric Dipole Antenna with Cavity

3.2 Measurements of Fabricated Differential Fed Magneto-Electric Dipole Antenna with Cavity

The return loss, gain and radiation patterns of the differential fed magneto-electric dipole antenna are measured and compared with the simulation results in this section. Firstly, port1 of the network analyzer is calibrated from 3 GHz to 10 GHz by using open, short and matched load. Then, in order to understand how well the matching between the antenna and its feeding structure is achieved, the return loss response is measured via N5222A PNA network analyzer of Keysight Technologies. A 180° hybrid coupler is used to feed the two port differential-fed antenna. The difference port (Δ) of the hybrid coupler was connected to the signal source of the measurement system, and the sum port (Σ) was terminated in a $50\ \Omega$ load. The output ports of the hybrid coupler were connected to the differential input port of the proposed antenna. As seen in Figure 3- 5 simulation and measurement results of the antenna are lower

than -10 dB through 3.4 GHz to 10 GHz. Thus, bandwidth requirement of the antenna is fulfilled.

The simulation result presented in Figure 3- 5 are different than the results of the optimized antenna which is presented in Figure 2- 46 of Chapter 2. Because in Chapter 2 the thickness of the conductors were assumed to be zero to accelerate the simulations, however here 2 mm is used for the antenna conductors and 0.5 mm is used for the feed structure to better model the manufactured antenna.

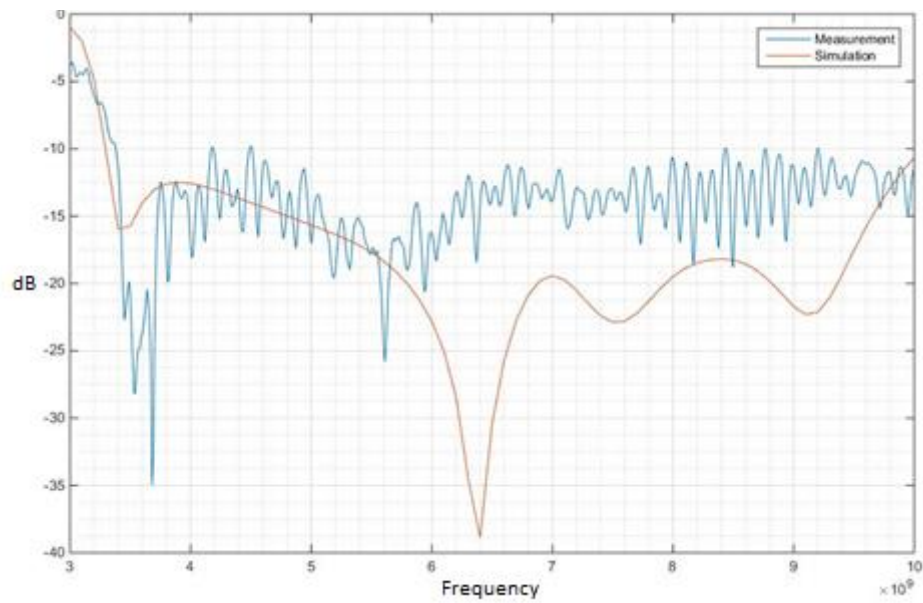


Figure 3- 5 Measured and Simulated Return Loss of the Differential Fed Magneto-Electric Dipole Antenna with Cavity

The ripples in the measurement results may be due to the multiple reflections from the antenna and the hybrid coupler as shown in Figure 3- 6.

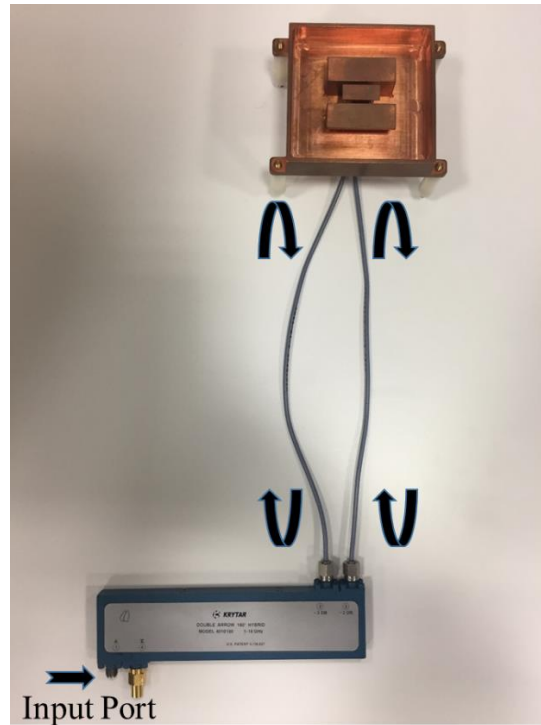


Figure 3- 6 General Measurement Set-up for the Differential Fed Magneto-Electric Dipole Antenna with Cavity

In order to investigate the agreement between the simulation and measurement results by eliminating the effects of directional coupler and the cables connecting the antenna and the directional coupler, the two-port s-parameter measurements of the manufactured antenna is performed. The S_{11} and S_{21} measurement results are compared with the corresponding simulation results in Figure 3- 7 and Figure 3- 8, respectively. As seen in the figures, the agreement up to 6GHz is good, but the results start to deviate from each other after this frequency. This may be due to the manufacturing process of the antenna. Antenna is not a solid conductor as modeled in HFSS, it is assembled by using screw and bolts. The contact of the conductors may not be perfectly achieved at higher frequencies.

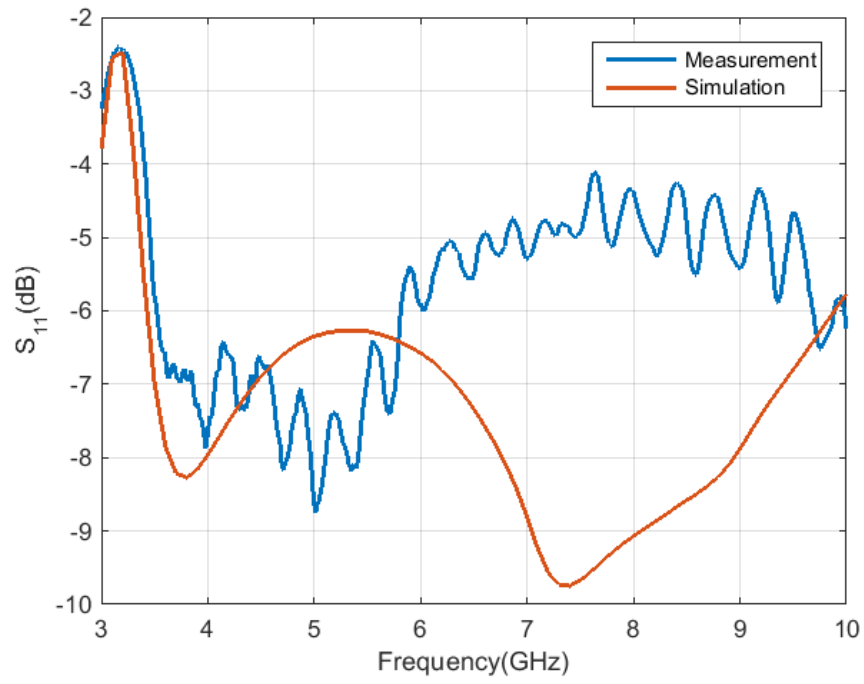


Figure 3- 7 Comparison of Simulation and Measurement Results for S_{11}

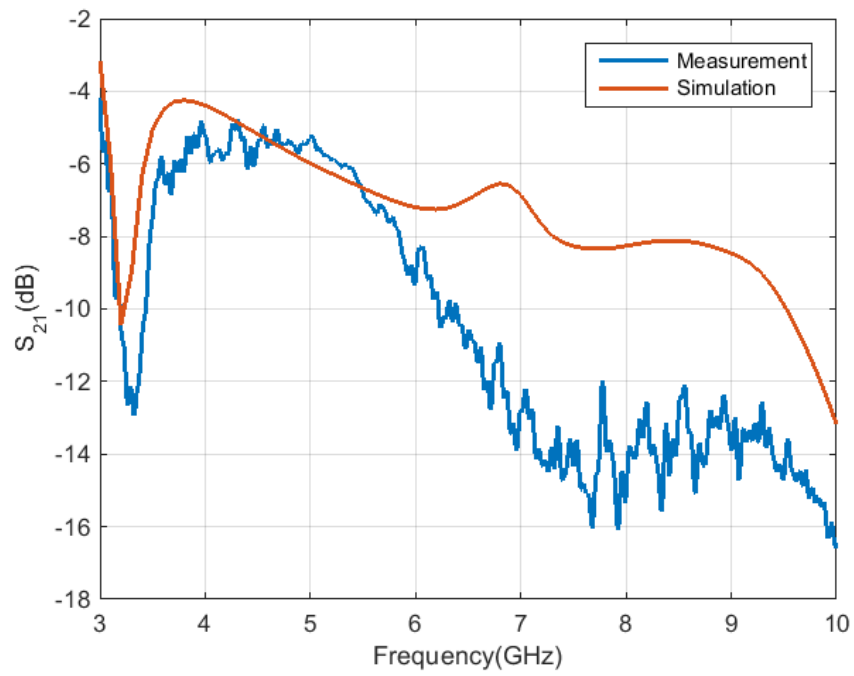


Figure 3- 8 Comparison of Simulation and Measurement Results for S_{21}

The differential input return loss is computed by using the measurement results of the two-port antenna. The measurement results and simulation results for the differential input return loss are compared in Figure 3- 9. The measurement results are quite different than the measurement results obtained by using the hybrid coupler. It is realized that when hybrid coupler is used the incident wave at Port 1 of the antenna will encounter a loss of 3dB compared to the input power at the input of the hybrid coupler. Similarly the reflected wave at the input port of the hybrid coupler will encounter 3 dB loss compared to the reflected wave at Port 1 of the antenna. Hence hybrid coupler provides 6 dB improvement in the input return loss. This is the reason why measurement results with hybrid coupler are better than computed differential input return loss by using two-port s-parameter measurement results.

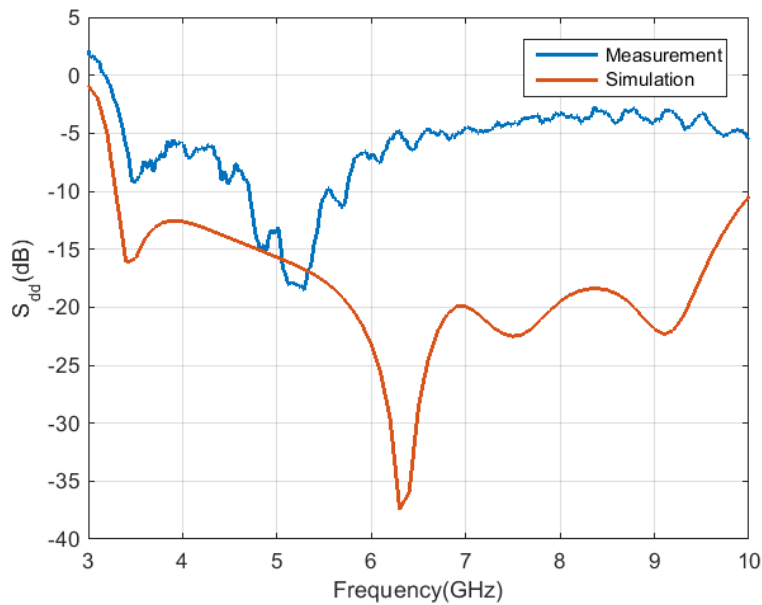


Figure 3- 9 Comparison of Simulation and Measurement Results for Differential Input Return Loss

After the return loss response is measured, radiation patterns of the antenna are explored. StarLab Spherical Nearfield Measurement System of SATIMO is used to obtain the far field patterns and far field measurement results are compared with the

simulation results in terms of the gain and radiation patterns. The near field measurement setup is presented in Figure 3- 10.

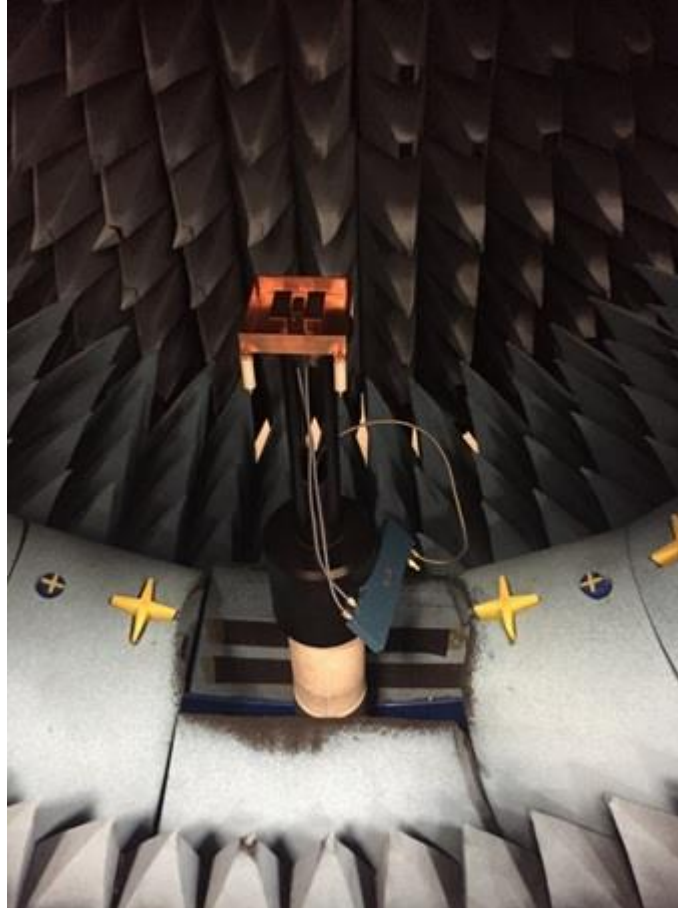


Figure 3- 10 Near Field Measurement Set-up for the Differential Fed Magneto-Electric Dipole Antenna with Cavity

The measured and simulated gain results of the antenna are presented in Figure 3- 11. As seen in the result, the simulated and measured gain results are in good agreement. Only a 200 MHz shift is observed at the low end of the bandwidth. The measured gain varies between 2.5 dB and 9 dB within the bandwidth with an average value of 6.4 dB.

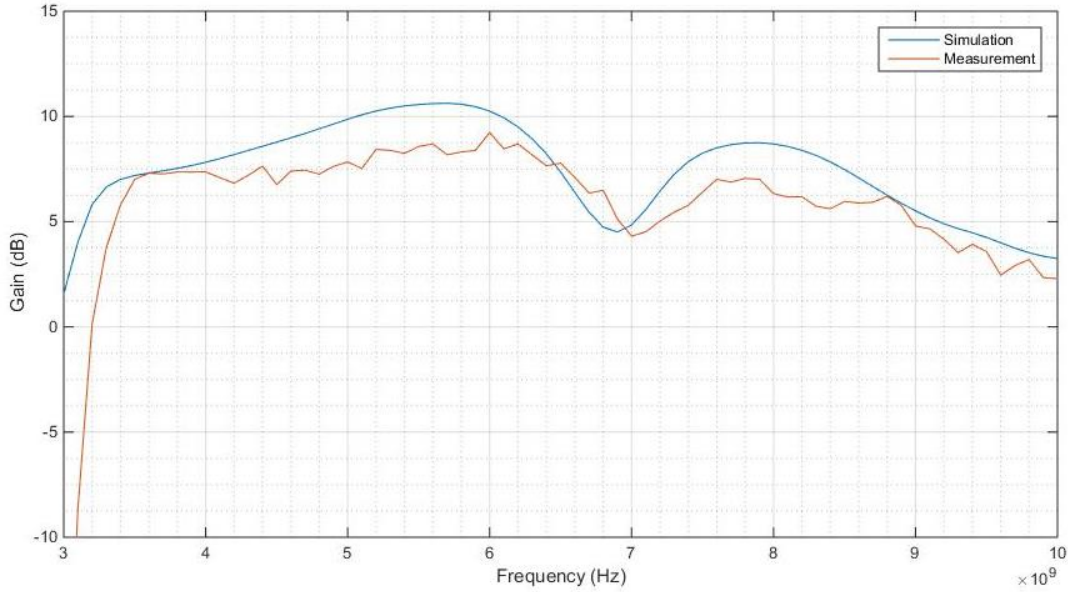


Figure 3- 11 Measured and Simulated Gains in Bore-sight Directions of the Differential Fed Magneto-Electric Dipole Antenna with Cavity

E and H plane radiation patterns are presented through Figure 3- 12 to Figure 3- 27 for eight different frequencies with 1 GHz step size between 3 GHz and 10 GHz. Although, at 3 GHz measured and simulated results of the antenna do not match, at all other frequencies measured and simulated results of the antenna are in good agreement. At 3 GHz it appears that the designed antenna can not radiate efficiently. Since the simulated model includes exactly the same parameters of the manufactured antenna (i.e., conductivity, thickness of the conductors), the discrepancy between the measurement and simulation results may be attributed to the measurement set-up.

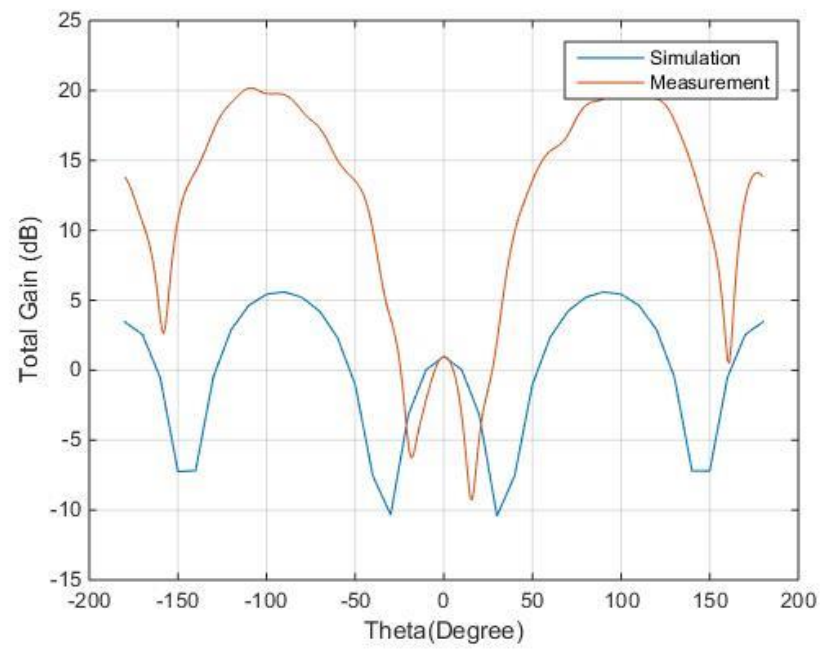


Figure 3- 12 E-Plane Radiation Patterns at 3 GHz

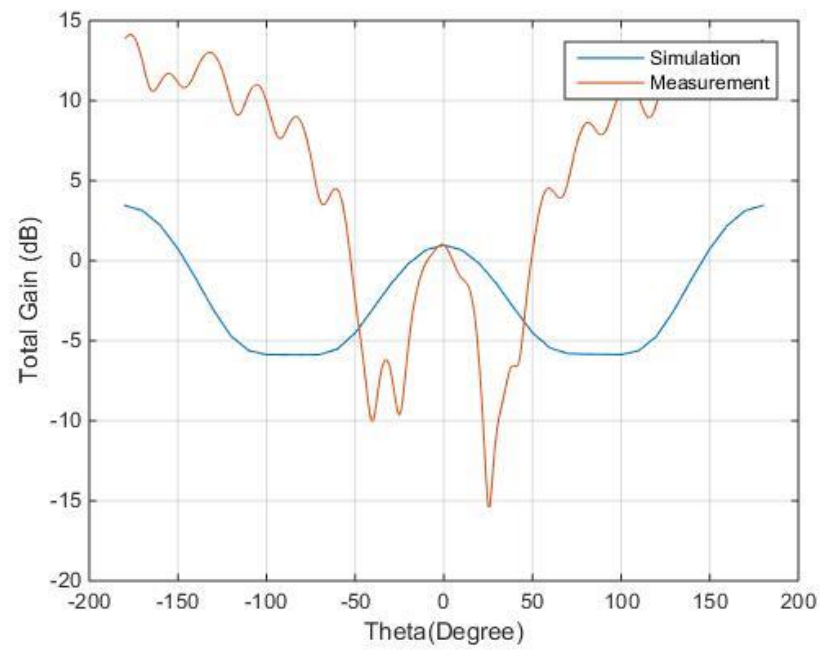


Figure 3- 13 H-Plane Radiation Patterns at 3 GHz

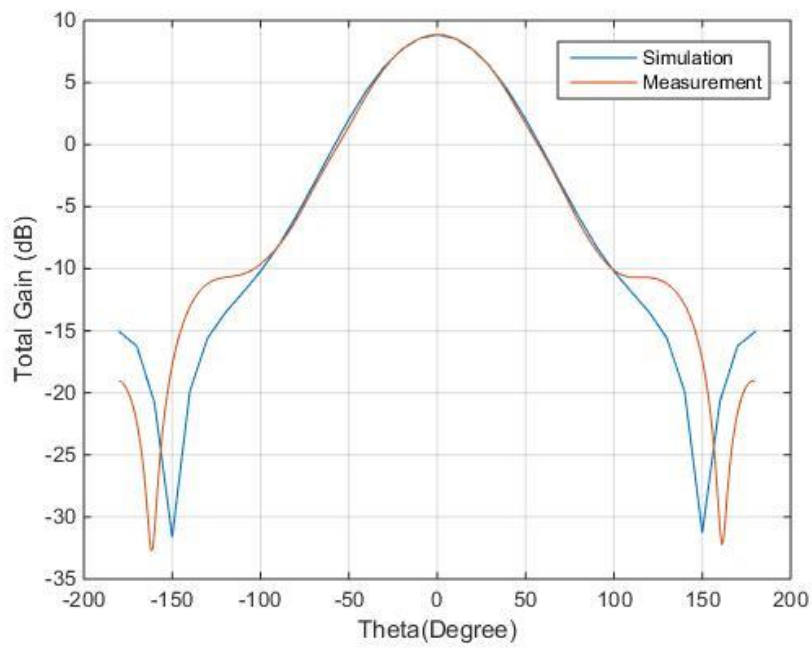


Figure 3- 14 E-Plane Radiation Patterns at 4 GHz

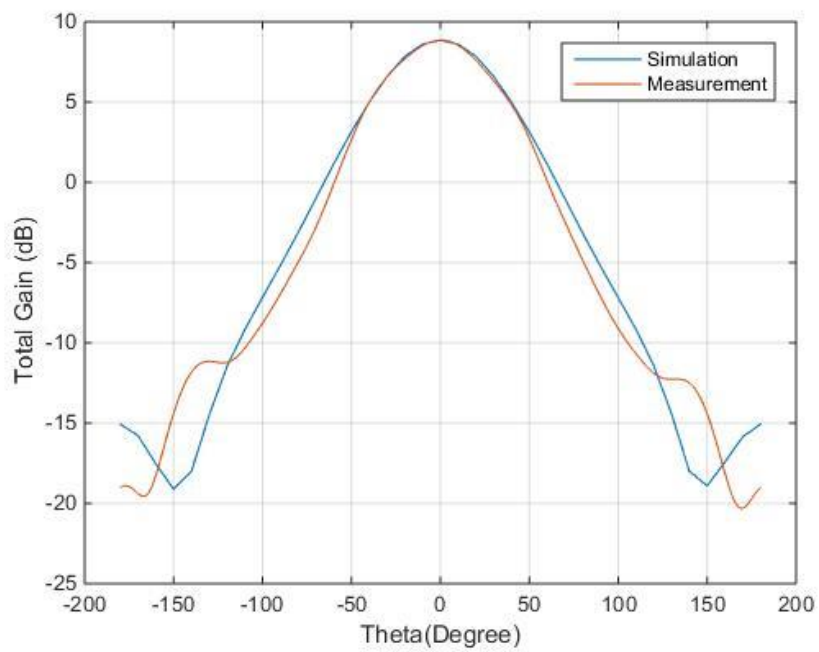


Figure 3- 15 H-Plane Radiation Patterns at 4 GHz

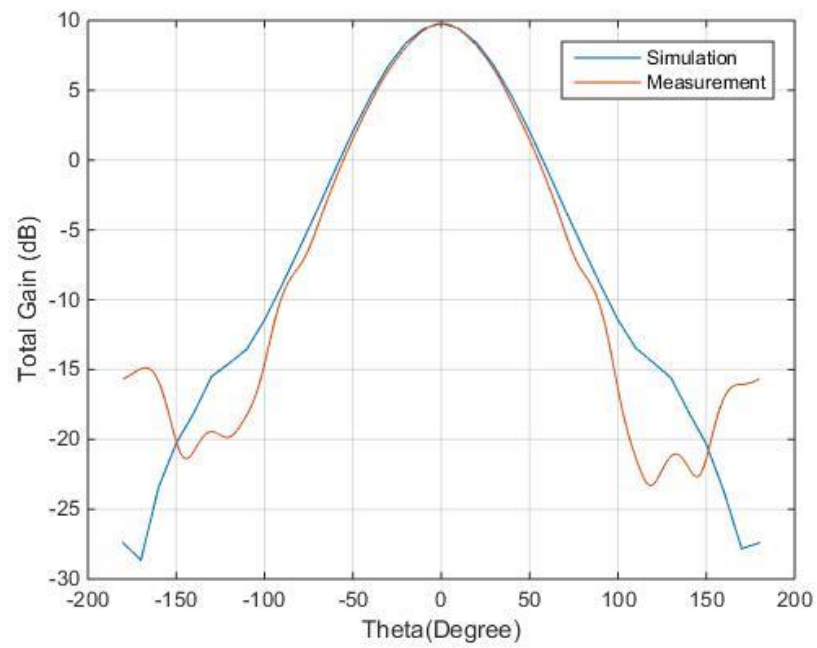


Figure 3- 16 E-Plane Radiation Patterns at 5 GHz

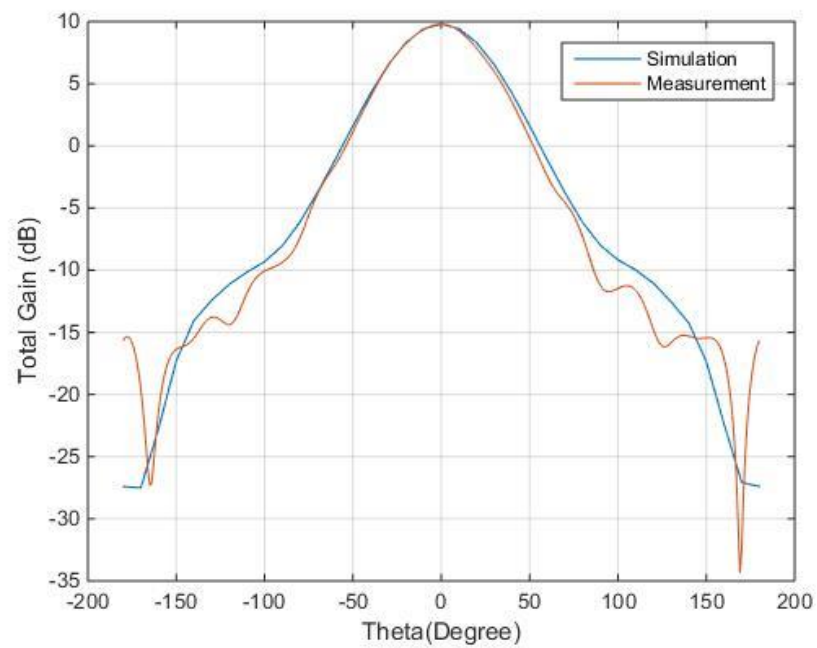


Figure 3- 17 H-Plane Radiation Patterns at 5 GHz

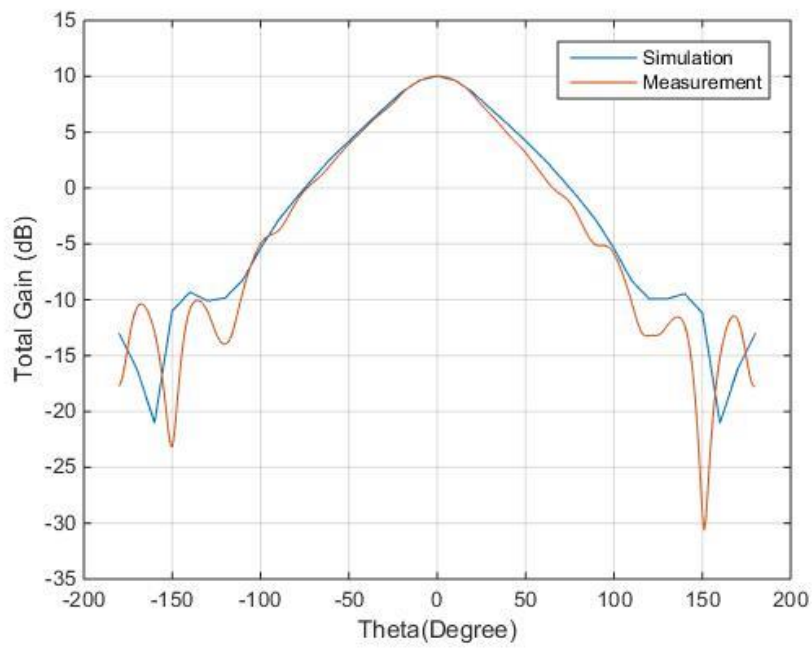


Figure 3- 18 E-Plane Radiation Patterns at 6 GHz

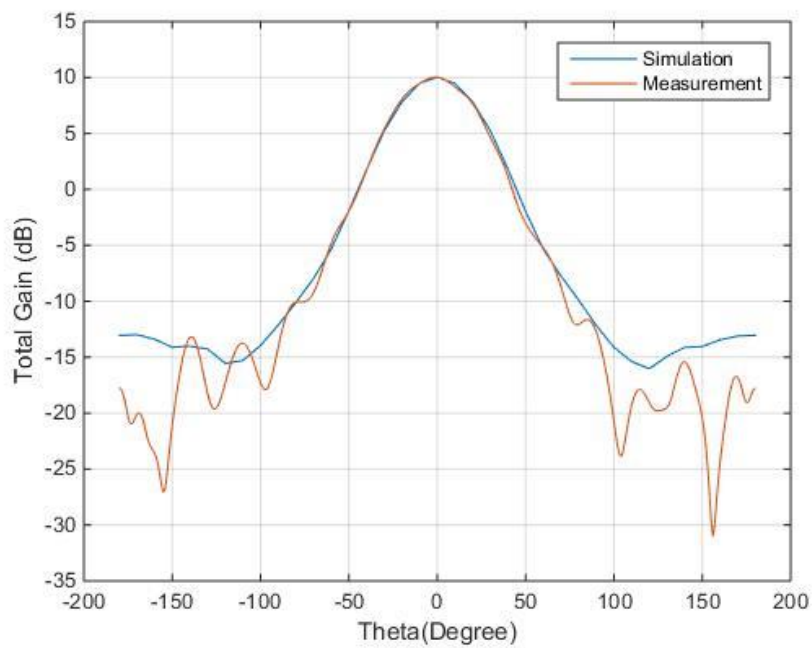


Figure 3- 19 H-Plane Radiation Patterns at 6 GHz

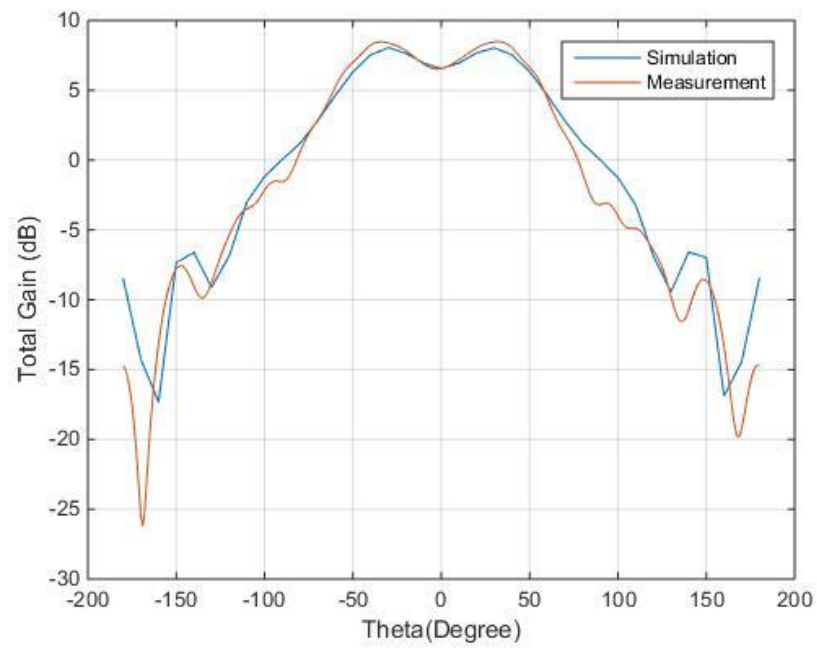


Figure 3- 20 E-Plane Radiation Patterns at 7 GHz

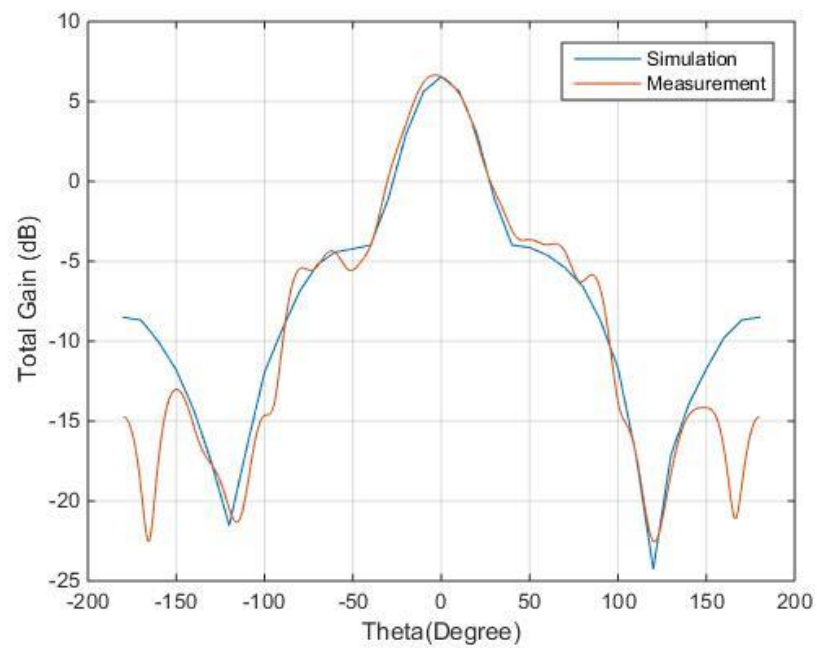


Figure 3- 21 H-Plane Radiation Patterns at 7 GHz

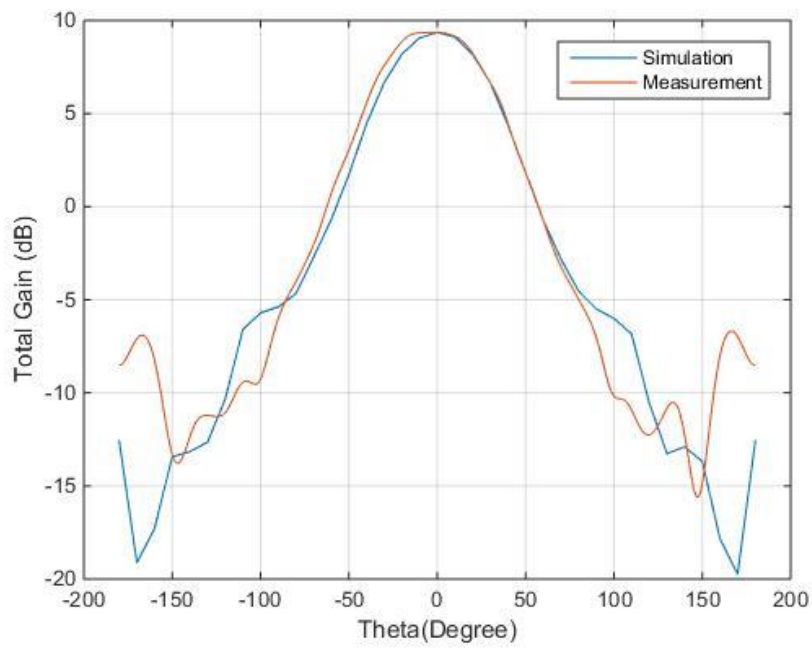


Figure 3- 22 E-Plane Radiation Patterns at 8 GHz

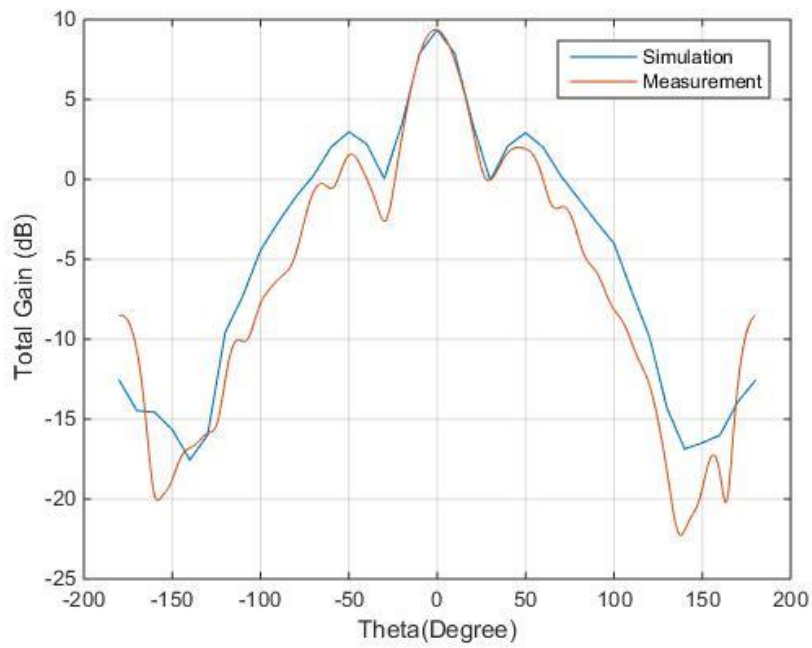


Figure 3- 23 H-Plane Radiation Patterns at 8 GHz

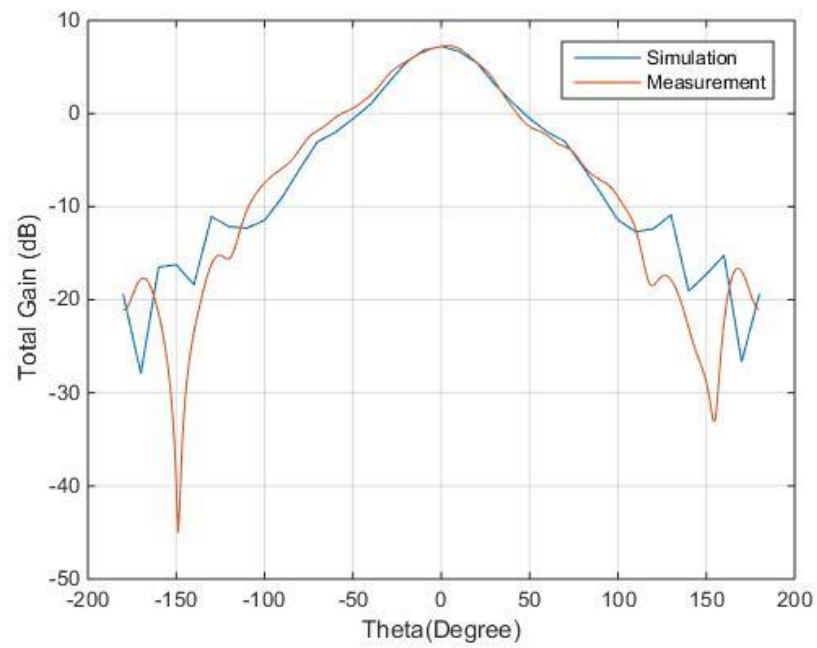


Figure 3- 24 E-Plane Radiation Patterns at 9 GHz

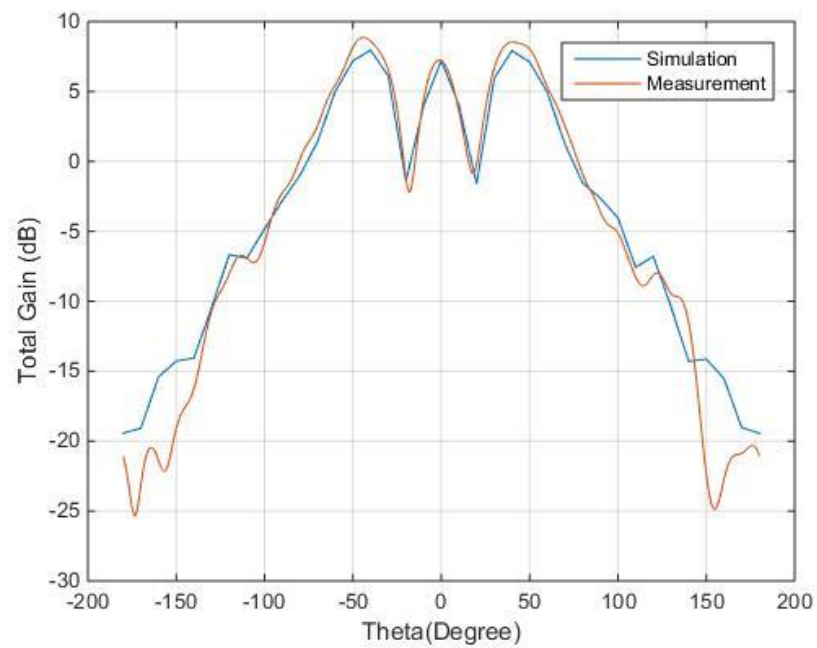


Figure 3- 25 H-Plane Radiation Patterns at 9 GHz

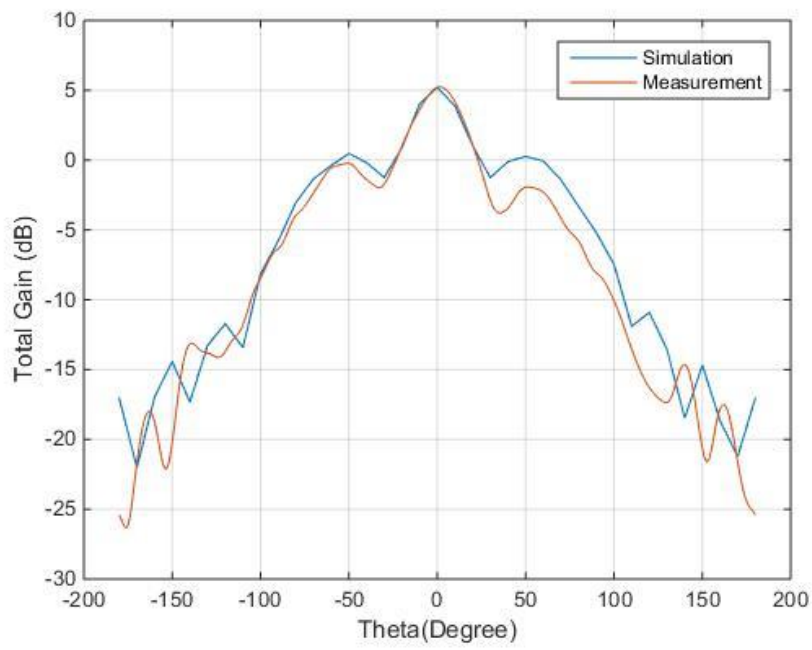


Figure 3- 26 E-Plane Radiation Patterns at 10 GHz

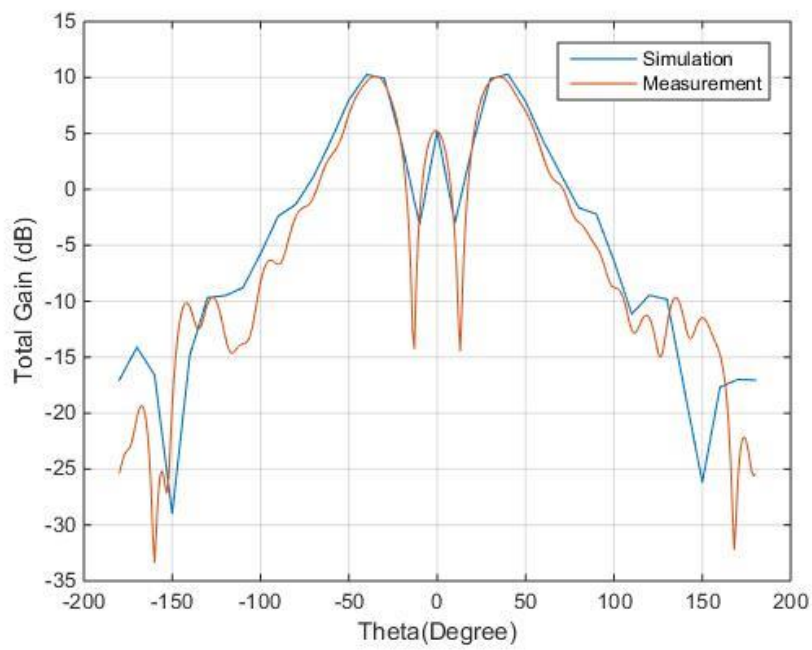


Figure 3- 27 H-Plane Radiation Patterns at 10 GHz

Measured 3dB beamwidths of the broadside beam are listed in Table 3- 1. It can be observed that the drop in the gain around 7 GHz is due to wide beamwidth in E-plane at this frequency.

Table 3- 1 Measured 3 dB Beamwidth of the Broadside Beam of the Antenna

Frequency	E-Plane	H-Plane
3 GHz	20°	31°
4 GHz	64°	69°
5 GHz	56°	55°
6 GHz	57°	47°
7 GHz	115°	37°
8 GHz	69°	27°
9 GHz	58°	20°
10 GHz	37°	15°

CHAPTER 4

CONCLUSIONS

In this thesis magneto-electric dipole antenna design with differential feeding structure is studied and an antenna operating in 3-10 GHz band is designed. The advantages of the designed antenna are that it has a low-cost and simple structure. The designed antenna has also a flat gain and good radiation pattern with very low cross-polarization. The simulated results demonstrated that it had a wide impedance bandwidth of 112% (3.3 GHz to 10 GHz). In order to achieve flat gain and to eliminate deteriorations in radiation patterns at higher frequencies, the differential fed magneto-electric dipole antenna is placed inside a cavity. The simulation results of the differential fed magneto-electric dipole antenna with cavity demonstrates that the return loss response and radiation patterns of the antennas fulfill the requirements and expectations of the design.

Finally, the design and simulation process of the differential fed magneto-electric dipole antenna with cavity is completed, this antenna with determined parameters is fabricated and measured. The fabrication of the antenna is accomplished in the facilities of ASELSAN Inc. using copper material. Totally, three parts which are ground plane with cavity, dipoles and differential feeding structure of the fabricated antenna are integrated manually. The return loss responses, gains and the radiation patterns of the fabricated differential fed magneto-electric dipole antenna with cavity are measured, and measurement results are compared with the simulation results in order to reveal the crucial fabrication parameters resulting in the deviation from the simulation.

Good agreement between the simulated and measured results of the differential fed magneto-electric dipole antenna with cavity is obtained in terms of the return loss, far field radiation patterns and gain. The measured bandwidth of the antenna for a return loss better than 10 dB is 110% (3.4 GHz to 10 GHz). The radiation patterns are measured at eight different frequencies, and observed to be in accordance with the simulation results in the operating bandwidth.

For the future work, instead of the differential feeding another structure that transforms the unbalanced input to balanced antenna terminals can be developed. Moreover, the dual polarized magneto-electric dipole antenna structures could also be studied as a future work.

REFERENCES

- [1] Q. Wu, B. S. Jin, L. Bian, Y. M. Wu, L. W. Li, *An Approach to the Determination of the Phase Center of Vivaldi-based UWB Antenna*, IEEE Transactions on Antennas and Propagation, pp. 564-566, 2006.
- [2] K. M. Luk, H. Wong, *A New Wideband Unidirectional Antenna Element*, International Journal of Microwave and Optical Technology, Vol. 1, No. 1, pp. 35-44, June 2006.
- [3] K. M. Luk, B. Wu, *The Magnetoelectric Dipole – A Wideband Antenna for Base Stations in Mobile Communications*, Proceedings of the IEEE, Vol. 100, No. 7, pp. 2297-2307, July 2012.
- [4] Z. N. Chen, K. M. Luk, *Antennas for Base Stations in Wireless Communications*, McGraw-Hill, Inc., 2009.
- [5] L. Ge, K. M. Luk, *A Low-Profile Magneto-Electric Dipole Antenna*, IEEE Transactions on Antennas and Propagation, Vol. 60, No. 4, pp. 1684-1689, April 2012.
- [6] S. W. Liao, Q. Xue, J. H. Xu, *A Differentially Fed Magneto-Electric Dipole Antenna with a Simple Structure*, IEEE Antennas and Propagation Magazine, Vol. 55, No. 5, pp. 74-84, October 2013.
- [7] H. W. Lai, H. Wong, *Substrate Integrated Magneto-Electric Dipole Antenna for 5G Wi-Fi*, IEEE Transactions on Antennas and Propagation, Vol. 63, No. 2, pp. 119-126, February 2015.
- [8] M. Li, K. M. Luk, *A Differential-fed Magneto-Electric Dipole Antenna for Ultra-wideband Applications*, IEEE Transactions on Antennas and Propagation, pp. 1482-1485, 2011.
- [9] L. Ge, K. M. Luk, *A UWB Magneto-Electric Dipole Antenna*, IEEE Asia-Pacific Conference on Antennas and Propagation, August 2012.
- [10] K. B. Ng, H. Wong, K. K. So, C. H. Chan, K. M. Luk, *60 GHz Plated Through Hole Printed Magneto-Electric Dipole Antenna*, IEEE Transactions on Antennas and Propagation, Vol. 60, No. 7, pp. 3129-3136, July 2012.

- [11] M. Li, K. M. Luk, *Wideband Magneto-Electric Dipole Antenna for 60 GHz Millimeter-Wave Communications*, IEEE Transactions on Antennas and Propagation, Vol. 63, No. 7, pp. 3276-3279, July 2015.
- [12] B. Q. Wu, K. M. Luk, *A Broadband Dual-Polarized Magneto-Electric Dipole Antenna with Simple Feeds*, IEEE Antennas and Wireless Propagation Letters, Vol. 8, pp. 60-63, 2009.
- [13] M. Li, K. M. Luk, *Wideband Magnetolectric Dipole Antennas with Dual Polarization and Circular Polarization*, IEEE Antennas and Propagation Magazine, Vol. 57, No. 1, pp. 110-119, February 2015.
- [14] ANSYS HFSS[®], <<http://www.ansys.com/hfss>>.
- [15] Bockelman, David E. and William R. Eisenstadt, *Pure-Mode Network Analyzer for On-Water Measurements of Mixed-Mode S-parameters of Differential Circuits*, IEEE Transactions on Advanced Packaging, Vol. 31, No. 2, May 2008.